Aus der Klinik für Nuklearmedizin
der Medizinischen Fakultät Charité – Universitätsmedizin Berlin

DISSERTATION

**Optimizing the Automated Analysis of Dopamine D2
Receptor Imaging for Research into Alcohol Use Disorders**

zur Erlangung des akademischen Grades
Doctor medicinae (Dr. med.)

vorgelegt der Medizinischen Fakultät
Charité – Universitätsmedizin Berlin

Von

David Paul Weber

aus Bremerhaven

Datum der Promotion: 03.12.2021

Vorwort

Teilergebnisse der vorliegenden Arbeit wurden im Rahmen einer Posterpräsentation mit zitierbarem Abstract veröffentlicht:

D. P. Weber, T. Gleich, T. Kodalle, G. Spitta, C. Lange, O. Butler, W. Brenner, A. Heinz, J. Gallinat, R. Buchert; Assessment of dopamine D2/3 receptor status in alcohol use disorders using F-18-fallypride PET and reference tissue approaches: methodological considerations; Dreiländertagung 2017 der Deutschen Gesellschaft für Nuklearmedizin

Table of Contents

List of Tables

List of Figures

List of abbreviations

AAL	Automated Anatomical Labeling
ADH	alcohol dehydrogenase
ALDH	aldehyde dehydrogenase
ANOVA	Analysis of variance
AUD	Alcohol use disorder
BMI	body mass index
BP	binding potential
BPND	non-displaceable binding potential
CIWA	Clinical Institute Withdrawal Assessment for Alcohol
CNS	Central nervous system
COV	coefficient of variation
CRF	Corticotropin-releasing factor
CT	Computed tomography
DA	Dopamine
DAT	dopamine transporter
DFG	Deutsche Forschungsgesellschaft
DOPA	Dihydroxyphenylalanine
DSM	Diagnostic and Statistical Manual of Mental Disorders
DSM-5	fifth edition of the DSM
DSM-IV	fourth edition of the DSM
FIRST	FMRIB's Integrated Registration & Segmentation Tool
fMRI	functional magentic resonance imaging
FMRIB	Oxford Centre for Functional MRI of the Brain
FSL	FMRIB Software Library
GABA	gamma-Aminobutyric acid
GH	growth hormone
HR	high risk
IBZM	Iodobenzamide
ICBM	International Consortium for Brain Mapping
LeAD	Learning and Alcohol Dependence
Logan	Logan's reference tissue method with k'2 term
Logan2	Logan's reference tissue method without k'2 term
LR	low risk
MNI	Montreal Neurological Institute
MRI	magnetic resonance imaging
nAChR	Nicotinic acetylcholine receptor
NPY	neuropeptide Y
PET	positron emission tomography
PTSD	Posttraumatic stress disorder
ROI	region of interest
rrss	relative residual sum of squares
rss	residual sum of squares
RTM	reference tissue model
SD	standard deviation
SLF	superior longitudinal fasciculus
SPECT	single-photon emission computed tomography
SRTM	simplified reference tissue model
SRTM2	two-step SRTM with global k'2
TAC	time activity curve
wm	white matter

Abstract

Alcohol use disorders (AUDs) are associated with significant disease burden worldwide, yet their etiology is still unclear. Previous research has linked AUDs with the dopaminergic neurotransmitter system. Specifically, striatal dopamine D2/3 receptor availability has been shown to be lower in alcohol-dependent subjects compared to controls. Recent imaging studies utilizing the PET-tracer [18F]fallypride were unable to consistently show this relationship. One reason for this inconsistency may be the use of suboptimal methods for the automated image analysis and thus a lack of sensitivity for between-group differences.

This study had both methodological and clinical goals. It aimed to optimize three steps in the automated image analysis process and to afterwards assess the relationship between D2/3 receptor availability and AUDs.

Twenty detoxified alcohol-dependent patients were compared with 19 control subjects with low-risk alcohol consumption and 19 control subjects with high-risk alcohol consumption. All subjects underwent [18F]fallypride-PET and MRI imaging. Quality parameters were compared between two different ROI identification methods, three different reference tissues and four different reference tissue models. Based on these analyses, a combination of methods was used to assess dopamine D2/3 receptor availability in the three groups.

The comparison of ROI identification methods showed significantly better anatomical fits using an automatic segmentation tool (FSL FIRST) compared with an atlas-based approach. The analysis of reference tissues showed an overall superiority of the superior longitudinal fasciculus (SLF) compared with both the cerebellum and a complete white matter probability mask. The SLF showed lower overall tracer uptake and lower heterogeneity of tracer uptake than the cerebellum. Compared to the cerebellum, the SLF also showed lower coefficients of variance in D2/3 receptor availability estimates. Using a complete white matter probability map as reference tissue was shown to be inferior in several quality parameters. The comparison of reference tissue models showed no significant differences between two variants of the simplified reference tissue model (SRTM) and two variants of the model proposed by Logan et al.

Using the optimized analysis process, significantly lower D2/3 receptor availability was found in detoxified alcohol-dependent patients compared to control subjects with low-risk

alcohol consumption in both the putamen and thalamus. No significant difference was found between low-risk and high-risk control subjects.

Lastly, it was found that the choice of methodology had a significant impact on the clinical research question - while some combinations of methodology showed a significant between-group difference, other combinations showed no such difference.

Zusammenfassung

Alkoholgebrauchsstörungen sind weltweit mit einer erheblichen Krankheitslast verbunden, ihre Ätiologie ist jedoch weiterhin unklar. Vorangegangene Untersuchungen haben Alkoholgebrauchsstörungen mit dem dopaminergen Neurotransmittersystem in Verbindung gebracht. Insbesondere wurde gezeigt, dass die Verfügbarkeit der striatalen Dopamin-D2/3-Rezeptoren bei alkoholabhängigen Personen im Vergleich zu Kontrollpersonen geringer ist. Diesen Zusammenhang konnten neuere Studien mit dem PET-Tracer [18F]fallypride nicht zuverlässig reproduzieren. Ein Grund hierfür könnte die Verwendung von suboptimalen Methoden für die automatisierte Bildanalyse und eine damit einhergehende mangelnde Sensitivität für Gruppenunterschiede sein.

In diesem Kontext verfolgte die vorliegende Studie sowohl methodische als auch klinische Fragestellungen. Sie zielte darauf ab, drei Schritte im automatisierten Bildanalyse-Prozess zu optimieren und anschließend die Beziehung zwischen D2/3-Rezeptor-Verfügbarkeit und Alkoholgebrauchsstörungen zu ermitteln.

Zwanzig alkoholabhängige Patienten nach Entzug wurden mit 19 Kontrollpersonen mit risikoarmem Alkoholkonsum und 19 Kontrollpersonen mit risikoreichem Alkoholkonsum verglichen. Alle Probanden wurden mittels [18F]fallypride-PET und MRT untersucht. Qualitätsparameter wurden zwischen zwei verschiedenen ROI-Identifikationsmethoden, drei verschiedenen Referenzgeweben und vier verschiedenen Referenzgewebemodellen verglichen. Basierend auf diesen Analysen wurde eine optimierte Kombination von Methoden verwendet, um die Verfügbarkeit von Dopamin-D2/3-Rezeptoren in den drei Gruppen zu beurteilen.

Der Vergleich der ROI- Identifikationsmethoden zeigte signifikant bessere anatomische Übereinstimmungen, wenn ein automatisches Segmentierungstool (FSL FIRST) statt eines atlasbasierten Ansatzes verwendet wird. Die Analyse der Referenzgewebe zeigte insgesamt eine Überlegenheit des superioren longitudinalen Faszikulus (SLF) im Vergleich sowohl zum Kleinhirn als auch zu einer Wahrscheinlichkeitsmaske für weiße Substanz. Der SLF zeigte im Vergleich zum Kleinhirn eine geringere Heterogenität der Traceraufnahme sowie eine insgesamt geringere Traceraufnahme. Im Vergleich zum Kleinhirn zeigte der SLF auch geringere Varianzkoeffizienten in den D2/3-Rezeptor-Verfügbarkeitsschätzungen. Dem gegenüber erwies sich die Verwendung einer Wahrscheinlichkeitsmaske für weiße Substanz als Referenzgewebe in mehreren Qualitätsparametern als unterlegen. Der Vergleich von Referenzgewebemodellen zeigte

keine signifikanten Unterschiede zwischen zwei Varianten des vereinfachten Referenzgewebemodells und zwei Varianten des von Logan et al. vorgeschlagenen Modells.

Unter Verwendung des optimierten Bildanalyse-Prozesses wurde eine signifikant niedrigere Verfügbarkeit von D2/3-Rezeptoren bei alkoholabhängigen Patienten nach Entzug im Vergleich zu Kontrollprobanden mit risikoarmem Alkoholkonsum sowohl im Putamen als auch im Thalamus gefunden. Zwischen den Probanden mit risikoarmem Alkoholkonsum und risikoreichem Alkoholkonsum wurde jedoch kein signifikanter Unterschied in der Rezeptorverfügbarkeit festgestellt.

In einer letzten Analyse wurde festgestellt, dass die Wahl der Methodik einen signifikanten Einfluss auf die klinische Forschungsfrage hatte: während einige Kombinationen der Methodik einen signifikanten Unterschied zwischen alkoholabhängigen Patienten nach Entzug und Kontrollprobanden zeigten, fand sich bei anderen Kombinationen kein solcher Unterschied.

1. Introduction

1.1. Burden of alcohol-related morbidity and mortality

Alcohol consumption presents a major global health issue. The world health organization estimates that in 2012 about 3.3 million deaths, or 5.9% of all deaths, were caused by alcohol consumption. In addition to that, alcohol was also estimated to have caused about 5.1% of the global burden of disease and injury in 2012 (World Health Organization, 2014).

In Germany, alcohol is among the psychoactive substances with the highest consumption. The 2012 Epidemiological Survey of Substance Abuse found that 90.2% of adults aged between 18 and 64 years had consumed alcohol within the previous 12 months, 9.8% had not and 3.6% had never consumed alcohol. 3.1% of respondents fulfilled the DSM-IV diagnostic criteria for alcohol abuse and another 3.4% fulfilled the DSM-IV criteria for alcohol dependence. Extrapolated to the German population an estimated 7.4 million adults consume more alcohol than the recommended daily allowance, 1.61 million adults fulfil the criteria for alcohol abuse and 1.77 million adults fulfil the criteria for alcohol dependence (Pabst, Kraus et al. 2013).

An estimated 74,000 people die each year in Germany because of alcohol consumption or a combination of alcohol consumption and tobacco abuse. A study based on data from 2007 estimated the economic cost of disease due to risky alcohol consumption and alcohol abuse at 26.7 billion euros per year. In 2013, of 19.2 million inpatient cases, 338,204 were due to psychological and behavioral disorders resulting from alcohol consumption, including acute intoxication (Die Drogenbeauftragte der Bundesregierung 2015).

According to the Statistical Report on substance abuse treatment in Germany, alcohol related disorders make up the most common main diagnoses in substance abuse treatment cases (50.4% of outpatient cases and 71.5% of inpatient cases) (Brand, Künzel et al. 2015).

1.2. Alcohol Use Disorders

Trying to categorize substance use into healthy, dangerous or pathological use is always difficult. At the same time, a clear differentiation is needed for research and treatment. Most commonly, the Diagnostic and Statistical Manual of Mental Disorders (DSM) is used

to provide guidelines for categorization. At the beginning of this research project, the fourth edition of the DSM (DSM-IV) (American Psychiatric Association 1994) was up to date, which listed the separate diagnoses of substance abuse and substance dependence. For both diagnoses, there were separate criteria, of which a certain number had to be present to justify the diagnosis. In 2013, the fifth edition of the DSM was released (DSM-5) (American Psychiatric Association 2013), which subsumes both categories under the term ″substance use disorders″. The criteria for this diagnosis are all the criteria of the former separate diagnoses except for the abuse criterion 3 "legal problems", which is no longer included in DSM-5. It has been replaced by a criterion for craving.

1.3. Etiology of alcohol use disorders
1.3.1. Established risk factors and heritability

Despite the well-known impact of alcohol use disorders on public health, there is no clear understanding of the mechanisms involved in alcohol abuse and alcohol dependence. To date, no comprehensive model exists that explains why fewer than 10% of the population suffer from alcohol use disorders while over 90% of the population consume alcohol. A variety of factors which are associated with alcohol dependence have been identified, however. Several reviews have tried to sum up the extensive existing research concerning risk factors and mechanisms leading to alcohol addiction (Hägele, Friedel et al. 2014; Vetreno and Crews 2014).

Among the mechanisms leading to alcohol addiction, several risk factors relating to behavior and habits have been found. Binge drinking and frequent exceeding of daily drinking recommendation are widely considered as the main risk factors for alcohol use disorders (Dawson, Grant et al. 2005; Crabbe, Harris et al. 2011). Furthermore, two factors connected with the commencement of alcohol consumption increase the risk of developing risky drinking behavior: young age at first alcohol consumption and a perception of feeling drunk during the first alcohol experience (Warner, White et al. 2007). Substance use in the peer group has also been associated with the alcohol problems of adolescents, as have aggressive and delinquent behavior (Barnow, Schuckit et al. 2002).

On top of behavioral risk factors, many studies have found strong evidence for the heritability of alcohol addiction. One of the strongest risk factors for the development of an alcohol use disorder is a positive family history of alcohol use disorders in close relatives (Nurnberger, Wiegand et al. 2004; Zimmermann, Blomeyer et al. 2007). Twin

studies comparing the concordance of alcohol use disorders amongst monozygotic and dizygotic twins have estimated the heritability of alcohol addiction to be around 50% (Kendler, Prescott et al. 1997). An adoption study showed that the influence of genetics on alcohol consumption is stronger than the influence of growing up with an alcohol addicted parent (Goodwin, Schulsinger et al. 1974). A positive family history for alcohol use disorders is also correlated with a preference for higher blood alcohol concentrations in an alcohol self-administration setting (Zimmermann, Mick et al. 2009). Several traits have been found to be connected to the heritability of alcohol use disorders, notably the trait of low sensitivity to the physiological effects of alcohol. This is an established risk factor for the development of an alcohol use disorder. In subgroups of study populations this trait appears to be linked to the heritability of alcohol use disorders (Schuckit and Smith 2000, Schuckit and Smith 2006).

Other heritable traits directly linked to an increased or decreased risk of developing an alcohol use disorder have been linked to specific genes relating to the metabolism of alcohol and its most important breakdown product, acetaldehyde. Two enzymes, crucial for the metabolic steps, alcohol dehydrogenase (ADH) and aldehyde dehydrogenase (ALDH), have variants that have been associated with significantly altered risks of developing an alcohol use disorder. There is strong evidence, for example, that the ADH variants ADH1B*2 and ADH1B*3 are protective against the development of alcohol dependence. Furthermore, the ALDH variant ALDH2*2 has been found to be strongly protective against alcohol dependence, with homozygotes being nearly completely protected (Hurley and Edenberg 2012). Furthermore, a polymorphism of the serotonin transporter gene HTTLPR was significantly related to both the low level of response phenotype and alcoholism (Hu, Oroszi et al. 2005). Additionally, homologues of the γ-aminobutyric acid receptor gene cluster have been associated with alcohol use disorders (Dick, Plunkett et al. 2006).

When looking at the etiology of alcohol use disorders it is important not to ignore the significant comorbidity of alcohol use disorders and other (severe) psychiatric disorders. Notably mood disorders, anxiety disorders, impulse control disorders and schizophrenia have been shown to be associated with alcohol use disorders (Kessler, Chiu et al. 2005; D'Souza, Gil et al. 2006; Enoch, White et al. 2008; Rubio, Jimenez et al. 2008).

1.3.2. Neurobiology of alcohol addiction

1.3.2.1.   Preclinical studies

Preclinical studies with various addictive substances have linked the development of addiction to a multitude of structural, neuronal and molecular changes in the central nervous system (Nestler and Aghajanian 1997; Robinson and Kolb 2004; Kumar, Choi et al. 2005). Various neuropharmacological sites and systems have been shown to be linked to alcohol addiction. Glutamate, GABA, nAChR/glycine, dopamine, 5-HT, cannabinoids, opioids and CRF/NPY have been associated with different dimensions of alcohol addiction, such as the initiation of alcohol consumption, maintenance of alcohol consumption, craving and reinstatement of alcohol seeking, and relapse to alcohol use (Nevo 1995; Vengeliene, Bilbao et al. 2008). Some of the changes occurring in the development of addiction resemble mechanisms of physiological learning (von der Goltz and Kiefer 2009).

Amongst the various neuropharmacological systems associated with alcohol addiction, the dopaminergic reward system with its mesolimbic and cortical structures is amongst the foremost studied regions and is perceived as a core region for alcohol addiction (Di Chiara 1997; Hyman, Malenka et al. 2006; Robinson and Berridge 2008; Belin, Jonkman et al. 2009; Heinz, Beck et al. 2009; Haber and Knutson 2010; Charlet, Beck et al. 2013; Engel and Jerlhag 2014). Alcohol and other drugs, along with non-drug related factors such as food and sex, stimulate dopaminergic neurotransmission and are thus subject to the dopaminergic influence on stimulus-response mechanisms, habit learning and incentive sensitization (Robinson and Berridge 2003).

Several preclinical studies have evaluated the effects of acute and chronic ethanol intake on the dopamine system. Rats who were subject to acute ethanol intake were shown to have an increased dopamine synthesis (Carlsson, Engel et al. 1974; Fadda, Argiolas et al. 1980) as well as an increased firing rate of dopaminergic neurons in the substantia nigra (Mereu, Fadda et al. 1984) and the ventral tegmental area (Gessa, Muntoni et al. 1985), along with an increased dopamine release in the nucleus accumbens and the striatum (Di Chiara and Imperato 1986, Di Chiara and Imperato 1988). Rats undergoing chronic ethanol intake were shown to have depleted DA stores (Fadda, Argiolas et al. 1980) and elevated extracellular dopamine concentrations in the nucleus accumbens, which persisted for up to two weeks in the absence of alcohol (Thielen, Engleman et al. 2004).

Other studies have focused on the effects of agonists and antagonists of the dopamine system on ethanol consumption. The administration of iv dopamine agonists reduced ethanol-induced locomotor stimulation in rats (Carlsson, Engel et al. 1974), reduced ethanol preference in common stock rats (Pfeffer and Samson 1988; Cohen, Perrault et al. 1998), showed varying dose- and receptor subtype-related changes in ethanol consumption in high alcohol-drinking rat lines (Dyr, McBride et al. 1993), and reduced ethanol intake in alcohol-preferring- and high alcohol-drinking rat lines (Russell, McBride et al. 1996). The administration of iv dopamine antagonists reduced alcohol preference in common stock rats (Pfeffer and Samson 1988), showed varying dose- and receptor subtype-related changes in ethanol consumption in high alcohol-drinking rat lines (Dyr, McBride et al. 1993), suppressed the alcohol-deprivation effect in chronic ethanol drinking mice (Salimov, Salimova et al. 2000), reduced drug-seeking behavior after withdrawal in common stock rats (Liu and Weiss 2002), reduced ethanol preference and intake in alcohol-preferring and non-alcohol preferring rats (Thanos, Katana et al. 2005), and reduced alcohol-seeking behavior in common stock rats (Vengeliene, Leonardi-Essmann et al. 2006).

It was further shown that the injection of antagonists aimed at the ventral tegmental nicotinic acetylcholine receptors blocks the increase in accumbal dopamine levels and reduces ethanol intake and preference in ethanol-preferring rats (Ericson, Blomqvist et al. 1998; Lof, Olausson et al. 2007).

Other studies have focused on the expression of dopamine receptors in different populations. Ethanol drinking rats were shown by in-vitro autoradiography to have a dose-dependent decrease of dopamine receptors in the caudate, nucleus accumbens and tuberculum olfactorium 24 hours after withdrawal, with no difference shown five days after withdrawal (Rommelspacher, Raeder et al. 1992). Ethanol-naïve, ethanol-preferring rat lines were shown to have decreased D2-receptor density compared to ethanol-naïve, non-ethanol-preferring rat lines in the olfactory tubercle, the caudate nucleus and the nucleus accumbens (Stefanini, Frau et al. 1992), as well as in the putamen and the ventral tegmental area (McBride, Chernet et al. 1993). Alcohol self-administering rats with adenoviral vector-induced increased D2 receptor expression in the nucleus accumbens were shown to have a decreased ethanol preference and ethanol intake compared to rats with unaltered D2 receptor status (Thanos, Volkow et al. 2001) [CAVE: two figures labeled incorrectly in the original paper, correction in issue 79.]. Ethanol-preferring rats were

shown to have increased D1 and D2 receptor densities in the anterior nucleus accumbens after chronic ethanol intake, compared to ethanol-naïve, ethanol-preferring rats (Sari, Bell et al. 2006). In contrast to these findings, ethanol-preferring rats were shown to have a downregulation of D1 and D2 receptors and an upregulation of D3, D4 & D5 receptors in the striatum after chronic ethanol intake, compared to ethanol-naïve, ethanol-preferring rats (Vengeliene, Leonardi-Essmann et al. 2006).

1.3.2.2. *Clinical studies*

The links between the dopaminergic system and alcohol have also been the subject of numerous clinical studies. Several studies have tried to indirectly analyze the dopaminergic system by looking at fMRI activity in the most important brain regions concerning the dopaminergic system. An altered ventral striatal activation pattern in alcohol-addicted patients compared to healthy controls was found, namely increased activation with alcohol-associated cues and decreased activation with non-alcohol rewards (Wrase, Schlagenhauf et al. 2007). The increase in ventral striatal activation was also shown in excessive drinkers compared to social drinkers (Ihssen, Cox et al. 2011). Other studies found opposing results with higher ventral striatal activity in social drinkers compared to heavy drinkers and found heavy drinkers to have a higher dorsal striatal activation instead (Vollstadt-Klein, Wichert et al. 2010).

Before DA receptor molecular imaging was widely used, DA receptor status used to be assessed indirectly by growth hormone (GH) response to an apomorphine challenge (Nair, Lal et al. 1982). Several studies found a reduced GH response in abstinent alcoholics in comparison to controls (Balldin, Berggren et al. 1992; Balldin, Berggren et al. 1993; Wiesbeck, Mauerer et al. 1995). More specifically, several follow-up studies found the GH response on admission and/or after detoxification to be significantly reduced in subsequent relapsers compared to subsequent abstainers (Dettling, Heinz et al. 1995; Heinz, Dettling et al. 1995; Heinz 1996; Schmidt, Dettling et al. 1996), as well as a significantly lower GH response in family positive alcoholics than in family negative alcoholics (Wiesbeck, Mauerer et al. 1995).

With the advent of molecular imaging, many different target sites of the dopamine system can be individually analyzed with a variety of radiotracers using single-photon emission computed tomography (SPECT) or positron emission tomography (PET) (see Figure 1).
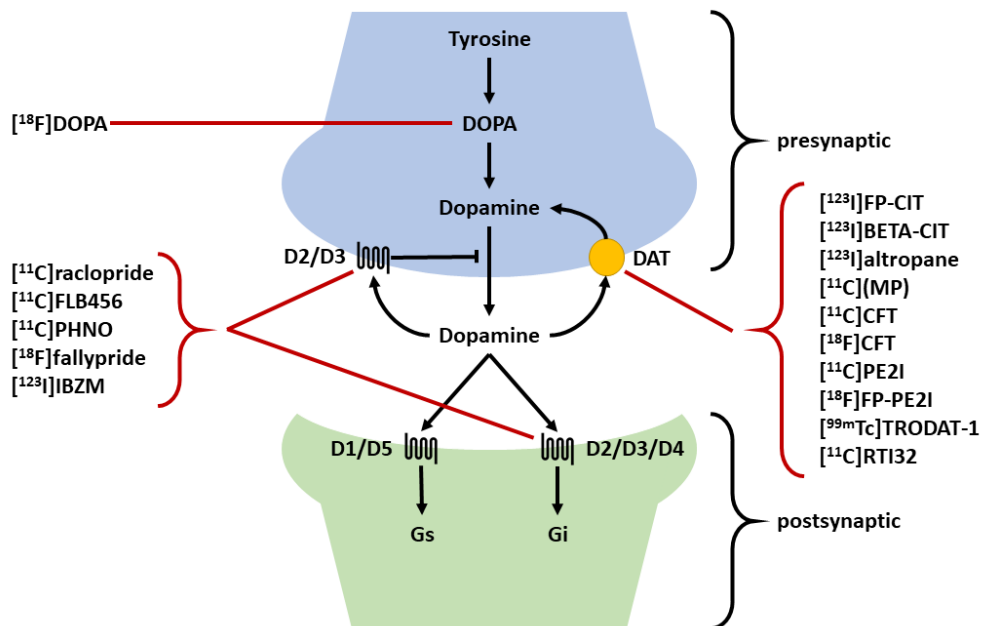
Figure 1. Simplified overview of the radiotracers of research into the dopamine system and their target structures. Adapted from Politis (2014).

Several studies have utilized PET with [11C]raclopride to access dopamine release in healthy subjects following alcohol cues or alcohol intake. It was shown that binding in the NAC and ventral putamen was significantly lower after alcohol intake, likely to be due to dopamine release in those areas (Boileau, Assaad et al. 2003). This increased striatal dopamine release upon alcohol intake was shown to be significantly stronger in men than in women (Urban, Kegeles et al. 2010). Another study found matching results of higher striatal dopamine release upon intravenous injection of alcohol, while showing lower striatal dopamine release after confrontation with alcohol cues only (Yoder, Morris et al. 2009).

Other studies have utilized [18F]DOPA-PET to measure striatal DOPA uptake with heterogenous results. One study showed that detoxified alcohol-dependent patients had significantly higher DOPA uptake in the left putamen and right caudate (Tiihonen, Vilkman et al. 1998), while another study could not repeat that finding, but found a significant negative correlation between alcohol craving and DOPA uptake in the striatum (Heinz, Siessmeier et al. 2005).

Several research groups have looked at the dopamine transporter (DAT) with SPECT to evaluate its interactions with alcohol dependence, with overall heterogenous results. One study found that non-violent alcohol-dependent patients after detoxification showed a significantly reduced DAT density compared to controls. Violent alcohol-dependent patients after detoxification on the other hand did not differ significantly (Tiihonen, Kuikka

et al. 1995). Other studies found a significant reduction in striatal DAT density in alcohol-dependent patients (Repo, Kuikka et al. 1999), no significant difference in DAT density (Volkow, Wang et al. 1996) and a significant reduction in DAT density on admission that disappeared after detoxification (Laine, Ahonen et al. 1999). One study showed that DAT availability was significantly lower in the putamen in subjects that showed one particular allelic variation of a genetic polymorphism linked to alcohol-dependence, but that reduced DAT availability did not correlate with alcoholism (Heinz 2000).

Several studies have utilized molecular imaging techniques to directly analyze DA receptors, most notably D2/D3 receptors. Several post-mortem autoradiography studies found lower DA receptor availability in alcohol-dependent patients compared to controls, notably in the nucleus accumbens, amygdala, caudate, putamen and globus pallidus (Noble, Blum et al. 1991; Tupala, Hall et al. 2001; Tupala, Hall et al. 2003).

Clinical studies using SPECT and PET imaging techniques to determine differences in DA receptor availability between alcohol-dependent patients and controls have so far had inconsistent results. Four studies with [11C]raclopride PET found a significantly reduced striatal binding potential in the patient group compared to controls (Hietala, West et al. 1994; Volkow, Wang et al. 1996; Martinez, Gil et al. 2005; Volkow, Wang et al. 2007). This finding was supported for the putamen and nucleus accumbens by a [18F]fallypride PET study, which also found a correlation with the severity of craving (Heinz, Siessmeier et al. 2004). Another study with [11C]raclopride PET found a significantly lower D2 receptor availability in both the caudate and putamen in the first six weeks of detoxification, but only in the caudate in a second scan 1-4 months later (Volkow, Wang et al. 2002). Another study with a similar design using [18F]fallypride PET found a significantly reduced DA binding potential in day 1 of detoxification in the Thalamus, insular cortex, hippocampus and lateral temporal cortex, but only a nonsignificant trend towards lower BPND in all other selected ROIs (Rominger, Cumming et al. 2012). Here, no difference was observed between day 1 of admission and a second scan 7-14 days later. A third scan after one year showed a significant increase of BPND in the striatum, caudate, putamen and lateral temporal cortex.

Other studies did not find significant differences in DA receptor BP between alcohol-dependent patients and control subjects. One study using [123I]Epidepride SPECT found no significant difference between patients and controls (Repo, Kuikka et al. 1999). Neither did another study using [18F]fallypride PET (Spreckelmeyer, Paulzen et al. 2011). Another

study using [18F]fallypride PET found significant differences in extrastriatal ROIs but only a nonsignificant trend in striatal ROIs (Rominger, Cumming et al. 2012). One study using [123I]IBZM SPECT found no difference in striatal DA receptor availability between alcohol-dependent patients and controls, but found a significant difference in follow-up between relapsers and abstainers, with a higher receptor availability in early relapsers (Guardia, Catafau et al. 2000).

One clinical study used a different approach, using [11C]raclopride PET with two non-patient groups, with and without family history of alcohol dependence. Family-positive subjects had significantly higher D2 receptor availability in caudate and ventral striatum compared to family-negative subjects (Volkow, Wang et al. 2006).

Although the etiology of alcohol addiction and the role of dopamine in it are not yet fully understood, some effort has been made to interpret the existing literature. Originally dopamine was thought to act as a mediator for hedonic effects of alcohol, i.e., the 'liking' (Wise 1988). This effect is now attributed instead to the opioid system (Berridge 2009; Berridge, Robinson et al. 2009). In recent years there has been a shift towards dopamine mediating the 'wanting' rather than the 'liking' of addictive substances. It would thus be responsible primarily for motivation (Robinson 1993, Robinson and Berridge 2001). This hypothesis has been supported by observations of continued substance intake or craving in addicted subjects even in the absence of pleasure derived from this behavior (Heinz, Lober et al. 2003). Concerning the dopamine receptor status in alcohol-dependent patients, it has been proposed that the continued frequent intake of alcohol is accompanied by continuously raised dopamine levels, which in turn leads to a downregulation of dopamine receptors (Heinz, Beck et al. 2009).

1.4. Research questions and hypotheses

Despite the numerous studies concerning the etiology and neurobiology of alcohol dependence, there is still no model that can adequately explain why only a small fraction of alcohol consumers progress toward an alcohol use disorder. The same holds true for the role of the dopaminergic system in alcohol use disorders. Concerning dopamine receptor status, the existing literature presents quite a few studies, both preclinical and clinical, that point towards a link between alcohol-dependence and a reduced DA receptor density, markedly in striatal brain regions - yet other studies fail to show this link (see 1.3.2). This project aims to answer the question of whether there is a reduction in striatal

dopamine D2/D3-receptor density in detoxified alcohol-dependent patients. It is hypothesized that this reduction does exist.

A second question is: if there is indeed a reduced dopamine receptor density in detoxified alcohol-dependent patients, is this a result of chronic alcohol consumption, or is this a preexisting condition that might bring with it a vulnerability to addiction? The question is thus, whether adults with high risk drinking profiles, but no alcohol-dependence, also have reduced dopamine receptor densities compared to healthy adults with a low-risk drinking profile. It is hypothesized that this reduction exists but is less severe than in alcohol-dependent patients.

The existing studies concerning dopamine receptor densities in alcohol-dependent patients have had varying results, but this might at least in part be due to those studies having varying methodologies, especially concerning image analysis. So far there is no consensus regarding the most accurate image analysis methodology. It would be advantageous to first compare the different methodologies and to then perform the image analysis with the most accurate methodology. It is the aim of this research to find out which image analysis methodologies offer the most advantages for the given clinical research question.

In region of interest (ROI)-based image analysis, different techniques exist to define ROIs for PET imaging. The first and most obvious method is manual segmentation, but this requires highly trained operators and is very time consuming. Manual segmentation is also difficult to reproduce exactly. A different approach is to circumvent the segmentation of individual brain images altogether and instead transpose the individual images into a template space. That way, existing atlases for that template space can be used. One of the most common templates is the Linear ICBM Average Brain Stereotaxic Registration Model (ICBM152) (Mazziotta, Toga et al. 2001), often used in conjunction with the AAL atlas (Tzourio-Mazoyer, Landeau et al. 2002). Alternatively, there are automated processes for the segmentation of brain structures. One such process is FMRIB's Integrated Registration & Segmentation Tool (FIRST) (Patenaude, Smith et al. 2011). In this project both approaches, namely normalized images in ICBM-space in conjunction with AAL atlas as well as a FIRST segmentation of individual images, were used and compared. This project aims to find out whether one of the approaches yields more accurate data. It was hypothesized that the individual segmentation in subject space would yield more accurate results.

A main difficulty in any in-vivo molecular imaging approach is that it relies on indirect measurements. It is not possible to literally count receptors in living subjects, so in PET imaging, mathematical models are used to estimate tracer binding potentials as a measure for binding site densities. These mathematical models usually rely on the comparison of the time activity curve (TAC) in the chosen ROI to a reference TAC. The gold standard is to use the TAC of the subjects' blood as a reference. While this approach is better in terms of needing fewer assumptions, it also relies on frequent blood takings during image acquisition, which is burdensome for the subjects. Alternatively, mathematical models exist that use other brain tissues as reference. Several different such models exist, and it is not clear if they can all be used interchangeably. In this project, the following reference tissue methods were used and compared: simplified reference tissue model (SRTM); two-step SRTM with global k'_2 (SRTM2); and Logan's reference tissue method with and without k'_2 term. It was hypothesized that all four mathematical models can be used, while SRTM2 would yield the best effect size.

All reference tissue models rely on a reference tissue that is assumed to have no specific binding for the tracer. In dopamine receptor trials the most commonly used reference tissue is the cerebellum. There is some evidence, however, that the cerebellum shows some specific D2/D3 binding, at least for [11C]FLB457 (Vandehey, Moirano et al. 2010) and [125I]epidepride, while no specific binding was found in the white matter (Tupala, Hall et al. 2001). This project aimed to answer if white matter is a better reference tissue than the cerebellum for D2/D3-receptor studies using [18F]fallypride. It was hypothesized that white matter as a reference tissue would yield more reliable results.

2. Materials and Methods

2.1. Project

This research is part of a larger study environment called "Learning and Alcohol Dependence (LeAD)", which is a joint project of Technische Universität Dresden and Charité Universitätsmedizin Berlin that aims to uncover interactions between learning and alcohol dependence. More information on this project can be found on the official website: www.lead-studie.de. The project is supported by the Deutsche Forschungsgesellschaft (DFG) under the name "FOR 1617: Learning and Habitisation as Predictors of the Development and Maintenance of Alcoholism" and project number 186318919. More information can be found on the DFG website: http://gepris.dfg.de/gepris/projekt/186318919?language=en. The LeAD project is made up of several subprojects; this research is part of subproject 5 "Dysfunctional interaction of dopamine and glutamate as a predictor for the development of alcohol use disorders (AUD)".

All subjects gave written informed consent. The study was conducted in accordance with the latest version of the Declaration of Helsinki and was approved by the Ethics Committee of the Charité - Universitätsmedizin Berlin (reference number EA1/245/11) and the German Federal Office for Radiation Protection (BfS, reference number Z5-22463/2-2011-021).

2.2. Cohort

We included three groups of subjects: alcohol-dependent patients after detoxification and controls matched according to age, sex and education who were divided into two groups, low-risk alcohol consumption and high-risk alcohol consumption. Twenty patients were enrolled into the study as well as 19 subjects in each control group. The patient sample was recruited from a group of patients already enrolled in subproject 2 of the LeAD study. That project had enrolled its patients from consecutive admissions in Berlin. The control subjects were recruited by advertising.

Inclusion criteria:

- men and women aged 25-54 years
- alcohol dependence according to DSM-IV

- minimum of 72 hours of abstinence, maximum of 21 days of abstinence for inclusion into subproject 2, PET scans were possible after more than 21 days of abstinence

- minimum of three years of alcohol dependence

- low severity of withdrawal symptoms (CIWA<8)

- ability to provide fully informed consent and to use self-rating scales

Exclusion criteria:

- lifetime history of DSM-IV bipolar or psychotic disorder

- current threshold DSM-IV diagnosis of any of the following disorders: current major depressive disorder, generalized anxiety disorder, post-traumatic stress disorder, borderline personality disorder, or obsessive compulsive disorder

- history of substance dependence other than alcohol or nicotine dependence

- current substance use other than nicotine and alcohol as evinced by positive urine screening

- history of severe head trauma or other severe central neurological disorder (dementia, Parkinson's disease, multiple sclerosis)

- pregnancy or nursing infants (for females)

- any alcohol intake in the last 24 hours before enrollment into subproject 2 as well as before PET scans

- use of medications or drugs known to interact with the CNS within the last 10 days or at least four half-lives post last intake, with testing at least four half-lives post last intake, before enrollment into subproject 2 as well as before PET scans. The only exception was detoxification treatment with benzodiazepines or chlomethiazole.

All inclusion and exclusion criteria, except for the alcohol-specific criteria, applied to both groups of control subjects as well. High-risk alcohol consumption for the control group was defined by presence of at least one of these criteria while not fulfilling the criteria for DSM-IV diagnoses of alcohol dependence:

- DSM-IV diagnosis of abuse

- Consumption of at least nine drinks (105 g of alcohol) per week

- Binge drinking (at least five drinks at one occasion)

2.3. Positron emission tomography with [18F]fallypride
2.3.1. [18F]fallypride

(S)-N-[(1-allyl-2-pyrrolidinyl)methyl]-5-(3-[18F]fluoropropyl)-2,3-dimethoxybenzamide or [18F]fallypride is a dopamine D2/D3-receptor tracer that was first described in 1995 (Mukherjee, Yang et al. 1995).

The first study on [18F]fallypride in humans was published in 2002 and found the distribution consistent in all subjects and established a rank order of receptor concentrations for relevant brain regions (see Table 1). The mean test-retest error observed was around 10%, while the largest test-retest error for one region in one subject was 27%.

[18F]fallypride was chosen for this study as it is a high affinity radioligand that can be used to assess dopamine D2/D3-receptor levels in both striatal as well as extrastriatal regions (Mukherjee, Yang et al. 1999; Slifstein, Hwang et al. 2004).

Table 1. Brain regions with [18F]fallypride activity rank and mean BP

Brain region	Rank	mean BP
Putamen	1	27.22
Caudate	2	23.57
Ventral striatum	3	13.98
Pituitary	4	3.93
Thalamus	4	3.23
Amygdala	5	2.40
Colliculi	6	1.99
Substantia nigra	7	1.49
Inferior temp.	8	1.04
Middle temp.	8	0.79
Parietal cortex	9	0.44
Occipital cortex	9	0.29
Frontal cortex	9	0.25

[a] derived from (Mukherjee, Christian et al. 2002)

In terms of stability with subjects' age, it has been shown that [18F]fallypride BP decreases by 10% per decade during healthy aging (Mukherjee, Christian et al. 2002).

[18F]fallypride has been used successfully to research the effects of amphetamine challenge on striatal regions and the extrastriatal limbic system, yet it wasn't successful in measuring changes in cortical synaptic dopamine (Slifstein, Narendran et al. 2004; Mukherjee, Christian et al. 2005; Riccardi, Li et al. 2006; Cropley, Innis et al. 2008). It has also been used to show differences in D2/D3 dopamine receptor levels in schizophrenia

(Kegeles, Slifstein et al. 2010). [18F]fallypride showed lower striatal effect sizes compared to previous [11C]raclopride studies (Slifstein, Kegeles et al. 2010).

The tracer was produced locally by the in-house radiochemistry unit in the Department of Nuclear Medicine of the Charité.

2.3.2. Scanner

PET for quantitative characterization of the dopamine D2/D3-receptor status was performed using a time-of-flight PET/CT system, the Philips Gemini TF 16, with a spatial resolution of about 7 mm (Surti, Kuhn et al. 2007). PET images were reconstructed using the iterative LOR-RAMLA algorithm of the scanner software with default parameter settings for brain.

2.3.3. Protocol

Two hundred MBq of [18F]fallypride were injected intravenously over 30 s following a low-dose cranial CT (Slifstein et al. 2010). PET emission data was acquired in three successive blocks, with a break between each block. The first two patients were scanned with a protocol that started with 50 minutes scan time, followed by 30 minutes pause, 60 minutes scan time, 60 minutes pause and finally 40 minutes scan time (Slifstein, Kegeles et al. 2010). The complete scanning procedure including breaks spanned four hours, which was demanding for the subjects. It also blocked the PET scanner for more than four hours for each patient. After the first two subjects had been scanned, it was established that the mathematical model was robust enough to allow for a shorter first block and a longer break between blocks 2 and 3 (see Figure 2 for all protocols). This allowed for two patients to be scanned interleaved, which saved scanner time and was also less demanding for the subjects. A low-dose CT was performed before each block for attenuation correction of the emission data of the respective block (120 kV, 40 mAs). As subjects moved during breaks, a separate low-dose CT for each block was required to avoid artifacts due to spatial mismatch between CT and PET caused by incomplete repositioning. The radiation exposure associated with each low-dose CT was < 0.5 mSv effective dose. The effective dose by intravenous injection of 200 MBq of [18F]fallypride is 4.3 mSv.
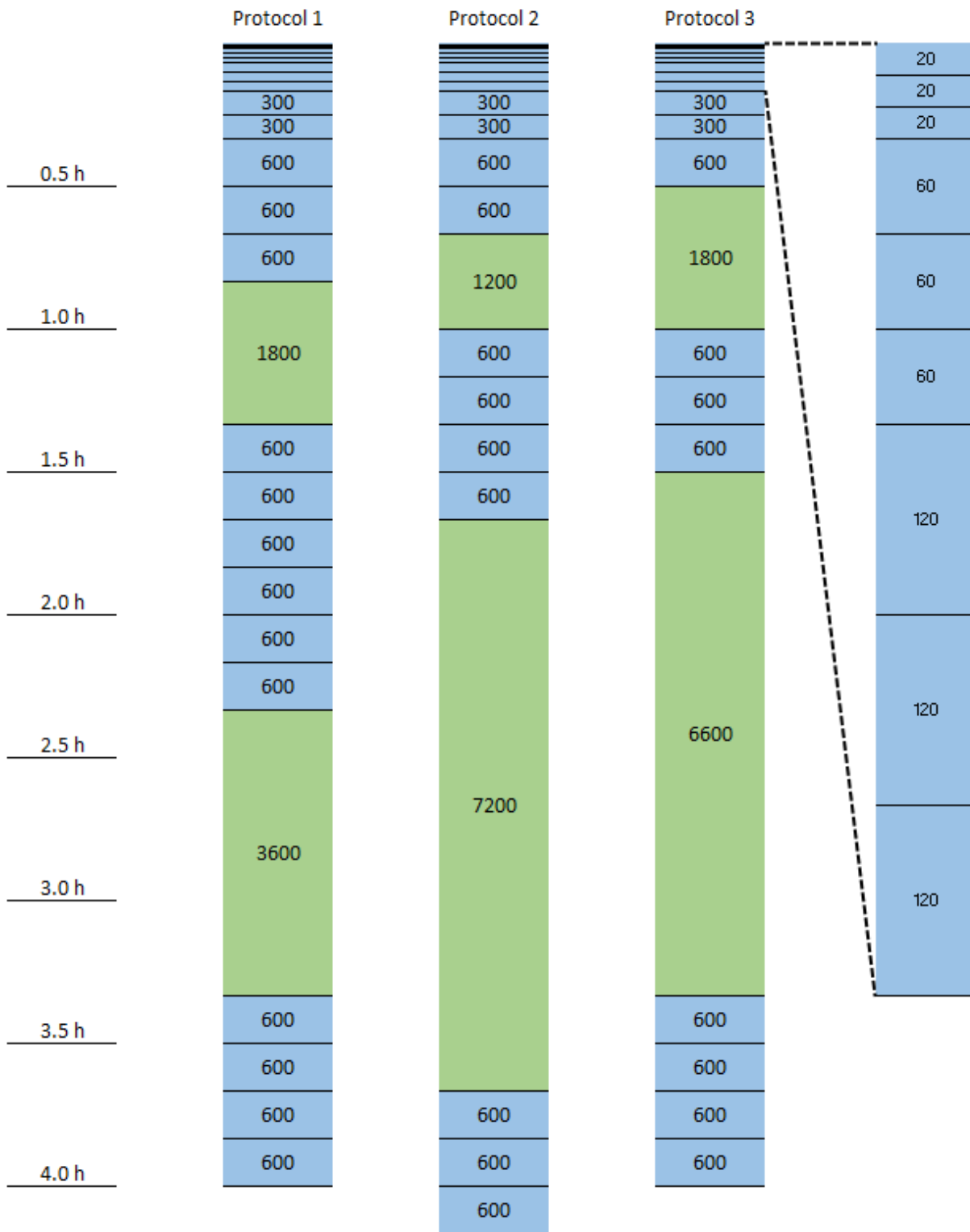
Figure 2: Overview of the three scanning protocols utilized for the PET scans. Each protocol consisted of three blocks with frames of varying lengths and a pause between each block of varying lengths, according to the protocol. The figure shows frames in blue and pauses in green; the boxes are proportional to the given duration. The duration of each frame or pause in seconds is labeled within each box. The column on the far right shows a magnified view of the first nine frames, which were identical in each protocol.

2.4. Computer-Assisted Image Analysis

In addition to PET imaging, all subjects underwent magnetic resonance imaging (MRI) in a 3-tesla scanner (Siemens TRIO). The resulting T1-weighted images were utilized in this study as anatomic reference images. Several steps were taken to prepare images for analysis (see Figure 3). The images derived from the PET scanner came as a collection of frames for each block with small motion artifacts due to movement during scanning blocks, and large spatial discrepancies between blocks due to patients getting up and lying down again. Furthermore, PET and MRI images were taken at different facilities with different spatial configurations.

In a first step, the images within each PET block were realigned to correct for motion artifacts within scanning blocks (see 2.4.1). Afterwards, the different image blocks were coregistered to one another to correct for spatial differences due to different positioning of the subject within the scanner for each block (see 2.4.2). As a result, all subjects' PET images were spatially aligned in subject PET space. For further analysis, the PET images were coregistered to the same subject's MRI (see 2.4.2). This resulted in PET being spatially aligned in MRI subject space, which enabled the reuse of MRI ROIs and MRI transformation information on PET images.

Several analyses required the use of brain anatomical information derived by other study groups, which are aligned to a common standard space. Throughout this study all analyses using standard space refer to the space described by the Montreal Neurological Institute (MNI) and are referenced as MNI space. The subjects' MRI images were transformed into MNI space (see 2.4.3) and the resulting transformation information was reused to transform the subjects' PET images into MNI space. As a result, both MRI and PET images were available in MNI space.

The two sets of commonly aligned PET and MRI images, in subject as well as MNI space, were used as a basis for all analyses. The steps taken for the analyses of these images are described in 2.4.4.
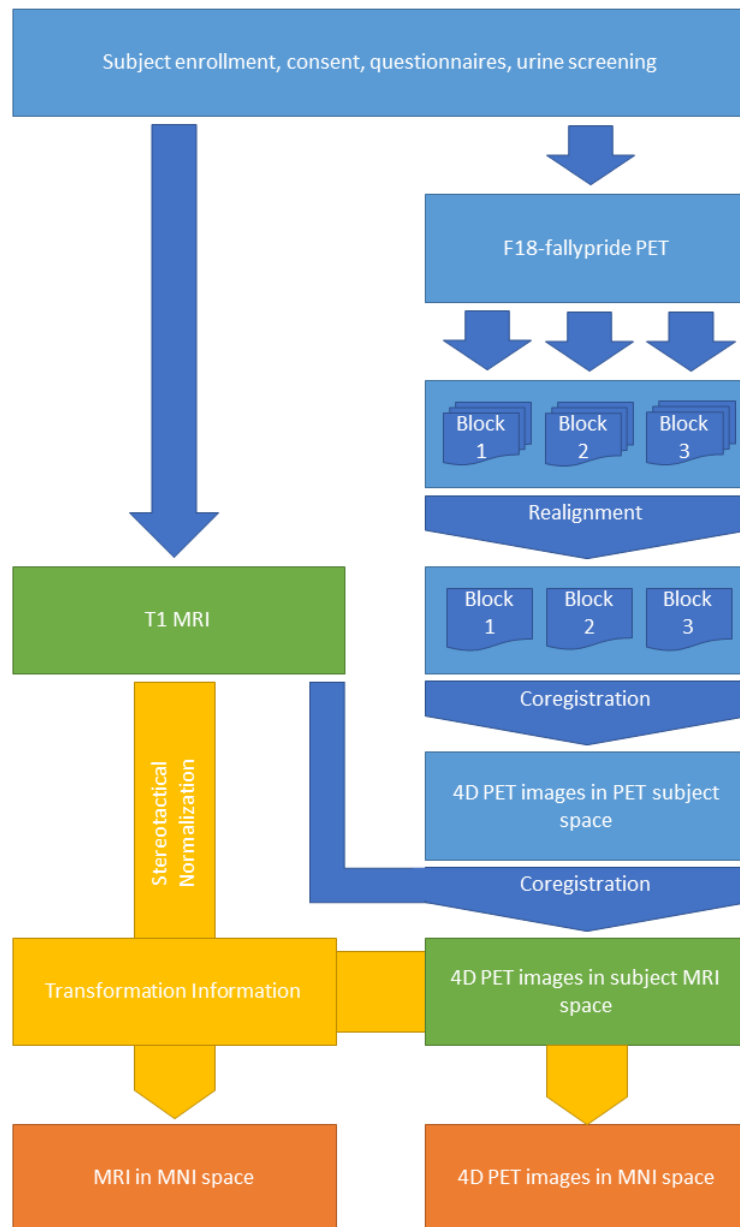
Figure 3. Flow chart of steps taken for image acquisition and preparation.

2.4.1. Realignment

All PET studies require subjects to lie still in the scanner during the image acquisition process, yet absolute rigidity is never achieved. Any movement of the subject can diminish the accuracy of image analysis (Herzog, Tellmann et al. 2005). Two mechanisms are mainly responsible for motion artifacts. Firstly, when using a mask to identify a ROI for the complete image series, movement artifacts may lead to regions (partially) shifting into or out of a ROI mask, and thus a misrepresentation between mask and brain and resulting inaccuracies in parametric estimations. Secondly, movement may lead to errors during attenuation and scatter correction. Realigning PET frames with the use of

coregistration algorithms has been shown to decrease the impact of motion artifacts on the accuracy of image analysis (Costes, Dagher et al. 2009).

To correct for motion artifacts during the scanning session, frames were automatically realigned within each block using the function spm_realign from spm8. In block 1 frame 6 was selected as the reference frame. In blocks 2 and 3 frames were realigned using the first frame as reference frame. Realignment settings for spm_realign were left at their default values.

No correction was performed for errors of attenuation and scatter correction. It is also not possible with this approach to correct for movement during a frame. It is unclear whether or not these residual motion errors lead only to statistical errors or whether they can potentially invalidate the outcome (Herzog, Tellmann et al. 2005).

Since realignment cannot correct for all motion errors, it is important to monitor the extent of the subject's movements. For this goal, realignment parameters for each frame were saved for each subject as three degrees of translation in mm and three degrees of rotation in degrees. A maximum voxel offset in mm was estimated from the degrees of rotation (see Equation (1)), with α being the degree of rotation and r being 100mm for a spherical approximation of the subject's brain.

$$offset = 2\pi r \frac{\alpha}{360°} \tag{1}$$

Realignment data was analyzed for each subject.

2.4.2. Coregistration

After realignment, coregistration was performed to move all PET and MRI images of a single subject into a single subject space. For this, all frames of the first block starting with frame 6 were used to create a static PET for coregistration with blocks 2 and 3 with the help of the spm8 function spm_reslice. The same procedure was used to create mean images over all frames from blocks 2 and 3. Using the spm8 function spm_coreg, the mean images of blocks 1 and 2, and of blocks 1 and 3 were coregistered. The respective coregistration matrices were used to coregister each frame of blocks 2 and 3 with block 1.

Frames 6 and 7 of the first block were used to create a perfusion PET with the help of the spm8 function spm_reslice. This perfusion image was taken as a source for coregistration with the subjects' T1-weighted MRI using spm_coreg. The resulting coregistration matrix

was used to coregister all realigned frames of block 1 and all frames from blocks 2 and 3 which were already realigned and coregistered to block 1. The resulting images, now in subjects' MRI space were resliced using spm_reslice and stored for use with individual ROIs.

2.4.3. Spatial normalization

Spatial normalization was performed to transform subjects' MRI and PET images into MNI standard space. The Linear ICBM Average Brain (ICBM152) Stereotaxic Registration Model (Mazziotta, Toga et al. 1995; Mazziotta, Toga et al. 2001; Mazziotta, Toga et al. 2001) was used as the target. They conform to the space described by the ICBM, NIH P-20 project, and approximate that of the space described in the 1988 atlas of Talairach and Tournoux (Talairach and Tournoux 1988; Ashburner, Barnes et al. 2008).

Spatial normalization was performed using the clinical_mrnormseg function from the clinical toolbox for SPM. This provides good performance with images of good spatial resolution and tissue contrast, such as the subjects' T1-weighted MRIs. The function is based on the unified segmentation normalization included in SPM8 (Brett, Leff et al. 2001; Ashburner and Friston 2005; Andersen, Rapcsak et al. 2010). Voxel size was set to 2mm and subjects' T1-weighted MRIs were selected as source images. Young healthy adults were selected as the target space.

The resulting transformation information for the transformation of the subjects' MRIs into MNI space was then used to transform all PET frames into MNI space with the help of the SPM8 function spm_write_sn.

2.4.4. ROI-based binding potential estimation

The clinical research question of this study is aimed at finding group differences in dopamine receptor status in different regions of interest (ROIs) of the brain. For this purpose, the non-displaceable binding potential (BP_{ND}) was estimated using different reference tissue models for tracer kinetic modelling (see 2.4.4.3) (Innis, Cunningham et al. 2007). These models use time activity curves (TACs) of both a ROI and a reference tissue to generate BP_{ND} estimates. The TACs are generated by masking 4D PET images and by calculating the average activity within the mask (see 2.4.4.2). Masks for ROIs and reference regions are generated using different ROI identification methods, either using standard atlases or by generating the mask from subjects' images (see 2.4.4.1). Different tissues were used as reference tissues (see 2.4.4.4). Figure 4 illustrates the different steps necessary for ROI-based binding potential estimation.
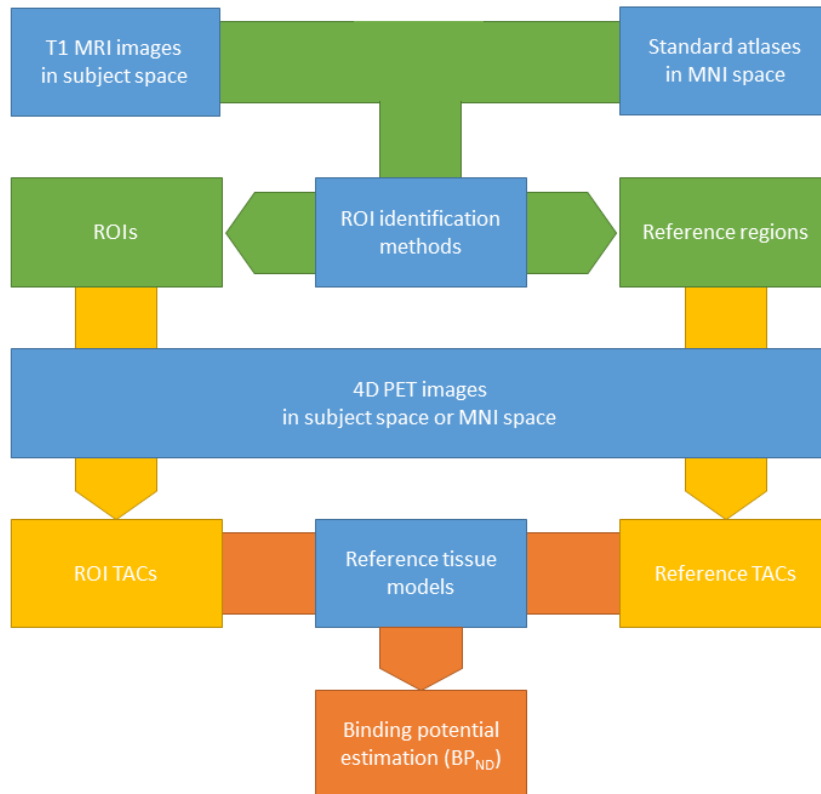
Figure 4. Flow chart of image analysis steps for binding potential estimation.

2.4.4.1.   Regions of Interest

Two different strategies for the identification of ROIs were utilized and compared. Firstly, standard atlases in MNI space were used in conjunction with normalized PET and MRI images. Secondly, individual regions of interest were identified for each subject with the FSL FIRST segmentation tool, and used in conjunction with MRI and PET images in subject space.

WFU_pickatlas (Maldjian, Laurienti et al. 2003; Maldjian, Laurienti et al. 2004) and its included AAL atlas (Tzourio-Mazoyer, Landeau et al. 2002) and IBASPM116 atlas (Alemán-Gómez Y. 2006) were used as standard atlases. From the AAL atlas, the left and right hemispherical representations for the amygdala, anterior part of the cingulate gyrus, caudate, inferior temporal gyrus, middle temporal gyrus, orbital frontal lobe, putamen, thalamus and insula, as well as the cerebellum were used. From IBASPM116, the hippocampus (left & right) was used.

The individual segmentations were performed with the FSL FIRST segmentation tool on each subject's MRI (Smith, Jenkinson et al. 2004; Woolrich, Jbabdi et al. 2009;, Patenaude, Smith et al. 2011; Jenkinson, Beckmann et al. 2012). The following areas were selected: putamen (l&r), caudate (l&r), accumbens (l&r), pallidum (l&r), thalamus

(l&r), hippocampus (l&r), amygdala (l&r) and brainstem. A voxel mask was created for each subject for the entire FSL segmentation, and the individual ROIs were separated by different mask values.

To systematically check the individual segmentations for errors, a procedure was written to allow the creation of axial slice images for visual confirmation of correct segmentation. The function spm_orthviews was used to create a three-dimensional TrueColor overlay of the FSL map over the subject's MRI. A custom colormap was created and fitted to the FSL map to allow for easily distinguishable ROIs. Axial slice images were created by automatically determining the highest and lowest axial slice within the FSL segmentation map that still included segmentation data. Slices were then created, each 4mm between these min and max values. The figures were conjoined in an ascending order and saved as high-quality images using the export_fig package. The resulting summary images (see Figure 5) were then assessed visually for each subject.
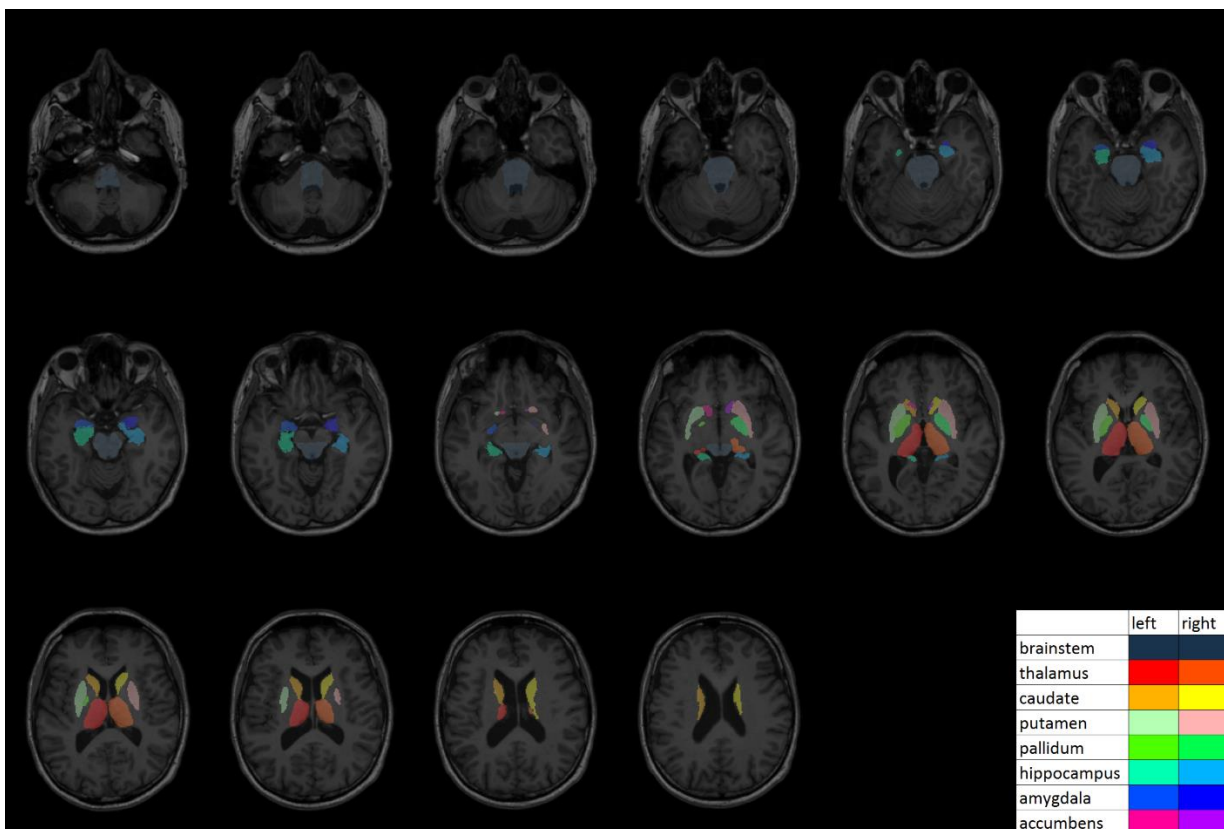
Figure 5: Example axial slices with TrueColor overlay of FSL segmentation.The image is in neurological convention, i.e., the left side of the patient is on the left side of the image.

2.4.4.2. Generating time activity curves

Time activity curves were generated by calculating the mean activity within the selected ROI for each frame. A mask was created from the selected atlases by a logical operation

that checked whether the voxel within that image belonged to the selected ROI-value. A temporary calculation image was created and written for this mask. For each frame, the voxels of the mask and the frame were being multiplied one by one, so that in the resulting image every voxel that was included in the mask had the activity value of the original frame and all other voxels were set to zero. All values were extracted that were larger than zero and the mean was calculated over these values. This represented the mean activity in the current frame within the selected ROI.

ROIs of FSL segmentation were used in conjunction with PET images in subject MRI-space, while ROIs of different atlases were used in conjunction with PET images in MNI space. Time activity curves of all ROIs were plotted and checked visually. An example is shown in Figure 6, while an example time-lapse series of PET activity is shown in Figure 7.
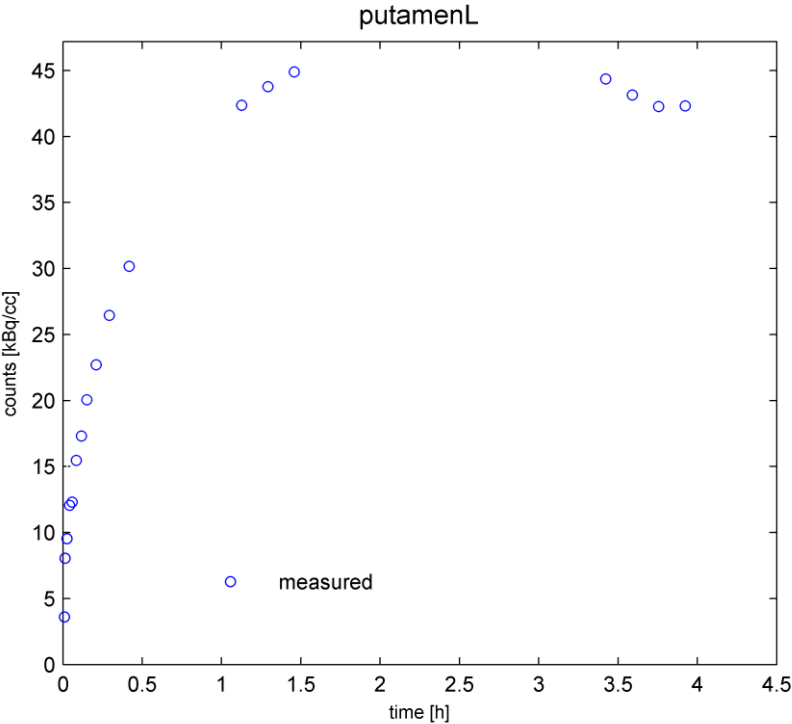
Figure 6: Example time activity curve for FSL ROI of left putamen.
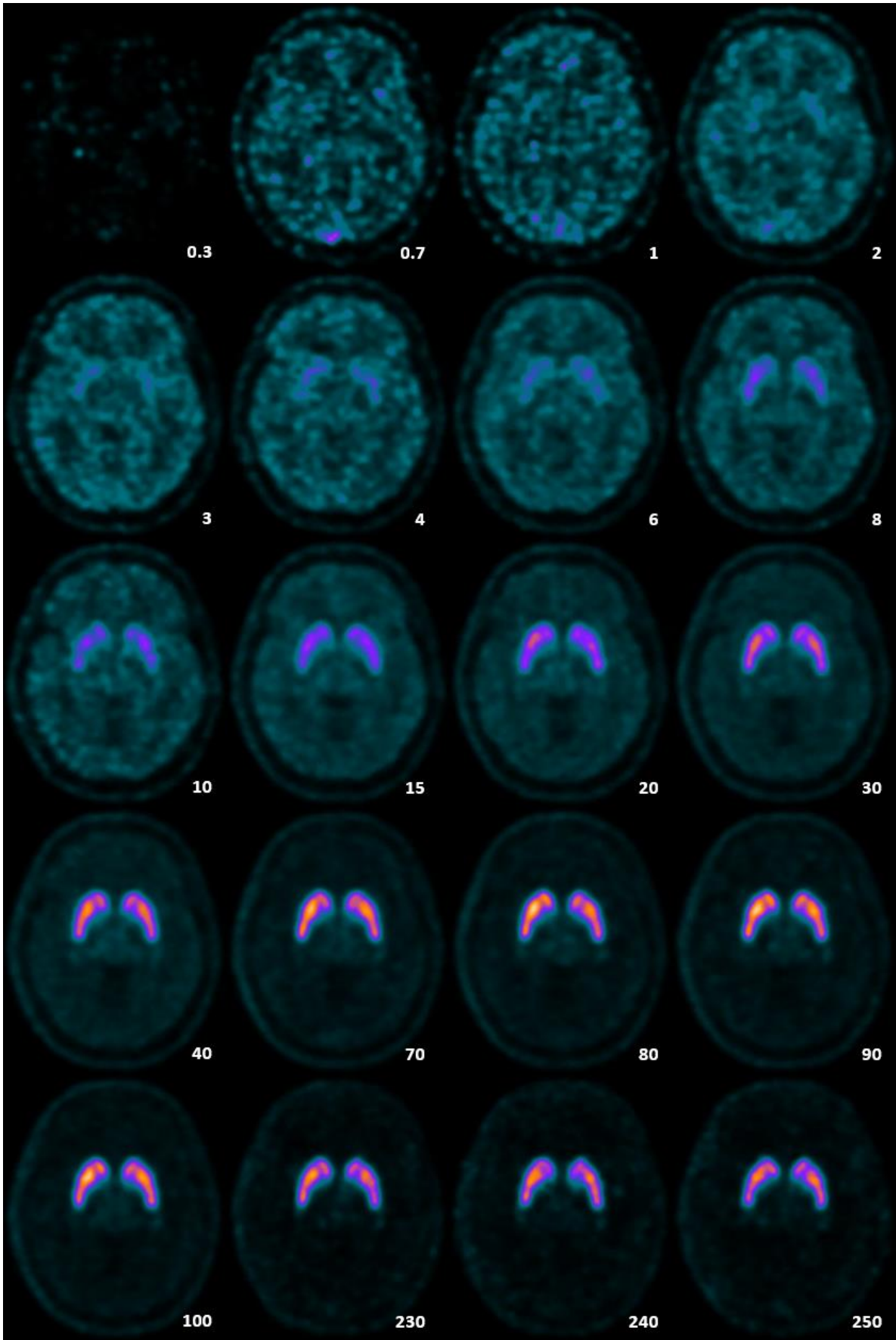
Figure 7. Example PET activity over time. Time in minutes after tracer application shown in lower right corner of each frame.

2.4.4.3.   Tracer kinetic modelling

The least complicated way to compare PET activity in different subjects or groups of subjects would be the comparison of single static PET images. This technique requires neither blood sampling nor a very time-consuming dynamic image acquisition. However, due to inherent biases and variability, this method is not sensitive enough for many research questions (Hoekstra, Paglianiti et al. 2000). Tracer kinetic modelling aims to fill this gap. The term describes several techniques that, by building mathematical dynamic models, try to differentiate the different states the tracer can be in (e.g. free in plasma, free in tissue, specifically bound, non-specifically bound), and how these states superimpose and make up the radioactivity detected by the scanner. Carson (2005), as well as Morris, Endres et al. (2004) have written extensive explanations and comparisons of tracer kinetic modelling techniques.

The different states that the radioligand can be in are commonly referred to as compartments. Figure 8 shows a basic three-compartment (two-tissue-compartment) model that describes the radioligand being in three different compartments: plasma, free or bound. In combination with different rate constants that describe the transition between compartments, a mathematical model for the concentrations over time can be written (see Equations (2) and (3)).
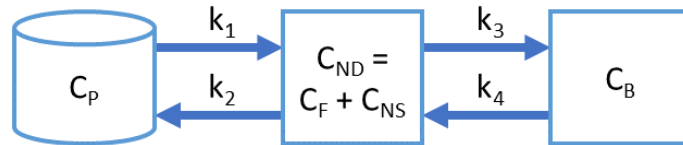
Figure 8. Example three-compartment (two-tissue-compartment) model. The radioactivity concentration of radioligand in plasma (C_P), the radioactivity concentration of non-displaceable radioligand ($C_{ND} = C_F + C_{NS}$ = free + nonspecifically bound), and that of radioligand specifically bound to receptors (C_B) and the first order rate constants k_1, k_2, k_3, and k_4. Adapted from Farde, Eriksson et al. (1989).

$$\frac{dC_{ND}}{dt} = k_1 C_P - k_2 C_{ND} - k_3 C_{ND} + k_4 C_B \tag{2}$$

$$\frac{dC_B}{dt} = k_3 C_{ND} - k_4 C_B \tag{3}$$

Each compartment model relies on assumptions about tracer dynamics in the different compartments and between compartments. These assumptions must be met at least approximately for a given model to be applicable. Originally, tracer dynamic modelling

most often used repeated invasive measurements of the arterial plasma concentration of the radioligand to supply a measured input function for the model and to thus reduce the estimated parameters. This is still considered to be the gold standard in tracer kinetic modelling. Unfortunately, measuring the arterial plasma function is highly burdensome for subjects and has other practical disadvantages as well.

As an alternative to tracer kinetic models with arterial input function, reference tissue models have been developed. These models rely on the comparison of the ROI to a reference region that is assumed not to have any specific binding for the radioligand. A reference region that complies with that assumption can be described with a much simpler compartment model (see Figure 9), and thus some of the parameters can be solved and enable the solution of the full model. Reference region models, though still relying on time-consuming dynamic PET imaging, are typically the optimal choice between optimizing for simplicity or accuracy (Morris, Endres et al. 2004).
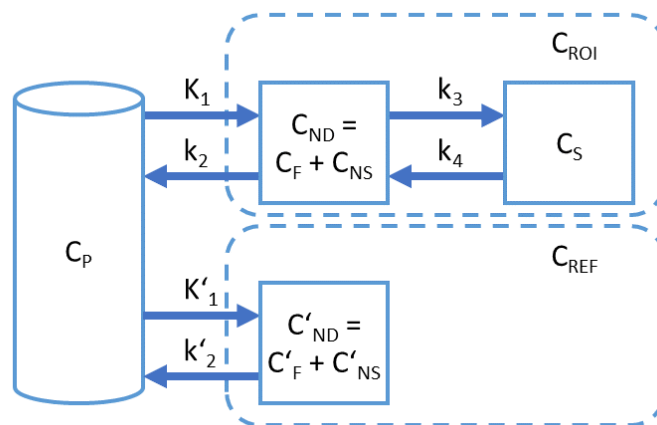
Figure 9. The original (full) reference tissue compartment model. It includes the compartments plasma (C_P), non-displaceable (= free + non-specifically bound) ($C_{ND} = C_F + C_{NS}$) and specifically bound (C_s), and the rate constants K_1, k_2, k_3 and k_4 for the ROI and K'_1 and k'_2 for the reference tissue. Adapted from (Oikonen 2018).

The first reference tissue method utilized in this study is the simplified reference tissue model (SRTM) that was proposed by Lammertsma and Hume (1996). They established that it is possible to reduce the original four-parameter model to a three-parameter model and still derive the same BP_{ND} values. SRTM has been shown to be a viable model for [18F]fallypride (Vernaleken, Peters et al. 2011).

When using SRTM for different ROIs in the same subject, a logical inconsistency arises. Because calculations are usually performed separately for each ROI, a different rate constant k'_2 is estimated for each ROI. As k'_2 is the rate constant for the transition of

radioligand from the reference compartment to the plasma compartment, it should be independent of the ROI analyzed. It was later shown that the coupling of k'$_2$ to a common value across brain regions reduces the variance of BP$_{ND}$ estimates and can thus lead to more sensitivity for between-group differences in BP$_{ND}$ (Endres, Hammoud et al. 2011). This method was included in this study and is referred to as SRTM2. Bilateral putamen and caudate ROIs were selected as receptor-rich areas for the calculation of the global k'$_2$.

A different method for tracer kinetic modelling was proposed by Logan, Fowler et al. (1996). The method exists in two variants, with and without a global k'$_2$ term. The two variants will be referred to as Logan and Logan2 in this study, for the variant with and without a global k'$_2$ term, respectively. Where a global k'$_2$ term was used, it was generated using the SRTM2 method with receptor-rich TACs (i.e., putamen and caudate). The Logan method does not originally have BP$_{ND}$ as the result parameter but results in a distribution volume ratio (DVR) between tissue and a reference tissue. However, this can easily be converted into a BP$_{ND}$ value (see equations (4) and (5)).

$$DVR = \frac{V_T}{V_{ND}} \tag{4}$$

$$BP_{ND} = \frac{V_S}{V_{ND}} = \frac{V_T - V_{ND}}{V_{ND}} = \frac{V_T}{V_{ND}} - 1 = DVR - 1 \tag{5}$$

As a quality control measure, TACs with the associated model fits were plotted and checked visually for all subjects (see Figure 10).

One important quality metric of tracer kinetic modelling is the fit of the model to the observed data. While searching for an optimal fit to the model with the MATLAB function fminsearch, the function also returns a function value which is the residual sum of squares (rss). This rss was divided by an estimation of the area under the curve of the time activity curve that was used as a basis for the model. In this way, a comparable measure was created, i.e., rrss = relative residual sum of squares.

All modelling was performed with custom software written for this project using MATLAB.
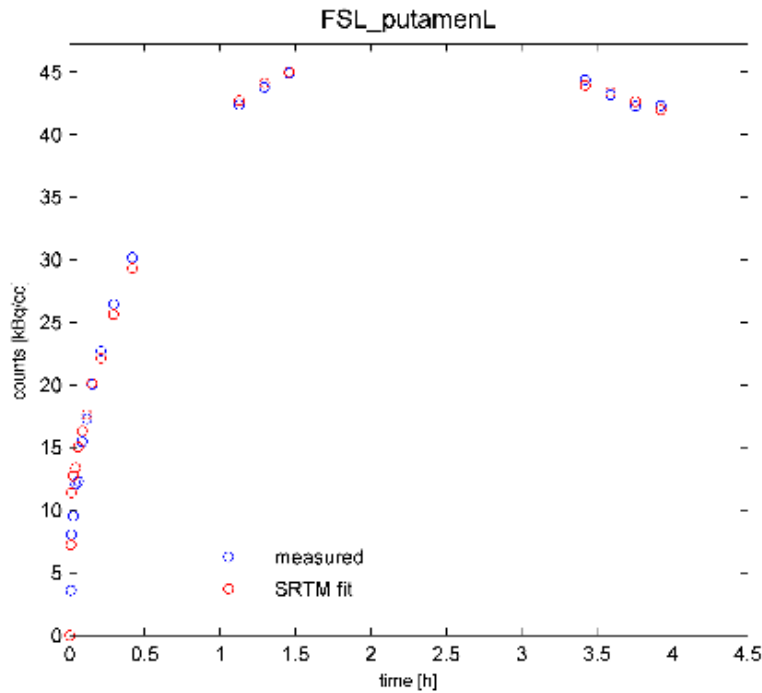
Figure 10: Example time activity curve for FSL ROI of left putamen (blue) with the respective SRTM fit (red).

2.4.4.4. Reference tissues

Without the use of invasive measurements of arterial plasma concentrations, tracer kinetic modelling for PET receptor studies relies on the use of a reference tissue that is assumed not to have any specific binding of the radioligand. For SRTM, the reference tissue must fit the two-compartmental model (= one-tissue compartmental model) at least reasonably well (Oikonen 2018). The clear majority of PET studies using dopamine receptor agonists such as [11C]raclopride or [18F]fallypride have used the cerebellum as reference tissue.

At the same time, there is some evidence that the cerebellum may not fulfill all requirements for a reference tissue. A post-mortem autoradiographic study on alcoholics found a detectable quantity of binding for the D2/D3 receptor ligand [125I]epidepride in the cerebellum, while not finding any binding or accumulation in the white matter (Tupala, Hall et al. 2001). Another study was able to show specific D(2)/D(3) binding in the cerebellum for [11C]FLB457 but not [18F]fallypride (Vandehey, Moirano et al. 2010). In a different study, the cerebellum TACs of [11C]raclopride imaging were fitted to both a two-compartment model (one-tissue compartment model) and a three-compartment model (two-tissue compartment model). Here, the three-compartment model offered the better fit (Farde, Eriksson et al. 1989). Despite these violations of reference region

requirements, it has been shown that the SRTM in conjunction with the cerebellum as reference tissue retains its sensitivity for detecting changes in BP, at least for [^{11}C]raclopride in humans (Lammertsma and Hume 1996).

Taking this evidence into account, it was decided to use the cerebellum as reference tissue, as well as two different white matter reference tissues. The mask for the cerebellum reference region (without vermis) was taken from the WFU_pickatlas, specifically the AAL atlas. It fits the MNI space and was thus used in conjunction with the normalized PET images. An example fit of the cerebellum ROI can be seen in Figure 11.

The first white matter reference tissue used was the superior longitudinal fasciculus (SLF). The corresponding ROI was taken from DTI-based fasciculi ROIs: Superior_longitudinal_fasciculus_L + Superior_longitudinal_fasciculus_R (Mori, Wakana et al. 2005; Wakana, Caprihan et al. 2007; Hua, Zhang et al. 2008). Both left and right SLF were taken together as a reference mask, and as they are in MNI space they were used in conjunction with the normalized PET images. An example fit of the SLF ROI can be seen in Figure 11.
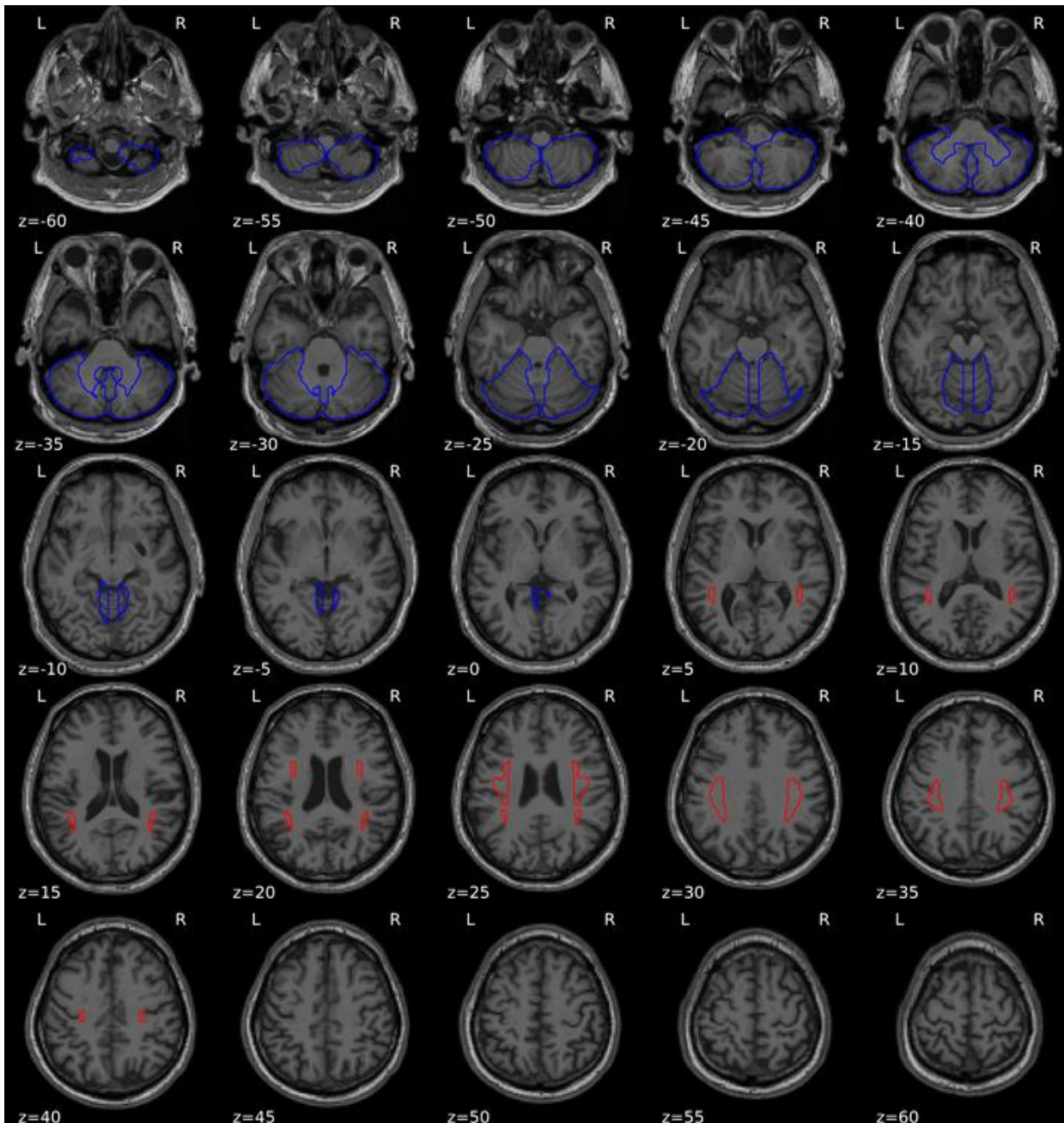
Figure 11. Example patient's normalized MRI with contours of cerebellum ROI (blue) and superior longitudinal fasciculus (SLF) ROI (red).

A second white matter reference mask was created using the clinical_mrnormseg function from the clinical toolbox for SPM8. This function creates a white matter mask from the subjects' T1-weighted MRIs. The created masks were probability masks with the voxel values representing the probability of the voxel being white matter. This was edited so that only voxels with a probability higher than 99.9% were included. An example fit of the total white matter mask can be seen in Figure 12.
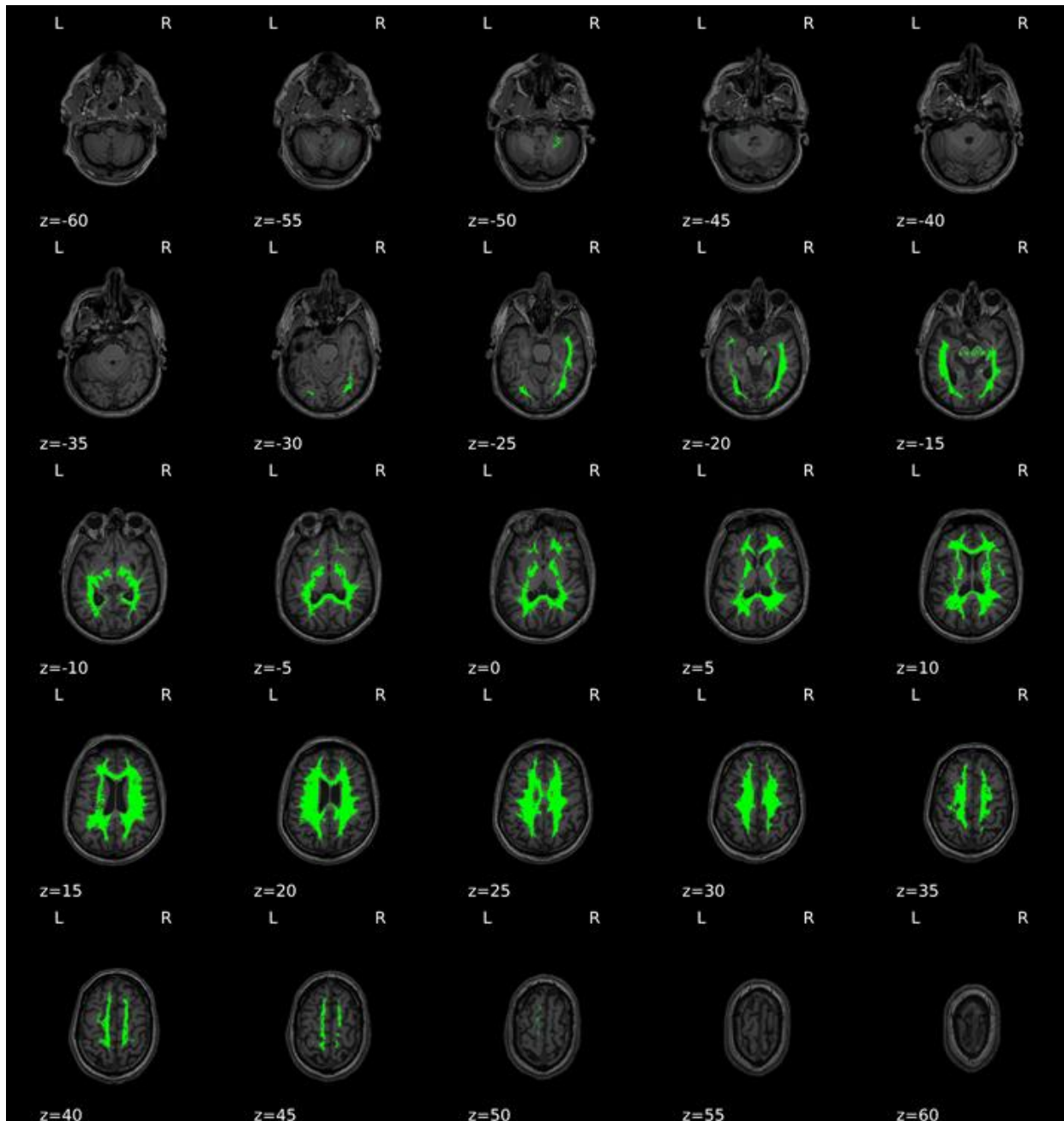
Figure 12. Example patient's MRI in neurological imaging convention with green overlay of generated 99.9% probability white matter mask.

2.5. Comparison of methods
2.5.1. Comparing reference regions

2.5.1.1.   Comparing coefficients of variation in reference regions

The homogeneity of voxel intensity in reference regions was compared by calculating the coefficient of variation within the reference regions' masks. The cerebellum and SLF were analyzed in conjunction with normalized subjects' MRIs and PETs in template/MNI space. The white matter mask was analyzed in conjunction with MRIs and PETs coregistered to the MRI in subject space. A single PET frame near the peak of the activity curve across

regions of interest (frame 2 of block 2) was selected for this comparison, as well as for the comparison of ROI identification techniques (see 2.5.2.1).

Coefficients of variation (see 2.8.2) within reference regions were calculated using the same steps as in 2.4.4.2 to extract all voxels within the reference region's mask. Coefficients of variation were calculated both for MRI intensities within reference region masks, as well as PET activity within reference region masks. Coefficients of variation for MRI intensities were used as a measure of anatomic homogeneity of the reference region, i.e., both SLF and white matter masks should have high homogeneity, and thus low coefficients of variation, being purely white matter regions. The cerebellum was anticipated to have higher coefficients of variation across subjects as it is a less homogenous tissue. High coefficients of variation could also point to areas of cerebrospinal fluid or other adjacent areas of the brain being erroneously included in the reference mask.

Coefficients of variation for PET activity within a reference region should ideally be very low, as this would be the case for a region with homogenous blood supply and no specific binding of the tracer. High coefficients of variation could be caused by areas of cerebrospinal fluid being included in the reference mask, which would add areas with activity lower than that of the theoretical unbound tissue compartment. Another possible reason for elevated coefficients of variation is spill-in by adjacent brain regions with high receptor availability, and thus high activity due to the limited spatial resolution of PET imaging.

2.5.1.2.   Comparing time activity curves of reference regions

Reference time activity ratio curves were created by dividing the time activity curve of one reference region by another reference region. In order to account for different measurement times due to differing protocols and varying breaks between image blocks (see 2.3.3), values were interpolated using a common minimum protocol for all subjects. To achieve this, the curves were linearized using the MATLAB function interp1 in linear mode and values for the common protocol were interpolated. Reference activity ratios were calculated for the following times: 40 s, 1 min, 2 min, 3 min, 4 min, 6 min, 8 min, 10 min, 15 min, 20 min, 30 min, 65 min, 75 min, 85 min, 203 min 20 s, 213 min 20 s and 223 min 20 s. Three curves were generated for each subject:

$$R_{c/SLF} = \frac{A_{cerebellum}}{A_{SLF}}$$

$$R_{c/wm} = \frac{A_{cerebellum}}{A_{white\ matter}}$$

$$R_{wm/SLF} = \frac{A_{white\ matter}}{A_{SLF}}$$

A higher ratio at the beginning of the curve might point toward spill-in by activity within blood vessels, a better perfusion or quicker tracer transport in that reference tissue, which should also be represented in lower R1 values (R1 = k_1/k'_1) in tissues compared to this reference tissue. A higher ratio in later stages of the curve might point toward activity of specific binding either in the reference region directly, or by spill-in of nearby areas with specific binding due to the limited special resolution of PET imaging. While differences in perfusion and tracer transport are represented in the mathematical model for the calculation of binding potentials, all mathematical models rely on the assumption that the reference region shows no specific binding (see 2.4.4.4).

Analysis was performed on the time activity ratio curves to check for group differences.

2.5.1.3. Comparing quality of fits of SRTM2

One important quality metric of tracer kinetic modelling is the fit of the model to the observed data. The relative residual sum of squares (rrss) (see 2.4.4.3) was used as a comparable measure for the fit of the model to the observed data. This measure was generated for all subjects on all FSL regions, with all three reference regions as reference regions and with SRTM2 as the mathematical model. A lower rrss stands for a better fit of the model to the observed data. In theory, a reference region that shows a smaller rrss fits the model better, which is a desirable outcome.

The analysis was performed both on the complete population and separately for the three subject groups.

2.5.1.4. Comparing coefficients of variation in result parameters

As the primary outcome for the clinical hypothesis is binding potential as a measure for receptor availability, it is of interest to determine which reference region would yield more stable BP values. To assess this, COVs (see 2.8.2) were calculated for BP values generated with the different reference regions. This analysis was performed on a per group basis. BPs of FSL ROIs of all subjects were calculated using SRTM2 and each of the three reference tissues. The BPs of the left and right hemispherical representations of each ROI were averaged. SPSS was used for each ROI and reference tissue to

calculate means and standard deviations for each group. COVs were calculated using these values and a variant of Levene's test was used as a statistical test (see 2.8.2).

2.5.2. Comparing ROI identification techniques

Two different techniques for the identification of ROIs were used and compared (see 2.4.4.1). It was hypothesized that the FSL segmentation in the subjects' MRIs would offer a superior fit to the real anatomical structures in comparison to standard atlases on normalized MRIs in template/MNI space. Five different areas were available in both the FSL segmentation and the AAL atlas: putamen, caudate, thalamus, amygdala and hippocampus. These areas were compared directly between the two atlases.

2.5.2.1.   *Comparing coefficients of variation of voxel intensity in selected regions of interest*

The homogeneity of regions of interest was compared between the two segmentation methods by calculating the coefficient of variation within the ROIs. ROIs taken from the AAL were analyzed in conjunction with normalized subjects' MRIs and PETs in template/MNI space. ROIs from the FSL segmentation were analyzed in conjunction with MRIs and PETs coregistered to MRI in subject space. A single PET frame near the peak of the activity curve across regions of interest (frame 2 of block 2) was selected for this comparison, as well as for the comparison of reference regions (see 2.5.1.1).

COVs within ROIs were calculated using the same steps as in 2.4.4.2 to extract all voxels within the ROI. COVs were calculated both for MRI intensities as well as PET activity. COVs for MRI intensities were used as a measure of the anatomic homogeneity of the ROI. High coefficients of variation could point to areas of cerebrospinal fluid or white matter being erroneously included in the ROI mask.

Coefficients of variation for PET activity were analyzed to see if the differences in the anatomic fit would have an influence on the PET analysis as well. High coefficients of variation for PET activity could be caused by areas of cerebrospinal fluid being included in the ROI mask, which would add areas with activity lower than that of the ROI, or by adjacent areas with higher receptor availability being included in the ROI mask, which would add areas with higher activity than that of the ROI.

2.5.2.2.   *Comparing quality of fits of SRTM2*

One important quality metric of tracer kinetic modelling is the fit of the model to the observed data. The relative residual sum of squares (rrss) (see 2.4.4.3) was used as a

comparable measure for the fit of the model to the observed data. This measure was generated for all subjects on all FSL and AAL regions, with SLF as reference region and SRTM2 as the mathematical model. A lower rrss stands for a better fit of the model to the observed data. The analysis was performed both on the complete population and separately for the three subject groups.

2.5.2.3.   *Comparing coefficients of variation in result parameters*

As the primary outcome for the clinical hypothesis is binding potential as a measure for receptor availability, it is of interest to determine which segmentation method would yield more stable BP values. To assess this, COVs were calculated for BP values generated for AAL and FSL ROIs. This analysis was performed both on the total population and on a per group basis to see if the coefficients of variation favor either segmentation method in general or whether there is a group bias involved. A variant of Levene's test was used to test for significant between-method differences (see 2.8.2).

2.5.3. Comparing reference tissue models

As the primary outcome for the clinical hypothesis is binding potential as a measure for receptor availability, it is of interest to determine which reference tissue model would yield more stable BP_{ND} values. To assess this, COVs were calculated for BP_{ND} values generated with the different reference tissue models. This analysis was performed on a per group basis. BP_{ND} values of FSL ROIs of all subjects were calculated using SLF as a reference tissue and each of the four reference tissue models. The BP_{ND} values of the left and right hemispherical representations of each ROI were averaged. SPSS was used for each ROI and reference tissue model to calculate means and standard deviations for each group. COVs were calculated using these values and a variant of Levene's test was used to test for significant between-method differences (see 2.8.2).

2.6.   Methods for the clinical research question

The combination of methods to use for the analysis of the clinical research question, i.e., of whether there are group differences in BP_{ND}, was to be dependent on the result of the comparison of methods. After analysis of the comparison of methodologies, it was decided to calculate BP_{ND} values for the clinical research question with SRTM2, using SLF as reference tissue on FSL ROIs. Group differences were analyzed by use of one-way ANOVA and post-hoc tests with Scheffé's method.

2.7. Influence of image analysis methodologies on clinical results

After having compared the different methodologies and having chosen a combination of methodologies, it was of interest to see whether the choice of methodology had an impact on the research question at hand. For this analysis, the putamen was chosen as ROI and BP_{ND} values were estimated for the putamen for all 24 combinations of ROI identification method, reference tissue and reference tissue model. For each of the 24 combinations, box plots for the three groups were plotted, and a one-way ANOVA was performed for each combination to see if different combinations of methods would yield different answers to the clinical research question.

2.8. Statistical tests
2.8.1. Use of common statistical tests

Common statistical tests were used to check for significant between-group differences. As for potentially confounding factors, the chi-squared test was used to check for between-group differences in gender and smoking status, whereas univariate ANOVA was used to test for between-group differences in body weight, height, BMI, age, injected dose of [^{18}F]fallypride and maximum realignment.

When comparing coefficients of variation of voxel intensities both in reference regions as well as in regions of interest, Welch's t-test was used to check for significant between-group differences.

For most other analyses, a one-way ANOVA was performed. If this showed a significant difference, it was followed by Levene's test to test for the equality of variances, and then depending on the result of Levene's test, Tamhane's T2 was used where variances were unequal and Scheffé's method was used where variances were equal.

2.8.2. Evaluating relative variation

For the comparison of different methodologies, it was necessary to find parameters that could suggest statistical superiority of one methodology over another. One such parameter is the relative variation, i.e., variation of measured or estimated values relative to their mean or median value. The reasoning is that a methodology that leads to more variable data will make it more difficult to distinguish group differences within that data.

One measure of relative variation is the coefficient of variation (COV), which is the standard deviation (SD) divided by the mean ($\bar{x}$) (see equation (6)) (Schultz 1985). This parameter was used repeatedly throughout this study.

$$COV = \frac{SD}{\bar{x}} \tag{6}$$

Several statistical tests exist to identify differences in variation between samples, of which Levene's Test is often included in software packages. In this test, each datum is converted to the absolute deviation of the datum (see equation (7)) to the mean over all data in the sample. Afterwards, an ANOVA is applied to these absolute deviations. This approach leads to an evaluation of the variation of absolute variations.

$$y(x) = |x - \bar{x}| \tag{7}$$

Alternative versions of Levene's Test exist that permit the evaluation of the variation of relative variations. A comparison of these tests concluded that the version using the relative deviation from the median (Med) as a basis for the ANOVA was the most robust (see equation (8)) (Schultz 1985). This test will be used for all evaluations of relative variations throughout this paper.

$$y(x) = \frac{|x - Med|}{Med} \tag{8}$$

3. Results

3.1. Study population

Fifty-eight subjects were enrolled in this study: 20 alcohol-dependent patients after detoxification, 19 healthy control subjects with high risk alcohol consumption, and 19 control subjects with low risk alcohol consumption. All subjects (n = 58) received a PET-scan between December 2013 and April 2016. The subjects had an average age of 45, weight of 84 kg, height of 178 cm and BMI of 26.5. The subjects were predominantly male, with females making up only 11-16% of the study population. There were no significant between-group differences in any of these parameters (see Table 2). The smoking status of the three groups was different, 53% of low-risk controls were current smokers, as compared to 89% and 84% in high-risk controls and patients (p = 0.017). Post-hoc analyses using the chi-squared test of independence showed a significant difference between low-risk and high-risk controls (p = 0.012) and between low-risk controls and patients (p = 0.036). The difference between high-risk controls and patients was non-significant (p = 0.631). Patients were abstinent for 9 to 96 days before PET imaging was performed - on average 36.4 (± 20.0) days.

Table 2. Study population

	Low-risk controls	High-risk controls	Patients	P
N	19	19	20	
Female	3 (16%)	2 (11%)	3 (15%)	0.879[†]
Current smokers	10 (53%)	17 (89%)	16 (84%)	0.017[†*]
Body weight mean (±SD)	82.0 (16.4)	85.7 (15.7)	85.1 (14.3)	0.737[‡]
Height mean (±SD)	178.7 (8.4)	177.3 (8.4)	177.9 (6.8)	0.845[‡]
BMI mean (±SD)	25.3 (4.1)	27.3 (4.5)	26.5 (3.4)	0.412[‡]
Age mean (±SD)	45.2 (8.7)	42.9 (9.1)	45.4 (8.4)	0.617[‡]
Days between PET imaging and last drink (±SD)			36.4 (20.0)	

* p < 0.05
† derived by chi-squared test of independence by group
‡ derived by univariate ANOVA by group

3.2. PET

On average, subjects received an injected dose of 196.9 (±9.9) MBq of [^{18}F]fallypride. Image acquisition was performed over 250 minutes (see 2.3.3). The maximum realignment per subject in any direction was on average 2.5 (±1.7) mm. There were no significant between-group differences (see Table 3). Example PET activity over time can be seen in Figure 7.

Table 3. Basic PET data

	Low-risk controls	High-risk controls	Patients	P
Injected dose in MBq mean (±SD) [min-max]	198.7 (14.0) [172.5-237.8]	194.4 (6.9) [174.2-208.3]	197.5 (7.2) [185.3-222.6]	0.386
Mean maximum realignment per subject in any direction (±SD)	2.1 (0.9)	2.7 (2.5)	2.6 (1.5)	0.617

P-values derived by univariate ANOVA by group

3.3. Comparing image analysis methodologies

The image analysis methodologies were analyzed before analyzing the clinical research question with the goal of identifying the optimum combination of methodologies for the clinical research question, and thus to be able to use this combination of methodologies to come as close as possible to the ground truth, within the limitations of this research project.

3.3.1. Comparing reference regions

3.3.1.1. Comparing coefficients of variation of voxel intensities in reference regions

For each subject, coefficients of variation of voxel intensities were calculated for all reference tissues for MRI intensities as well as PET activity as a measure of homogeneity within the reference regions (see Figure 13). The average coefficient of variation in MRI intensities was about five times higher for all subjects in the cerebellum (0.303 ±0.031) than in either SLF (0.056 ±0.014) or white matter mask (0.058 ±0.009) ($p < 0.0001$), both of which were found to be very homogenous in MRI intensities and did not differ significantly ($p = 0.18$). The average coefficients of variation in PET activity within reference tissues was found to be 4-6 times higher in the white matter mask (1.161 ±0.111) ($p < 0.0001$) than in either cerebellum (0.269 ±0.023) or SLF (0.195 ±0.023), of which SLF was significantly lower than cerebellum ($p < 0.0001$).
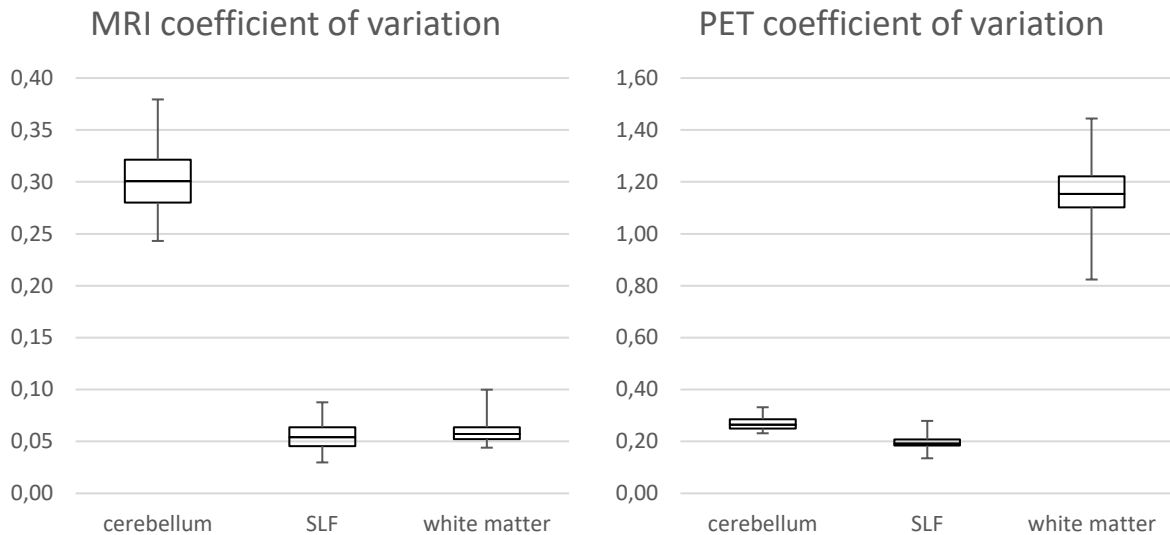
Figure 13. MRI and PET coefficients of variation of voxel intensity in reference tissues. Whiskers show maximum and minimum values.

3.3.1.2. *Comparing time activity curves of reference regions*

Relative time activity curves were generated for each subject to compare the relative activity over time between reference regions. These relative time activity curves showed similar trends over all subjects (see Figure 14).

When comparing the relative activity within the cerebellum with that within the white matter mask, in the first minute, the cerebellar activity is on average 2.11 ±0.22 times higher than that within the white matter mask. The activity ratio reaches an equilibrium of 0.99 ±0.06 after 15 minutes and then falls to 0.69 ±0.05 at 65 minutes, and further to 0.60 ±0.06 after 223 minutes.

When comparing the relative activity within the cerebellum with that within the SLF, in the first minute, the cerebellar activity is on average 2.50 ±0.32 times higher than that within the white matter mask. The activity ratio reaches an equilibrium of 1.01 ±0.08 after 30 minutes and then begins to rise again up to 1.24 ±0.13 after 223 minutes.

When comparing the relative activity within the white matter mask with that within the SLF, in the first minute, the activity within the white matter mask is on average 1.19 ±0.12 times higher than that within the white matter mask. The activity ratio rises further to about 1.26 ±0.05 after 30 minutes, 1.47 ±0.08 after 65 minutes and up to 2.08 ±0.18 after 223 minutes.

Overall, the cerebellum shows significantly higher activity at early time points, reaches an equilibrium at some stage with the white matter regions, and then ends up with an activity

between the two other reference tissues. The complete white matter mask shows a similar time activity curve in the early stages compared to the SLF but shows significantly higher activity in later stages than both the cerebellum and the SLF. The SLF shows the lowest activity overall, reaches equilibrium with the cerebellum in the second half hour and then has significantly lower activity in later stages than either the cerebellum or the white matter mask.
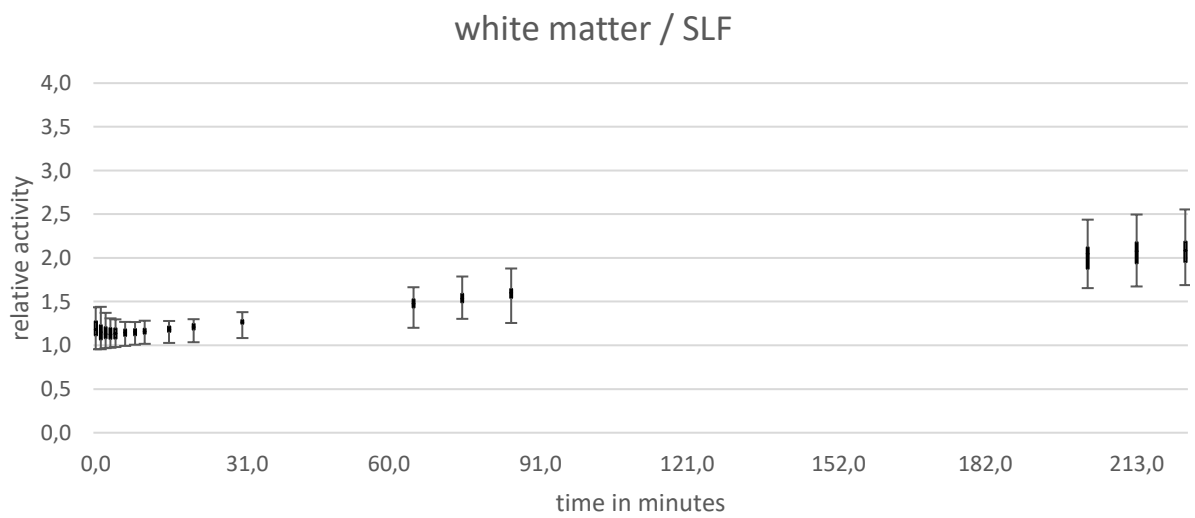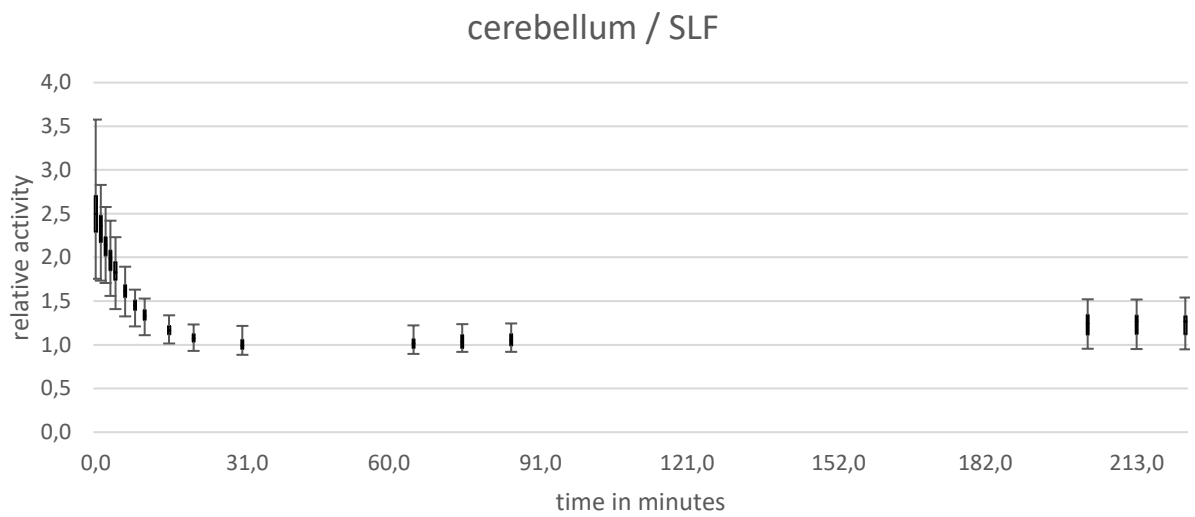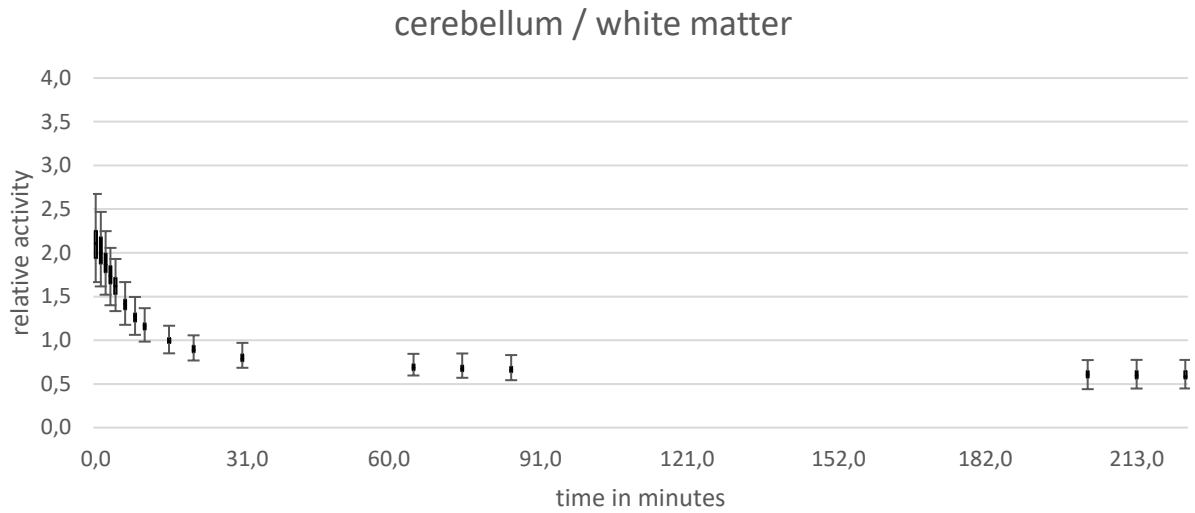
Figure 14. Relative time activity curves of reference regions averaged over all subjects. Whiskers show maximum and minimum values across subjects.

3.3.1.3. Comparing quality of fits of SRTM2

When using different reference tissues for the reference tissue model, there is a potential for a different quality of fit for the estimated curves, i.e., using one reference tissue over another might lead to an estimated curve that more closely resembles the measured values (see Figure 15). The quality of fit for the SRTM2 reference tissue model was calculated for FSL ROIs with all three reference tissues (see Table 4). The relative residual sum of squares was used to derive a scalar measure for the quality of fit.

Analysis of variance showed a main effect of chosen reference tissue on rrss values for caudate ($p = 0.027$), thalamus ($p < 0.0001$), hippocampus ($p < 0.0001$) and amygdala ($p < 0.0001$). No effect was shown for putamen, accumbens and pallidum.

Post hoc analyses were performed after checking for equality of variance either with Scheffé's method or with Tamhane's T2 (see 2.8). The post hoc analyses for caudate using Scheffé's method indicated that rrss values were lower when using cerebellum as reference tissue compared to white matter ($p = 0.028$), but did not differ significantly between cerebellum and SLF ($p = 0.54$) or SLF and white matter ($p = 0.29$). Post hoc analyses using Tamhane's T2 for the thalamus indicated that rrss values were lower when using white matter as reference tissue compared to cerebellum ($p < 0.0001$) and SLF ($p < 0.0001$), and lower when using SLF compared to cerebellum ($p < 0.0001$). The same was indicated for the hippocampus: rrss values were lower when using white matter as reference tissue compared to cerebellum ($p < 0.0001$) and SLF ($p < 0.0001$), and lower when using SLF compared to cerebellum ($p < 0.0001$). For the amygdala, post hoc analyses using Tamhane's T2 indicated that rrss values were lower when using SLF as reference tissue compared to cerebellum ($p < 0.0001$) and white matter ($p < 0.0001$), and lower when using white matter compared to cerebellum ($p < 0.0001$).

Table 4. rrss of SRTM2 fit on FSL ROIs using different reference tissues

	Cerebellum	SLF	whiteM
Putamen	0.33 (±0.16)	0.32 (±0.13)	0.34 (±0.16)
Caudate *	0.32 (±0.14)	0.35 (±0.13)	0.40 (±0.21)
Accumbens	0.72 (±0.35)	0.72 (±0.32)	0.73 (±0.32)
Pallidum	0.63 (±0.35)	0.65 (±0.35)	0.65 (±0.59)
Thalamus **	5.93 (±2.71)	1.22 (±0.53)	0.73 (±0.38)
Hippocampus **	4.15 (±1.82)	1.27 (±0.49)	0.64 (±0.34)
Amygdala **	3.32 (±1.95)	0.96 (±0.61)	1.83 (±0.89)

* p = 0.027, ** p < 0.0001; p-values derived by one-way ANOVA
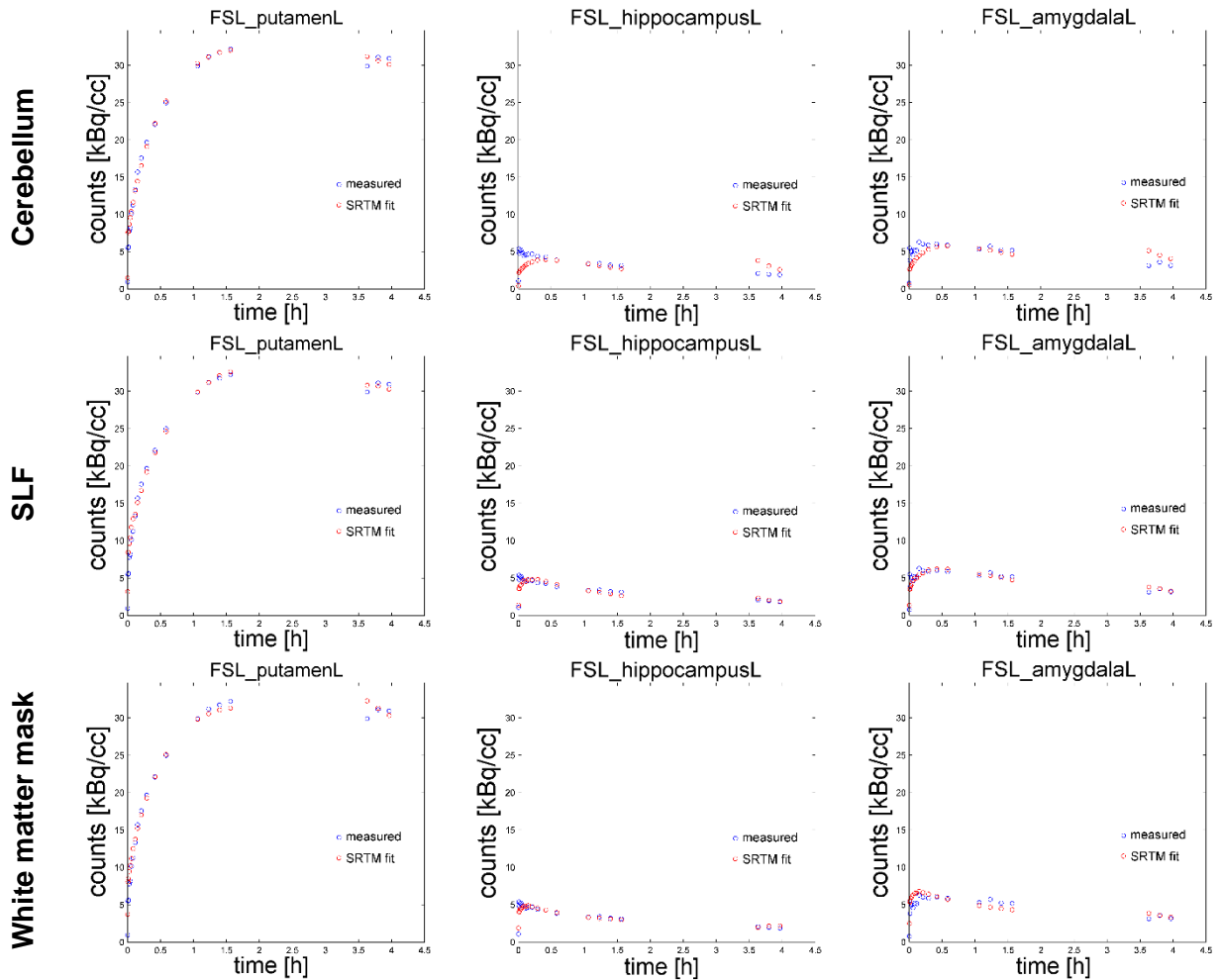
Figure 15. Example SRTM2 fits for one subject for FSL ROIs for left putamen, hippocampus and amygdala. Using cerebellum (top), SLF (middle) and white matter mask (bottom) as reference tissues. Measured values are shown in blue (independent of reference tissue), model fits are shown in red (dependent on reference tissue).

3.3.1.4.   Comparing coefficients of variation in result parameters

Potential differences in quality parameters may end up influencing the accuracy of binding potential estimation. This may in parts be represented in the data by a higher standard deviation relative to the mean (i.e., coefficient of variation) in the resulting binding potential estimations, depending on using one method over another. To compare the influence of the reference tissue used on COVs of binding potential estimations, the binding potential was estimated for all subjects' FSL ROIs using SRTM2 as a reference tissue model and all three reference tissues. The binding potentials were then averaged per subject for both hemispherical representations of each ROI. Mean and standard deviation was calculated by group, as well as a per-group COV for each ROI and reference tissue. The non-weighted average of the per-group COVs was calculated for a resulting overall COV per ROI and reference tissue (see Table 5). A variant of Levene's Test (see 2.8.2) showed that the choice of reference tissue had a significant effect on

variances of BP estimations for the putamen (p = 0.048), thalamus (p = 0.033) and hippocampus (p = 0.001). No significant effect was observed for the caudate (p = 0.105), accumbens (p = 0.592), pallidum (p = 0.592) and amygdala (p = 0.785). For all ROIs with significant differences in variance, using SLF as reference tissue resulted in the lowest COV, using cerebellum as a reference tissue resulted in the highest COV, while using the white matter mask was in-between.

Table 5. Overall COV of binding potential estimations using SRTM2 on FSL ROIs

ROI	Group	cerebellum	whiteM	SLF
Putamen	**LR**	11.3%	9.1%	9.5%
	HR	11.4%	10.9%	7.4%
	Patient	11.3%	7.6%	8.7%
	Overall	11.3%	9.2%	8.5%
Caudate	**LR**	12.6%	10.0%	10.2%
	HR	11.4%	9.9%	8.6%
	Patient	13.3%	11.0%	12.7%
	Overall	12.4%	10.3%	10.5%
Accumbens	**LR**	15.5%	13.6%	12.9%
	HR	14.1%	16.5%	12.4%
	Patient	10.8%	13.1%	10.6%
	Overall	13.5%	14.4%	12.0%
Amygdala	**LR**	18.7%	19.8%	19.2%
	HR	19.8%	18.2%	18.5%
	Patient	17.0%	11.8%	12.9%
	Overall	18.5%	16.6%	16.9%
Thalamus	**LR**	23.9%	17.9%	19.0%
	HR	22.8%	15.8%	13.8%
	Patient	24.6%	14.5%	15.0%
	Overall	23.7%	16.0%	15.9%
Pallidum	**LR**	15.9%	17.0%	15.2%
	HR	17.1%	20.5%	16.7%
	Patient	20.1%	18.5%	16.8%
	Overall	17.7%	18.6%	16.2%
Hippocampus	**LR**	29.3%	20.3%	16.8%
	HR	51.8%	29.4%	22.2%
	Patient	38.1%	21.9%	13.4%
	Overall	39.7%	23.9%	17.5%

3.3.2. Comparing methodologies for ROI identification

Two different methodologies for the identification of ROIs were compared: the AAL atlas in conjunction with images for both MRI and PET normalized in template (MNI) space;

and FSL FIRST segmentation of individual MRIs with both MRI and PET images in subject space.

3.3.2.1. *Comparing coefficients of variation of voxel intensity in selected regions of interest*

Coefficients of variation of voxel intensity were calculated for selected AAL and FSL ROIs, representing the same anatomical regions, for MRI intensity as well as PET activity as a measure of homogeneity within the ROIs. It can be assumed that the difference in voxel intensity within the same tissues is expected to be lower than the difference between tissues, thus coefficients of variation of voxel intensity within ROIs can be used as a measure for ROI fits. MRI intensity showed no significant difference for the putamen between AAL with 7.02 ($\pm$0.56) and FSL with 6.9 ($\pm$0.46) ($p = 0.19$). In all other ROIs there was a highly significant difference ($p < 0.0001$), with COVs of MRI intensity being higher in AAL ROIs than in FSL ROIs (see Figure 16). Specifically, the COV was about 4-fold higher in AAL caudate ROIs with 27.91 ($\pm$8.84), as compared to 6.73 ($\pm$1.41) in FSL caudate ROIs ($p < 0.0001$). In AAL thalamus ROIs the COV was on average 25% higher with 15.25 ($\pm$5.6), as compared to 12.04 ($\pm$1.96) in FSL thalamus ROIs ($p = 0.0001$). In AAL amygdala ROIs the COV was about 2.5 times higher than in FSL amygdala ROIs with 17.02 ($\pm$3.55) compared to 6.68 ($\pm$0.82) ($p < 0.0001$), respectively. For the hippocampus, AAL ROIs were about twice as high as FSL ROIs with 20.3 ($\pm$3.29) compared to 9.24 ($\pm$0.89) ($p < 0.0001$), respectively.
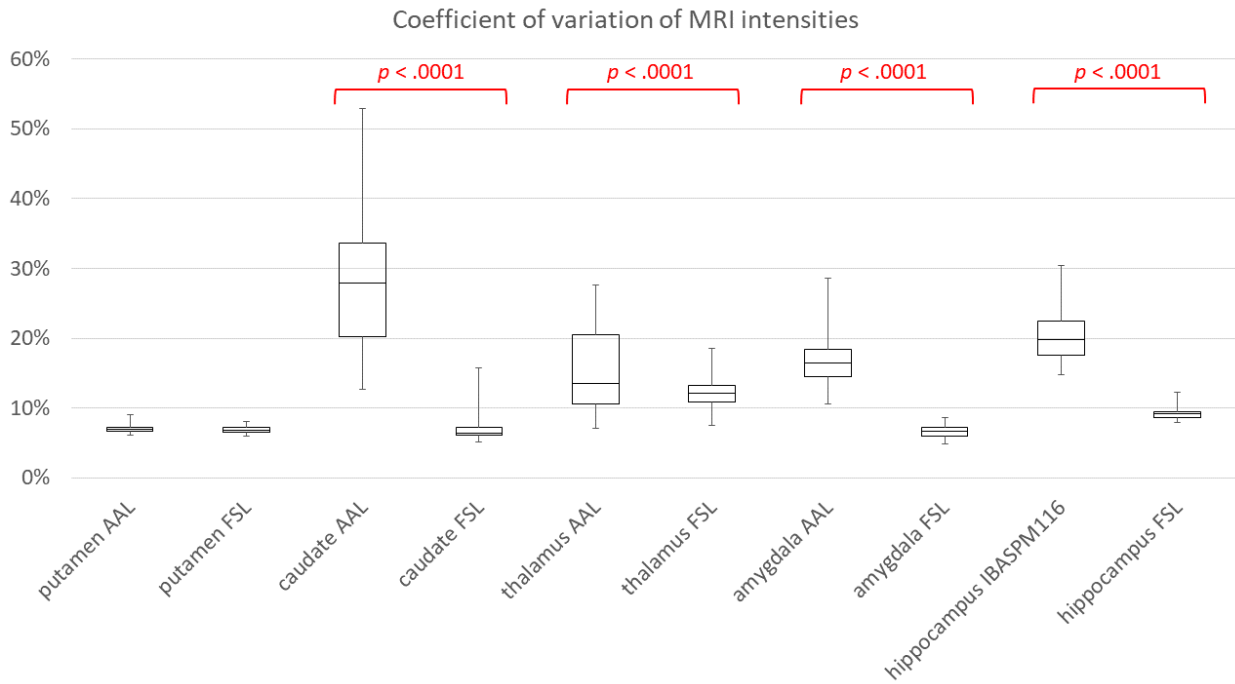
Figure 16. Coefficient of variation of MRI intensities.

PET activity also showed highly significant differences between COVs in AAL ROIs compared to FSL ROIs (see Figure 17). In AAL putamen ROIs, COVs were on average 45% higher than in FSL putamen ROIs with 37.03 (±3.62) compared to 25.43 (±2.5) (p < 0.0001), respectively. In AAL caudate ROIs, COVs were on average 52.54 (±10.59), as compared to 32.97 (±3.12) on average for FSL caudate ROIs (p < 0.0001). COVs for the amygdala were about 35% higher in AAL with 43.85 (±6.28), as compared to FSL with 32.57 (±3.39) (p < 0.0001). For the hippocampus, COVs were about 40% higher in AAL with 50.92 (±4.74), as compared to FSL with 36.19 (±4.56) (p < 0.0001). In the thalamus, no significant difference in COV of PET activity was observed between AAL ROIs with 32.7 (±4.01) and FSL ROIs with 32.49 (±3.76) (p = 0.77). Figure 18 visualizes the different ROI fits of AAL and FSL.
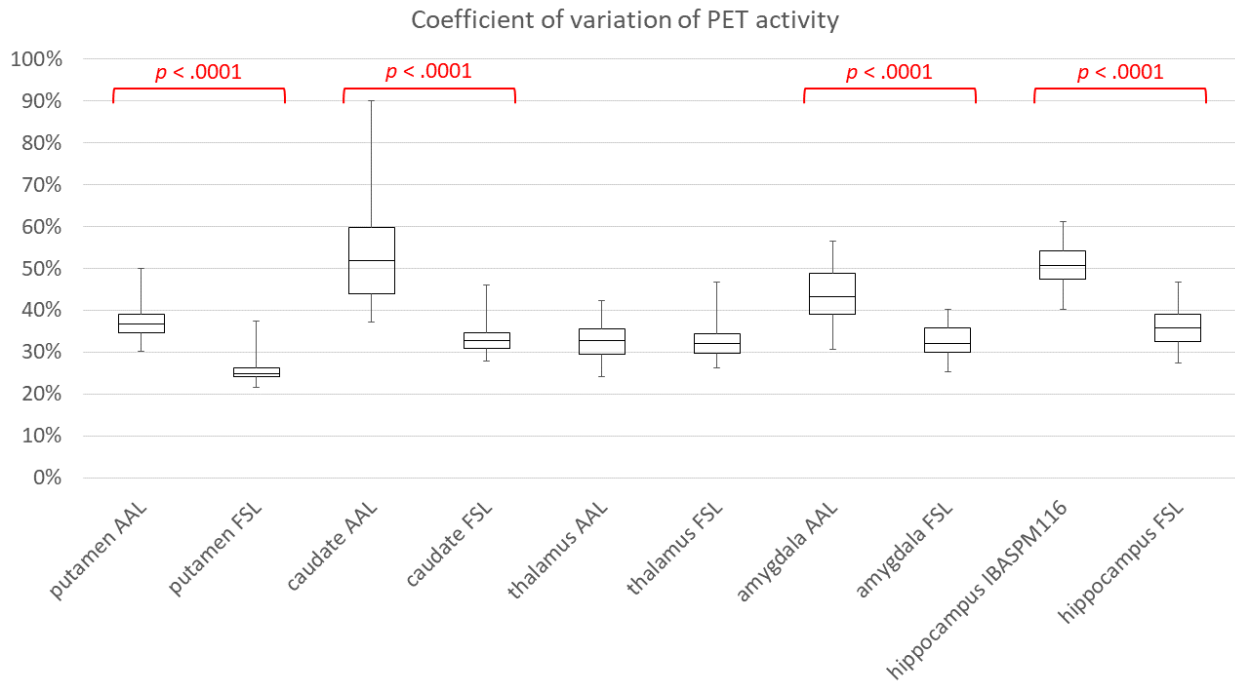
Figure 17. Coefficient of variation of PET activity.
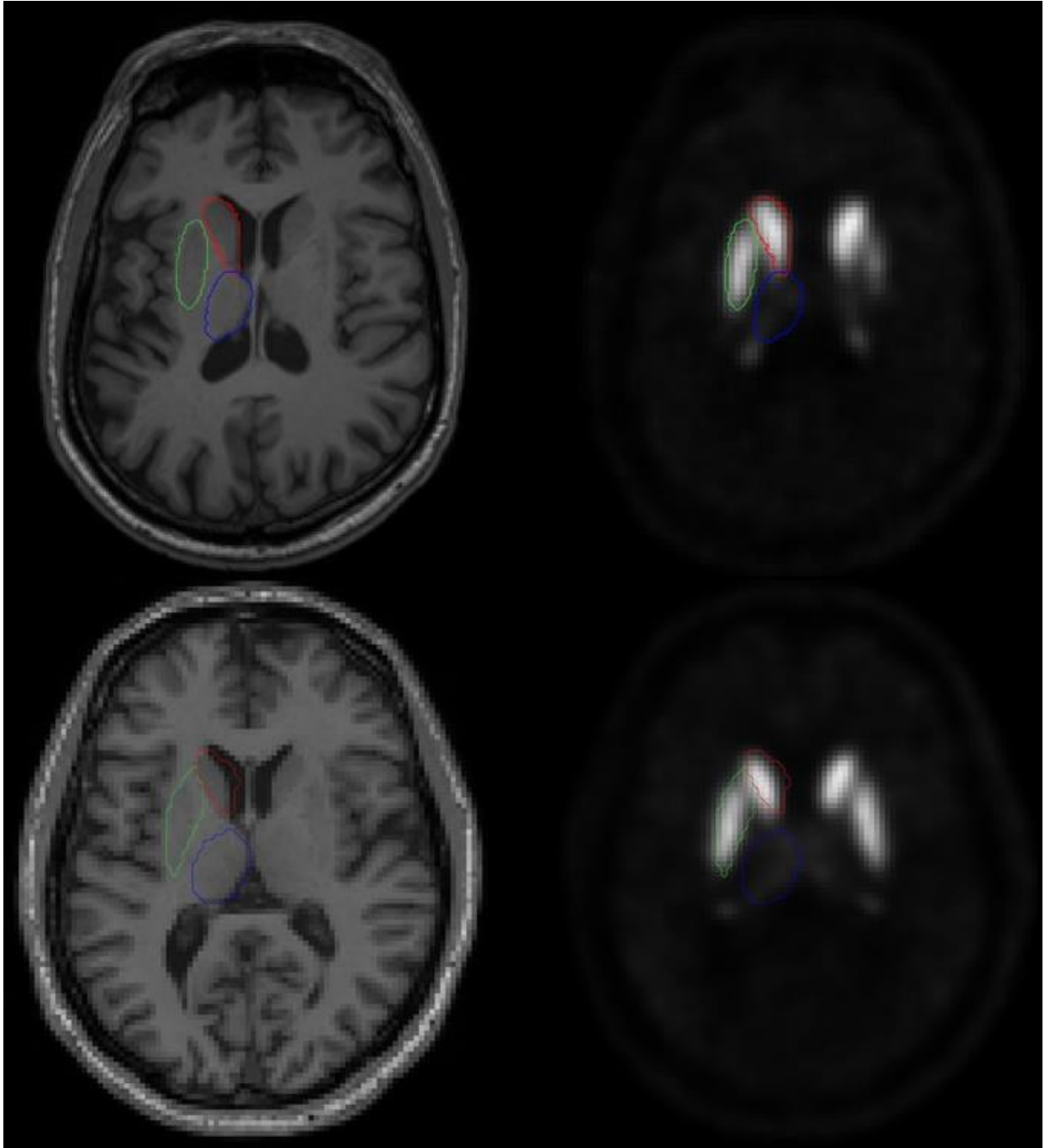
Figure 18. Example images of ROI fits. Top left shows an example of an axial slice of a subject's MRI image in neurologic convention, in conjunction with the subject's FSL FIRST segmentation of the left putamen (green), caudate (red) and thalamus (blue). Top right, the same subject's PET (image block 2, image 2) with the same FSL FIRST segmentation. Bottom left shows the same subject's normalized MRI in conjunction with the AAL ROIs for the left putamen (green), caudate (red) and thalamus (blue). Bottom right shows the same subject's normalized PET image (image block 2, image 2) with the same AAL ROIs.

3.3.2.2. *Comparing quality of fits of SRTM2*

When using different methodologies for the identification of ROIs, there is a potential for a different quality of fit for the estimated curves, i.e., using one methodology over another for the same anatomical region might lead to an estimated curve that more closely resembles the measured values. In contrast to the fits compared for different reference regions, the measured values are different in this case. The quality of fit for the SRTM2 reference tissue model was calculated for AAL and FSL ROIs with SLF as reference tissue (see Table 6). The relative residual sum of squares was used to derive a scalar measure for the quality of fit. Using one-way ANOVA the choice of ROI identification methodology had a highly significant effect on rrss values for the caudate nucleus, with AAL showing lower rrss values 0.24 (±0.09) than FSL 0.32 (±0.13) ($p < 0.0001$). There was no significant difference for the putamen, thalamus, amygdala or hippocampus.

Table 6. ROI identification method comparison: rrss of SRTM2 fits with SLF as reference tissue

	Putamen	Caudate*	Thalamus	Amygdala	Hippocampus
AAL	0.27 (±0.12)	0.24 (±0.09)	1.10 (±0.57)	0.88 (±0.47)	1.30 (±0.49)
FSL	0.32 (±0.13)	0.35 (±0.13)	1.22 (±0.53)	0.96 (±0.61)	1.27 (±0.49)

* $p < 0.0001$

3.3.2.3. *Comparing coefficients of variation in result parameters*

Potential differences in quality parameters may end up influencing the accuracy of binding potential estimation. This may in part be represented in the data by a higher standard deviation relative to the mean (i.e., coefficient of variation (COV)) in the resulting binding potential estimations, depending on using one method over another. To compare the influence of different ROI identification methodologies on COVs of binding potential estimations, the binding potential was estimated for all subjects' FSL and AAL ROIs using SRTM2 as reference tissue model and SLF as reference tissue. The binding potentials were then averaged per subject for both hemispherical representations of each ROI. Mean and standard deviation was calculated by group. A per-group COV for each AAL and FSL ROI was calculated. The non-weighted average of these per-group COVs was calculated for a resulting overall COV per ROI (see Table 7). The resulting COVs were 1.4-1.6-fold higher in AAL representations of the caudate and amygdala than in the respective FSL representation. A variant of Levene's Test (see 2.8.2) showed that the choice of ROI identification method had a significant effect on variances of BP estimations

for the caudate (p = 0.003) and amygdala (p = 0.021). No significant difference was observed for the putamen (p = 0.144), thalamus (p = 0.897) and hippocampus (p = 0.9).

Table 7. ROI identification method comparison: overall COVs of binding potential estimations

	Putamen	Caudate*	Thalamus	Amygdala*	Hippocampus
AAL	0.10	0.18	0.16	0.24	0.17
FSL	0.09	0.11	0.16	0.17	0.17

* p < 0.05

3.3.3. Comparing reference tissue models

3.3.3.1.   Comparing coefficients of variation in result parameters

To compare the influence of different reference tissue models on COVs of binding potential estimations, the binding potential was estimated for all subjects' FSL ROIs using SLF as reference tissue and all four reference tissue models. The binding potentials were then averaged per subject for both hemispherical representations of each ROI. Mean and standard deviation was calculated by group. A per-group COV for each ROI and model was calculated. The non-weighted average of these per-group COVs was calculated for a resulting overall COV per ROI and model (see Table 8). A variant of Levene's Test (see 2.8.2) showed that the choice of reference tissue model had no significant effect on variances of BP estimations for any of the analyzed ROIs: putamen (p = 0.99), caudate (p = 0.99), accumbens (p = 0.99), pallidum (p = 0.99), thalamus (p = 0.13), amygdala (p = 0.38). The SRTM did not converge for the hippocampus ROI in six subjects.

Table 8. Reference tissue model comparison: overall COVs of binding potential estimations

	SRTM	SRTM2	LOGAN	LOGAN2
Putamen	0.09	0.09	0.08	0.08
Caudate	0.11	0.11	0.10	0.10
Accumbens	0.12	0.12	0.12	0.11
Pallidum	0.16	0.16	0.16	0.15
Thalamus	0.12	0.16	0.13	0.13
Hippocampus[†]	n/a	0.17	0.19	0.18
Amygdala	0.13	0.17	0.15	0.15

† for the ROI hippocampus, the model SRTM did not converge for five subjects' left hemispherical representation and six subjects' right hemispherical representation.

3.4. Clinical results

Clinical results were calculated using the SLF as reference tissue and SRTM2 as reference tissue model with FSL ROIs (see Figure 19). One-way ANOVA showed significant group differences in BP_{ND} in the putamen (p = 0.027), caudate (p = 0.04) and thalamus (p = 0.012). No significant group differences were observed in the accumbens (p = 0.564), pallidum (p = 0.469), hippocampus (p = 0.174) and amygdala (p = 0.145).

Levene's test implied equal variance between groups for the putamen, caudate and thalamus, so Scheffé's method was used for post hoc analyses (see 2.8).

Post hoc analyses for the putamen using Scheffé's method indicated that BP_{ND} values in patients (28.85 ±2.51) were significantly lower than those in LR (31.14 ±2.95) (p = 0.027). No significant difference was found between BP_{ND} values in HR (30.01 ±2.23) and patients (p = 0.379), or LR and HR (p = 0.407).

Post hoc analyses for the caudate using Scheffé's method indicated no significant differences between BP_{ND} values in patients (23.36 ±2.97) and LR (25.13 ±2.55) (p = 0.116), HR (25.34 ±2.19) and patients (p = 0.069), or LR and HR (p = 0.969).

Post hoc analyses for the thalamus using Scheffé's method indicated that BP_{ND} values in patients (1.47 ±0.22) were significantly lower than those in LR (1.69 ±0.32) (p = 0.047) or HR (1.71 ±0.24) (p = 0.026). No significant difference was found between BP_{ND} values in LR and HR (p = 0.972).
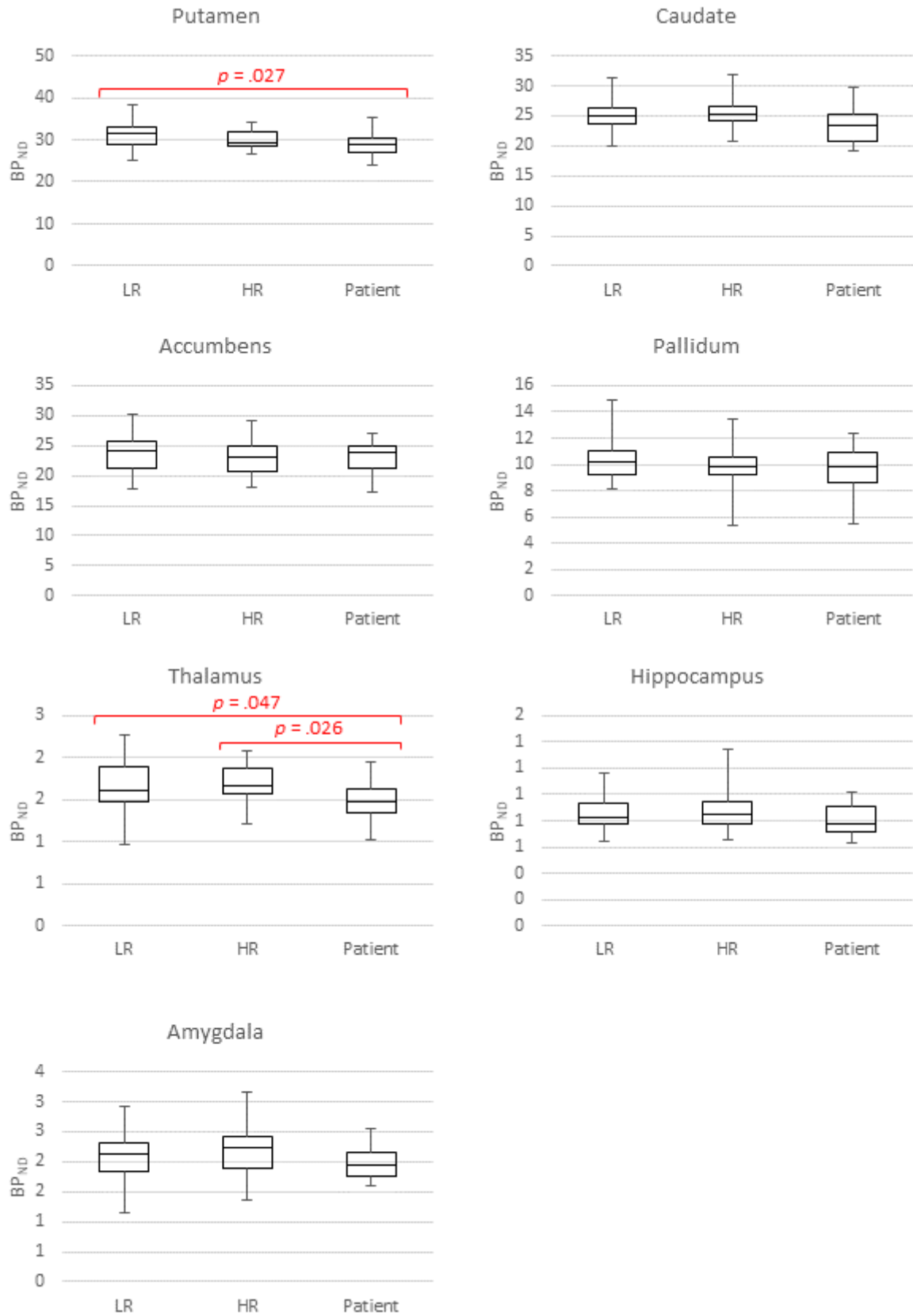
Figure 19. Non-displaceable [^{18}F]fallypride binding potential in patients, as well as controls with low risk (LR) or high risk (HR) alcohol consumption.

3.5. Influence of image analysis methodologies on clinical results

After having compared the different methodologies and having chosen a combination of methodologies that potentially has the lowest error rates, it was of interest to see whether the choice of methodology has an impact on the research question at hand. For this analysis, the putamen was chosen as ROI and BP_{ND} values were estimated for the putamen for all combinations of methodologies analyzed.

Figure 20 shows the distribution of BP_{ND} estimations by group for all combinations of methodologies. When comparing different ROI identification methods, there is a trend toward higher absolute BP_{ND} estimations in FSL ROIs compared to AAL ROIs, while the overall group difference seems similar for both methods. The same can be said about the different reference tissue models, which show similar distributions, with SRTM and SRTM2 having similar values, slightly higher in absolute terms than Logan and Logan2, which also show very similar distributions. The highest difference can be observed in reference tissues. The white matter mask shows significantly lower absolute values, while also showing lower within-group differences. The SLF shows the highest absolute values without having higher within-group differences compared to the cerebellum.

One-way ANOVA was performed for group differences for all combinations of image analysis methodologies to see whether the choice of methodology would ultimately have an influence on the answer to the clinical research question (see Table 9). The choice of methodology has a vital impact on the BP_{ND} estimations and group distributions, and this leads to contrary answers to the research question at hand, with p-values ranging from 0.027, where one would interpret a group difference to 0.599, and where one would not expect a group difference to be present.

Table 9. One-way ANOVA derived p-values for group differences for the putamen using different image analysis methodologies.

	AAL			FSL		
	cerebellum	SLF	whiteM	cerebellum	SLF	whiteM
SRTM	0.537	0.037*	0.030*	0.520	0.030*	0.064[†]
SRTM2	0.543	0.037*	0.032*	0.528	0.027*	0.066[†]
Logan	0.577	0.052[†]	0.034*	0.480	0.037*	0.048*
Logan2	0.599	0.076[†]	0.046*	0.478	0.048*	0.052[†]

All values given represent one-way ANOVA derived p-values for group difference between the three groups analyzed for the clinical research question: alcohol-dependent patients after detoxification and controls with low-risk or high-risk alcohol consumption.
* P-values < 0.05, usually considered significant
[†] P-values between 0.1 and 0.05, where one might consider a trend towards a group difference
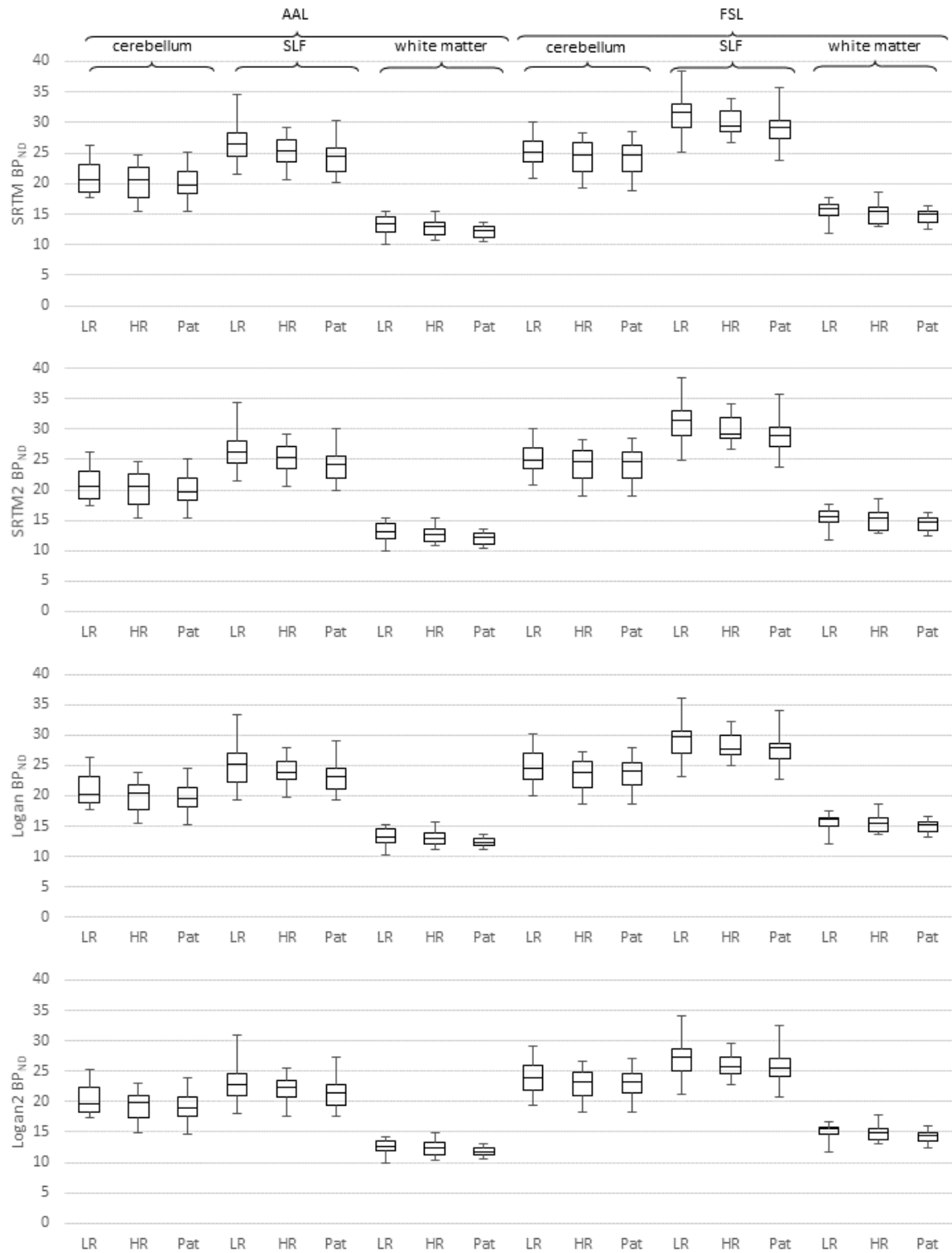
Figure 20. Influence of image analysis methodologies on clinical results. The image shows the distribution of BP_{ND} estimations for the putamen using combinations of different methodologies for the three different groups: patients (Pat) and controls with low risk (LR) and high risk (HR) alcohol consumption. From top to bottom, four different reference tissue models are used: SRTM, SRTM2, Logan and Logan2. Within the individual figures, the nine boxes on the left are based on a putamen ROI identified by the AAL atlas, while the nine boxes on the right use putamen ROIs identified by FSL FIRST segmentation. For each segmentation method three different reference tissues were used, from left to right: cerebellum, superior longitudinal fasciculus (SLF) and white matter mask.

4. Discussion

4.1. Main findings

The aim of this prospective [18F]fallypride-PET study was three-fold: first, to compare alternative methods for different steps of tracer kinetic modelling to find the combination of methods that yields the lowest error rates; second, to use these methods to analyze the dopamine D2/3 receptor status of detoxified alcohol-dependent patients as well as control subjects with low-risk and high-risk alcohol consumption; and finally, it was of interest to show if the choice of methodology would impact on the clinical research question.

Different options for three aspects of tracer kinetic modelling were analyzed and compared: reference tissues, ROI identification techniques and reference tissue models. For reference tissues the cerebellum, which is nearly exclusively used as reference tissue for dopamine receptor PET, was compared to two different white matter regions, the SLF and a probabilistic white matter mask. In these comparisons the SLF was shown to be more homogenous than the cerebellum in both MRI intensity as well as PET activity. It also showed less activity in later stages of imaging, pointing towards residual specific binding in the cerebellum. Finally, the SLF provided lower per-group COV in BP_{ND} estimations for the putamen, thalamus and hippocampus. The probabilistic white matter mask was shown to be inferior overall compared to the SLF, most likely due to spill-in effects. Thus, the SLF was shown to be superior overall as a reference tissue.

Atlas-based ROI identification in conjunction with spatially normalized images was compared to automatic segmentation of ROIs in subjects' T1 MRIs with the FSL FIRST algorithm. The FSL ROIs showed more homogenous MRI intensities for caudate, thalamus, amygdala and hippocampus, and more homogenous PET activity for putamen, caudate, amygdala and hippocampus, which points towards a better anatomic representation of the underlying ROIs. FSL ROIs also provided lower per-group COVs in BP_{ND} estimations for the caudate and amygdala. Overall, the FSL ROIs seemed to be the better choice.

Four different reference tissue models were compared: SRTM without and with (SRTM2) global k'$_2$ term, as well as the Logan method with and without (Logan2) k'$_2$ term. The influence of the chosen reference tissue on the COV of BP_{ND} estimations was analyzed, and was without any significant difference other than that the SRTM did not converge for

several subjects for the hippocampus ROI. It was thus decided that no method was clearly superior.

It was decided to analyze the between-group differences with SRTM2 as the reference tissue model, and FSL ROIs and SLF as reference tissue. With this combination, it was shown that patients had significantly lower BP_{ND} values than low-risk controls in the putamen and thalamus, as well as significantly lower BP_{ND} values than high-risk controls in the thalamus. No significant differences were found between low-risk and high-risk controls.

In a last analysis, it was shown that the choice of methodology had a major influence on the ability to show the between-group difference for the putamen ROI. It was shown that no combination of methodologies using the cerebellum as reference tissue showed any group difference, while SLF and the white matter mask both showed similar results. AAL ROIs were more likely to show a group difference in conjunction with the white matter mask, while FSL ROIs were more likely to show a group difference with SLF. The influence of the reference tissue model was also comparatively small with SRTM and SRTM2, both being more likely to show a group difference than Logan and Logan2.

4.2. Findings
4.2.1. Comparison of methodologies
A detailed discussion and literature overview of the different methodologies would go beyond the limitations of this study. Here, only the aspect of their differing results for this specific research question will be discussed.

4.2.1.1.   Comparing quality of fits
For the comparison of reference tissues as well as for the comparison of ROI identification techniques, the fit of the SRTM2 model to the observed data was assessed by comparing the relative residual sum of squares (rrss) (see 2.4.4.3). The analysis of the data showed several paradoxical results, most notably for the caudate, and the fit was calculated to be significantly better with AAL ROIs than with FSL ROIs, even though FSL ROIs were shown to be significantly better at representing the true anatomic representation of the caudate. When looking at all the data, the rrss as a measurement for the quality of fits did not seem to be a useful measure for the comparison of methodologies. It was decided not to rely on this measure for the evaluation of methods. Consequently, the rrss results are not featured in the further discussions below.

4.2.1.2. Reference tissues

As far as reference tissues are concerned, the first question was whether using a white matter region instead of the cerebellum would offer advantages. Evidence exists that the cerebellum is not optimal. A post-mortem autoradiographic study on alcoholics found a detectable quantity of binding for the D2/D3 receptor ligand [125I]epidepride in the cerebellum, while not finding any binding or accumulation in the white matter (Tupala, Hall et al. 2001). Another study was able to show specific D2/D3 binding in the cerebellum for [11C]FLB457 but not [18F]fallypride (Vandehey, Moirano et al. 2010). In a different study the cerebellum TACs of [11C]raclopride imaging were fitted to both a two-compartment model (one-tissue compartment model) and a three-compartment model (two-tissue compartment model). Here the three-compartment model offered the better fit (Farde, Eriksson et al. 1989). These findings suggest that not all reference region requirements are fully met by the cerebellum, yet it has been shown that at least for [11C]raclopride, the SRTM in conjunction with the cerebellum as reference tissue retains its sensitivity for detecting changes in BP (Lammertsma and Hume 1996). To date, the cerebellum is nearly exclusively used as the reference tissue for [18F]fallypride studies, but recently it has been suggested that white matter regions, such as the SLF, may offer advantages like lower COVs of BP_{ND} estimations and larger effect sizes for group differences in striatal BP_{ND} (Ishibashi, Robertson et al. 2013).

The comparisons of the cerebellum and the SLF in this study point toward the cerebellum being less homogenous, both in MRI voxel intensities as well as PET voxel intensities. Also, comparatively higher activity was shown in the cerebellum in later stages of imaging. It was also found that using the cerebellum leads to higher relative variance in BP_{ND} estimations. All these findings are suggestive of SLF being a more reliable reference tissue than the cerebellum. The underlying reason for this may be that due to specific binding, or other reasons, the cerebellum does not fully meet the assumptions for reference tissues for SRTM.

The next question is whether the choice of reference tissue influences the clinical research question. At least in this study, group differences were shown while using the SLF as reference tissue, but this sensitivity was not retained when using the cerebellum as reference tissue. Of course, by itself this is no proof for the superiority of one reference tissue over another, because the ground truth is not known. At the same time, it shows the impact the choice of reference region has on research outcomes.

Concerning the choice of white matter region, this study compared a white matter voxel probability mask with 99.9% probability of being white matter, with an atlas-derived ROI for the SLF. It was shown that the white matter mask was much less homogenous in PET imaging and showed significantly higher activity in later stages of imaging, as compared with SLF. SLF also showed comparatively lower COVs in BP_{ND} estimations for some ROIs. It is suspected that this is due to spill-in by PET activity of regions with high dopamine D2 receptor concentrations into the white matter mask. A good example for this is the capsula interna which is correctly identified as white matter and thus included in the mask, and which should theoretically have had a low PET activity, assuming for no dopamine D2/D3 receptors in white matter, but it had a relatively high activity. This can be adequately explained by the striatal regions nearby and the low spatial resolution of PET. Overall, the SLF seems to be clearly superior as reference tissue compared with the white matter probability mask.

4.2.1.3. *Comparing ROI identification techniques*

Identification of ROIs for PET studies can be achieved by three different strategies: manual delineation in individual subjects' images; (semi-) automatic segmentation in individual subjects' images; or transformation of individual images into a standard space and utilization of predefined standard atlases. Manual delineation is a highly time-consuming process with a high inter- and intra-operator variability. For this reason, most recent studies have utilized either of the two automatic strategies. In this study, both approaches were compared: the automatic segmentation technique FSL FIRST was used to create individual ROIs for each subject to be used in conjunction with MRI and PET images in subject space, and additionally all images were transformed into MNI standard space and used in conjunction with atlas-derived ROIs (AAL mostly). The comparison showed that atlas-derived ROIs were significantly less homogenous than the FSL representations. The within-ROI COV of MRI voxel intensity was significantly higher in AAL ROIs compared to FSL ROIs in the caudate, thalamus, amygdala and hippocampus. Only the putamen ROIs did not differ significantly in the MRI COV of voxel intensity. The comparison of within-ROI COV of PET intensity showed a similar picture with significantly higher COVs in AAL representations of the putamen, caudate, amygdala and hippocampus than in FSL representations. These findings support the subjective impression that the FSL ROIs fit better visually. AAL ROIs often seemed to partially include adjacent white matter or ventricles. Additionally, COV of BP_{ND} estimations were

compared. Here the FSL ROIs yielded significantly lower COVs for the caudate and amygdala compared with AAL ROIs. Overall, the FSL approach is likely to be superior, mainly due to the better anatomic representation.

4.2.1.4.   Comparing reference tissue models

It was previously shown that Logan and SRTM are viable RTMs for [^{18}F]fallypride, with highly correlating BP$_{ND}$ estimations (Siessmeier, Zhou et al. 2005). In this study, no significant effect of the choice of reference tissue model on the variance of BP$_{ND}$ estimations was detected. Both SRTM variants and Logan variants were shown to produce very similar results and are probably both viable as reference tissue models. Because SRTM variants have been used by the vast majority of [^{18}F]fallypride studies, it may be advantageous to choose a SRTM variant for better comparison with other studies.

Concerning different SRTM variants, using a global k$_2$' term (SRTM2) is logically sound and other studies have shown that it offers advantages (Endres, Hammoud et al. 2011). In this study it was shown that the SRTM with individual k$_2$' terms for each ROI did not converge for some subjects' hippocampus ROI; otherwise, the two variants did not differ significantly. Overall SRTM2 seems to be the most reasonable choice as reference tissue model for [^{18}F]fallypride.

4.2.2. Clinical research question

4.2.2.1.   Group difference between patients and controls

In this study, significant group differences in BP$_{ND}$ in the putamen, caudate and thalamus were shown. Post hoc analyses showed significantly lower BP$_{ND}$ in the putamen in patients than in low risk controls, and significantly lower BP$_{ND}$ in the thalamus in patients than in both low-risk or high-risk controls. In the caudate, patients also showed a trend towards lower BP$_{ND}$ than in either control group, but this did not reach significance. A comparable [^{18}F]fallypride study also found a group difference between recently detoxified patients (at day 1 and days 7-14 of admission) and controls in the thalamus (Rominger, Cumming et al. 2012). In contrast to the present study, this previous study also found a group difference in hippocampus, but only observed a trend towards lower BPND in the putamen of detoxified patients. In terms of methodology, they used the cerebellum as reference tissue, a Logan variant as reference tissue model and an atlas-based approach with normalized dynamic images as ROI identification technique. A different [^{18}F]fallypride study found no significant differences in baseline BP$_{ND}$ between detoxified (8 to 126 days) alcohol-dependent patients and controls (Spreckelmeyer,

Paulzen et al. 2011). They used parametric modelling with a SRTM variant, the cerebellum as reference region and AAL atlas-based ROIs on normalized images. One could speculate that the findings of this study concerning the cerebellum as reference tissue and on atlas-based ROI identification techniques could provide a reason as to why no significant group difference was observed for the putamen by Rominger et al., or any ROI by Spreckelmeyer et al. Another major difference in these studies is the imaging date of the patient group, which was day 1 and days 7-14 of admission in the study by Rominger et al., 8 to 126 days after detoxification for Spreckelmeyer et al., and 9-96 days after the last drink in this study. It has been observed before that patients show elevated BP_{ND} later after detoxification compared to early after detoxification (Volkow, Wang et al. 2002; Rominger, Cumming et al. 2012), so the imaging delay after detoxification could have potentially lessened the group difference in this study and in the study of Spreckelmeyer et al. due to rising BP_{ND} after detoxification.

The main reason to suspect a group difference in D2/3 receptor binding potential to be present between detoxified alcohol-dependent patients and controls lies in several PET studies with other tracers that have shown a significant group difference. Studies with [^{11}C]raclopride, which has a lower affinity compared with [^{18}F]fallypride, have found lower dopamine D2/3 receptor binding potential estimations in detoxified alcoholics compared with healthy controls in whole striatum ROIs (Hietala, West et al. 1994; Volkow, Wang et al. 1996), the caudate and putamen (Volkow, Wang et al. 2002), the limbic, associative and sensorimotor striatum (Martinez, Gil et al. 2005) and the ventral striatum (Volkow, Wang et al. 2007). Finally a PET study with [^{18}F]-DMFP found a significantly lower D2 receptor availability in detoxified alcoholics in the putamen and nucleus accumbens (Heinz, Siessmeier et al. 2004).

Overall it seems likely that a group difference exists, but that this group difference was not seen in certain studies due to suboptimal image analysis methodologies.

4.2.2.2.   Group difference between high-risk and low-risk controls
If there is a reduced dopamine receptor density in detoxified alcohol-dependent patients, the next question is whether this is a result of alcohol-dependence or a preexisting condition. To investigate this question, the dopamine receptor status of healthy subjects with high-risk alcohol consumption was compared to that of subjects with low-risk alcohol consumption. It was hypothesized that high-risk subjects would be between low-risk subjects and detoxified alcohol-dependent patients in dopamine receptor availability.

In this study, no significant between-group differences were found between high-risk subjects and low-risk subjects. Thus, the data do not support this hypothesis.

4.2.3. Influence of methodology on clinical research question

It was proposed that one reason for the differing results in PET studies on dopamine receptor availability and alcohol dependence may be the difference in image analysis methodology. Primarily, $[^{18}F]$fallypride studies have failed to reliably show the group differences that were observed with $[^{11}C]$raclopride. It was suggested that this difference may result from different tracer dynamics and their influence on tracer kinetic modelling. This study has shown that different options for different steps of tracer kinetic modelling offer different quality outcomes. This is especially true for reference tissues, where the cerebellum, though nearly exclusively used as reference tissue in $[^{18}F]$fallypride and $[^{11}C]$raclopride studies, was shown to be inferior to the SLF in several quality parameters. The next question is thus whether the choice of methodology is of consequence for the clinical research question. In this study the BP_{ND} within the putamen was estimated for all subjects with all 24 combinations of methodologies analyzed: two ROI identification techniques, three reference tissues and four reference tissue models. The resulting value distributions were plotted by group and were analyzed for between-group differences.

It was shown that the choice of methodology has a major influence on the interpretation of the clinical research question. This was especially true for the choice of reference region, which had a major influence on BP_{ND} estimations. No combination of methodologies that used the cerebellum as reference tissue showed a significant between-group difference (p-values between 0.478 and 0.599), whereas all combinations using one of the white matter reference tissues showed either a trend towards a between-group difference or a significant between-group difference (p-values between 0.027 and 0.076). Concerning ROI identification techniques, atlas-based ROIs were more likely to show significant between-group differences in combination with the white matter probability mask, whereas the individual FSL segmentations were more likely to show significant between-group differences in combination with the SLF as reference tissue. As for reference tissue models, the two SRTM variants and the two Logan variants showed very similar results, without any clear pattern.

Overall it is possible that the choice of methodology, and markedly the choice of reference tissue, can have a major influence on the ability to detect between-group differences in $[^{18}F]$fallypride studies. It is likely that this is a contributing factor in $[^{18}F]$fallypride studies

not being able to show the group differences that have previously been observed with [^{11}C]raclopride studies.

4.3. Strengths

In general, the quality of the PET data in this study was very good. It utilized a large study population of 58 subjects overall, with 20 patients and 19 each in both control groups. This is more than most other dopamine receptor PET studies comparing detoxified alcohol-dependent patients with controls. The following list offers an overview of other studies' participant numbers (patients / controls): 17/14 (Rominger, Cumming et al. 2012), 11/11 (Spreckelmeyer, Paulzen et al. 2011), 9/8 (Hietala, West et al. 1994), 10/17 (Volkow, Wang et al. 1996), 14/11 (Volkow, Wang et al. 2002), 15/15 (Martinez, Gil et al. 2005), 20/20 (Volkow, Wang et al. 2007), and 11/13 (Heinz, Siessmeier et al. 2004). In terms of imaging quality, the injected dose was very similar for all subjects, being between 172.5 and 237.8 MBq and equally distributed in all three groups (mean by group 198.7, 194.4 and 197.5 MBq). Also, there was only limited head movement overall. The realignment parameters for all groups were very similar. There was an average maximum realignment in any direction of 2.1 (±0.9) mm, 2.7 (±2.5) mm and 2.6 (±1.5) mm for low-risk controls, high-risk controls and patients, respectively. Another advantage of this study is the utilization of [^{18}F]fallypride, which is a high affinity tracer that offers excellent sensitivity and specificity for the D2/3 receptors in both receptor-rich as well as other areas (Mukherjee, Christian et al. 2002). It can also be argued that the extra care taken into looking into the different advantages and disadvantages of methodological options represents a strength of this study for the evaluation of the clinical research question.

4.4. Limitations

Some general limitations concerning the applicability of this research's findings stem directly from the methodology and are common across all PET receptor studies. The estimation of the BP$_{ND}$ is a multi-step process that leads to a measure that is comparable across groups of subjects but is limited as quantitative measure of receptor density, because several factors can influence the BP$_{ND}$, including varying endogenous dopamine levels. Another limitation stems from the decision to not measure the arterial plasma function. Measuring the input function directly from the subjects' arterial blood is considered the gold standard in tracer kinetic modelling, but is highly burdensome for the subjects as well as time-consuming and expensive. The main problem connected to not measuring the arterial input function is that the SLF as reference tissue is not yet verified

as a viable reference region for SRTM and [18F]fallypride. It can be argued that the indirect validation performed in this study does not represent adequate validation. Another weakness in the scientific accuracy of this study is the use of the same data for both methodological considerations as well as the clinical research question. This offers the potential for statistical effects influencing each other, i.e., a group difference that could be statistically significant by chance only, without a real-world representation, may also be represented in lower per-group COVs for a certain methodology. It would have been more scientifically sound to use different data sets for the identification of the best methodology and the clinical research question.

Other limitations stem from the subject sample. The main difficulty here is the differing smoking habits of the three groups. Low-risk controls were significantly less likely to be current smokers than either the high-risk group or the patients. For this reason, it is impossible to pinpoint differences between patients and low-risk controls to just their drinking habits. It is impossible to fully differentiate between the effects of nicotine dependence and alcohol dependence. Another limitation concerning the subject sample is the gender ratio, with very few women in each group. Thus, the findings are not necessarily generalizable for both genders. Concerning the patient sample, it is not clear if the sample is fully representative of detoxified alcohol-dependent patients. The patients that took part in the study had to be highly functional in their daily lives to be able to fulfill the requirements of the research project, with several appointments for questionnaires and imaging. They may thus represent a subgroup of alcohol-dependent patients that is particularly functional.

For the comparison with other studies, it is important to note that the length of detoxification was comparatively long. A more significant effect might have been found earlier after detoxification, as it was previously shown that striatal BP_{ND} tends to be higher after one year of detoxification than one day after detoxification (Rominger, Cumming et al. 2012).

Concerning the results of the methodological comparisons, it is unclear if they are generalizable. It would be very interesting to see whether similar results can be achieved with other [18F]fallypride data sets, especially concerning the SLF as reference tissue.

Finally, it remains to be said that even if the difference in binding potential that was observed in this study has a real-world counterpart, this is only correlation and not proof

of a causation. It is still unclear whether this is a preexisting condition that acts as a risk factor for alcohol dependence or a result of chronic ethanol intoxication.

4.5. Perspectives

Concerning the methodological considerations, as a next step it is of interest to see if it is possible to fully validate the SLF as reference tissue with a separate data set that includes an arterial input function. Afterwards, it would be interesting to see if any of the other [18F]fallypride studies looking for group differences between detoxified alcohol-dependent patients and controls reach similar results with the SLF as reference tissue.

Within this project, one of the next steps is the correlation of PET data with questionnaires and memory function tests that were performed by the same subjects. This will allow for more insight into the links between the dopamine system and learning.

Another aspect of this project is a follow-up of all subjects. For the patient population, the severity of craving over extended time and relapse rates will be monitored. Here, it will be of interest to see if future relapsers and abstainers differ in PET imaging after detoxification, or if there is a correlation with BP_{ND} in one of the ROIs and the severity of craving.

Subjects in the high-risk group will be followed up on after three years. The primary outcome parameters alcohol consumption and AUD will be assessed as well as smoking. Additionally, all psychometric, neuropsychosocial and learning tests will be repeated to explore the potential impact of ethanol-intake over the three years. Again, it will be interesting to see if any correlation to current PET data can be uncovered.

4.6. Conclusions

The present findings contribute to the understanding of the influence of different methodological options for the image analysis of [18F]fallypride, as well as the understanding of differences in the dopamine receptor status of detoxified alcohol-dependent patients and healthy controls.

Concerning the methodological options, it was shown that the use of the cerebellum as reference tissue is inferior to the use of the SLF in several parameters, namely the coefficient of variance of both MRI and PET intensity in the reference tissue, the fit of the SRTM2 model to the measured TACs, and the coefficient of variance in BP_{ND} estimations when using that reference tissue. It was also found that the activity within the cerebellum is equal to the activity within the SLF 30 to 60 minutes after dose injection, but is

significantly higher in later images. Overall, this points toward the SLF being a better reference tissue for parametric modelling when using [^{18}F]fallypride, with the caveat that the SLF has not yet been validated using the gold standard method, i.e., parametric modelling with an arterial input function. It was also shown that the choice of reference tissue has a major impact on the ability to show a significant group difference in BP$_{ND}$ estimations, in that the cerebellum as reference tissue prevented the group difference from being shown. Additionally to the findings concerning reference tissues, it was shown that automatic segmentation with FSL FIRST provides better anatomical fits than the combination of spatial normalization with atlas-based ROIs. No significant difference was observed between the use of two different SRTM variants and two Logan variants as reference tissue models.

When using the optimal combination of methodologies, it was shown that detoxified alcohol-dependent patients have a significantly lower BP$_{ND}$ in the putamen than controls with low-risk alcohol consumption, and significantly lower BP$_{ND}$ in the thalamus than either control group. No significant difference was found between control subjects with high-risk alcohol consumption and control subjects with low-risk alcohol consumption.

5.   Literaturverzeichnis

Alemán-Gómez Y., M.-G. L., Valdés-Hernandez. P. (2006). IBASPM: Toolbox for automatic parcellation of brain structures. Presented at the 12th Annual Meeting of the Organization for Human Brain Mapping, June 11-15, 2006, Florence, Italy. Available on CD-Rom in NeuroImage, Vol. 27, No.1.

American Psychiatric Association (1994). Diagnostic and statistical manual of mental disorders, Fourth Edition. Washington, DC.

American Psychiatric Association (2013). Diagnostic and statistical manual of mental disorders (DSM-5®), American Psychiatric Pub.

Andersen, S. M., S. Z. Rapcsak and P. M. Beeson (2010). "Cost function masking during normalization of brains with focal lesions: still a necessity?" Neuroimage 53(1): 78-84.

Ashburner, J., G. Barnes, C. Chen, J. Daunizeau, G. Flandin, K. Friston, D. Gitelman, S. Kiebel, J. Kilner and V. Litvak (2008). "SPM8 manual." Functional Imaging Laboratory, Institute of Neurology: 41.

Ashburner, J. and K. J. Friston (2005). "Unified segmentation." Neuroimage 26(3): 839-851.

Balldin, J., U. Berggren, G. Lindstedt and A. Sundkler (1993). "Further Neuroendocrine Evidence for Reduced D(2)-Dopamine Receptor Function in Alcoholism." Drug and Alcohol Dependence 32(2): 159-162.

Balldin, J. I., U. C. Berggren and G. Lindstedt (1992). "Neuroendocrine evidence for reduced dopamine receptor sensitivity in alcoholism." Alcohol Clin Exp Res 16(1): 71-74.

Barnow, S., M. A. Schuckit, M. Lucht, U. John and H. J. Freyberger (2002). "The importance of a positive family history of alcoholism, parental rejection and emotional warmth, behavioral problems and peer substance use for alcohol problems in teenagers: a path analysis." J Stud Alcohol 63(3): 305-315.

Belin, D., S. Jonkman, A. Dickinson, T. W. Robbins and B. J. Everitt (2009). "Parallel and interactive learning processes within the basal ganglia: relevance for the understanding of addiction." Behav Brain Res 199(1): 89-102.

Berridge, K. C. (2009). "Wanting and Liking: Observations from the Neuroscience and Psychology Laboratory." Inquiry (Oslo) 52(4): 378.

Berridge, K. C., T. E. Robinson and J. W. Aldridge (2009). "Dissecting components of reward: 'liking', 'wanting', and learning." Curr Opin Pharmacol 9(1): 65-73.

Boileau, I., J.-M. Assaad, R. O. Pihl, C. Benkelfat, M. Leyton, M. Diksic, R. E. Tremblay and A. Dagher (2003). "Alcohol promotes dopamine release in the human nucleus accumbens." Synapse 49(4): 226-231.

Brand, H., J. Künzel, B. Braun, R. Walter-Hamann and T. Wessel (2015). SUCHTHILFE IN DEUTSCHLAND 2014. JAHRESBERICHT DER DEUTSCHEN SUCHTHILFESTATISTIK (DSHS). http://www.suchthilfestatistik.de, IFT Institut für Therapieforschung.

Brett, M., A. P. Leff, C. Rorden and J. Ashburner (2001). "Spatial normalization of brain images with focal lesions using cost function masking." Neuroimage 14(2): 486-500.

Carlsson, A., J. Engel, U. Strombom, T. H. Svensson and B. Waldeck (1974). "Suppression by dopamine-agonists of the ethanol-induced stimulation of locomotor activity and brain dopamine synthesis." Naunyn Schmiedebergs Arch Pharmacol **283**(2): 117-128.

Carson, R. E. (2005). Tracer kinetic modeling in PET. Positron Emission Tomography, Springer**:** 127-159.

Charlet, K., A. Beck and A. Heinz (2013). "The dopamine system in mediating alcohol effects in humans." Curr Top Behav Neurosci **13**: 461-488.

Cohen, C., G. Perrault and D. J. Sanger (1998). "Preferential involvement of D3 versus D2 dopamine receptors in the effects of dopamine receptor ligands on oral ethanol self-administration in rats." Psychopharmacology (Berl) **140**(4): 478-485.

Costes, N., A. Dagher, K. Larcher, A. C. Evans, D. L. Collins and A. Reilhac (2009). "Motion correction of multi-frame PET data in neuroreceptor mapping: Simulation based validation." NeuroImage **47**(4): 1496-1505.

Crabbe, J. C., R. A. Harris and G. F. Koob (2011). "Preclinical studies of alcohol binge drinking." Ann N Y Acad Sci **1216**: 24-40.

Cropley, V. L., R. B. Innis, P. J. Nathan, A. K. Brown, J. L. Sangare, A. Lerner, Y. H. Ryu, K. E. Sprague, V. W. Pike and M. Fujita (2008). "Small effect of dopamine release and no effect of dopamine depletion on [18F]fallypride binding in healthy humans." Synapse **62**(6): 399-408.

D'Souza, D. C., R. B. Gil, S. Madonick, E. B. Perry, K. Forselius-Bielen, G. Braley, L. Donahue, T. Tellioglu, Z. Zimolo, R. Gueorguieva and J. H. Krystal (2006). "Enhanced sensitivity to the euphoric effects of alcohol in schizophrenia." Neuropsychopharmacology **31**(12): 2767-2775.

Dawson, D. A., B. F. Grant and T. K. Li (2005). "Quantifying the risks associated with exceeding recommended drinking limits." Alcohol Clin Exp Res **29**(5): 902-908.

Dettling, M., A. Heinz, P. Dufeu, H. Rommelspacher, K. J. Graf and L. G. Schmidt (1995). "Dopaminergic responsivity in alcoholism: trait, state, or residual marker?" American Journal of Psychiatry **152**(9): 1317-1321.

Di Chiara, G. (1997). "Alcohol and dopamine." Alcohol Health Res World **21**(2): 108-114.

Di Chiara, G. and A. Imperato (1986). "Preferential stimulation of dopamine release in the nucleus accumbens by opiates, alcohol, and barbiturates: studies with transcerebral dialysis in freely moving rats." Ann N Y Acad Sci **473**: 367-381.

Di Chiara, G. and A. Imperato (1988). "Drugs abused by humans preferentially increase synaptic dopamine concentrations in the mesolimbic system of freely moving rats." Proc Natl Acad Sci U S A **85**(14): 5274-5278.

Dick, D. M., J. Plunkett, L. F. Wetherill, X. Xuei, A. Goate, V. Hesselbrock, M. Schuckit, R. Crowe, H. J. Edenberg and T. Foroud (2006). "Association between GABRA1 and drinking behaviors in the collaborative study on the genetics of alcoholism sample." Alcohol Clin Exp Res **30**(7): 1101-1110.

Die Drogenbeauftragte der Bundesregierung (2015). Drogen- und Suchtbericht 2015.

Dyr, W., W. J. McBride, L. Lumeng, T. K. Li and J. M. Murphy (1993). "Effects of D1 and D2 dopamine receptor agents on ethanol consumption in the high-alcohol-drinking (HAD) line of rats." Alcohol **10**(3): 207-212.

Endres, C. J., D. A. Hammoud and M. G. Pomper (2011). "Reference tissue modeling with parameter coupling: application to a study of SERT binding in HIV." Phys Med Biol **56**(8): 2499-2513.

Engel, J. A. and E. Jerlhag (2014). "Alcohol: mechanisms along the mesolimbic dopamine system." Prog Brain Res **211**: 201-233.

Enoch, M. A., K. V. White, J. Waheed and D. Goldman (2008). "Neurophysiological and genetic distinctions between pure and comorbid anxiety disorders." Depress Anxiety **25**(5): 383-392.

Ericson, M., O. Blomqvist, J. A. Engel and B. Söderpalm (1998). "Voluntary ethanol intake in the rat and the associated accumbal dopamine overflow are blocked by ventral tegmental mecamylamine." European Journal of Pharmacology **358**(3): 189-196.

Fadda, F., A. Argiolas, M. R. Melis, G. Serra and G. L. Gessa (1980). "Differential effect of acute and chronic ethanol on dopamine metabolism in frontal cortex, caudate nucleus and substantia nigra." Life Sci **27**(11): 979-986.

Farde, L., L. Eriksson, G. Blomquist and C. Halldin (1989). "Kinetic analysis of central [11C]raclopride binding to D2-dopamine receptors studied by PET--a comparison to the equilibrium analysis." J Cereb Blood Flow Metab **9**(5): 696-708.

Gessa, G. L., F. Muntoni, M. Collu, L. Vargiu and G. Mereu (1985). "Low doses of ethanol activate dopaminergic neurons in the ventral tegmental area." Brain Res **348**(1): 201-203.

Goodwin, D. W., F. Schulsinger, N. Moller, L. Hermansen, G. Winokur and S. B. Guze (1974). "Drinking problems in adopted and nonadopted sons of alcoholics." Arch Gen Psychiatry **31**(2): 164-169.

Guardia, J., A. M. Catafau, F. Batlle, J. C. Martin, L. Segura, B. Gonzalvo, G. Prat, I. Carrio and M. Casas (2000). "Striatal dopaminergic D(2) receptor density measured by [(123)I]iodobenzamide SPECT in the prediction of treatment outcome of alcohol-dependent patients." Am J Psychiatry **157**(1): 127-129.

Haber, S. N. and B. Knutson (2010). "The reward circuit: linking primate anatomy and human imaging." Neuropsychopharmacology **35**(1): 4-26.

Hägele, C., E. Friedel, T. Kienast and F. Kiefer (2014). "How Do We 'Learn' Addiction? Risk Factors and Mechanisms Getting Addicted to Alcohol." Neuropsychobiology **70**(2): 67-76.

Heinz, A. (1996). "Psychopathological and Behavioral Correlates of Dopaminergic Sensitivity in Alcohol-Dependent Patients." Arch Gen Psychiatry **53**(12): 1123.

Heinz, A. (2000). "Genotype Influences In Vivo Dopamine Transporter Availability in Human Striatum." Neuropsychopharmacology **22**(2): 133-139.

Heinz, A., A. Beck, J. Wrase, J. Mohr, K. Obermayer, J. Gallinat and I. Puls (2009). "Neurotransmitter systems in alcohol dependence." Pharmacopsychiatry **42 Suppl 1**: S95-S101.

Heinz, A., M. Dettling, S. Kuhn, P. Dufeu, K. J. Graf, I. Kurten, H. Rommelspacher and I. G. Schmidt (1995). "Blunted growth hormone response is associated with early relapse in alcohol-dependent patients." Alcohol Clin Exp Res **19**(1): 62-65.

Heinz, A., S. Lober, A. Georgi, J. Wrase, D. Hermann, E. R. Rey, S. Wellek and K. Mann (2003). "Reward craving and withdrawal relief craving: assessment of different motivational pathways to alcohol intake." Alcohol Alcohol **38**(1): 35-39.

Heinz, A., T. Siessmeier, J. Wrase, H. G. Buchholz, G. Grunder, Y. Kumakura, P. Cumming, M. Schreckenberger, M. N. Smolka, F. Rosch, K. Mann and P. Bartenstein (2005). "Correlation of alcohol craving with striatal dopamine synthesis capacity and D2/3 receptor availability: a combined [18F]DOPA and [18F]DMFP PET study in detoxified alcoholic patients." Am J Psychiatry **162**(8): 1515-1520.

Heinz, A., T. Siessmeier, J. Wrase, D. Hermann, S. Klein, S. M. Grusser, H. Flor, D. F. Braus, H. G. Buchholz, G. Grunder, M. Schreckenberger, M. N. Smolka, F. Rosch, K. Mann and P. Bartenstein (2004). "Correlation between dopamine D(2) receptors in the ventral striatum and central processing of alcohol cues and craving." Am J Psychiatry **161**(10): 1783-1789.

Herzog, H., L. Tellmann, R. Fulton, I. Stangier, E. Rota Kops, K. Bente, C. Boy, R. Hurlemann and U. Pietrzyk (2005). "Motion artifact reduction on parametric PET images of neuroreceptor binding." J Nucl Med **46**(6): 1059-1065.

Hietala, J., C. West, E. Syvalahti, K. Nagren, P. Lehikoinen, P. Sonninen and U. Ruotsalainen (1994). "Striatal D2 dopamine receptor binding characteristics in vivo in patients with alcohol dependence." Psychopharmacology (Berl) **116**(3): 285-290.

Hoekstra, C. J., I. Paglianiti, O. S. Hoekstra, E. F. Smit, P. E. Postmus, G. J. J. Teule and A. A. Lammertsma (2000). "Monitoring response to therapy in cancer using [18F]-2-fluoro-2-deoxy-d-glucose and positron emission tomography: an overview of different analytical methods." European Journal of Nuclear Medicine **27**(6): 731-743.

Hu, X., G. Oroszi, J. Chun, T. L. Smith, D. Goldman and M. A. Schuckit (2005). "An expanded evaluation of the relationship of four alleles to the level of response to alcohol and the alcoholism risk." Alcohol Clin Exp Res **29**(1): 8-16.

Hua, K., J. Zhang, S. Wakana, H. Jiang, X. Li, D. S. Reich, P. A. Calabresi, J. J. Pekar, P. C. van Zijl and S. Mori (2008). "Tract probability maps in stereotaxic spaces: analyses of white matter anatomy and tract-specific quantification." Neuroimage **39**(1): 336-347.

Hurley, T. D. and H. J. Edenberg (2012). "Genes encoding enzymes involved in ethanol metabolism." Alcohol Res **34**(3): 339-344.

Hyman, S. E., R. C. Malenka and E. J. Nestler (2006). "Neural mechanisms of addiction: the role of reward-related learning and memory." Annu Rev Neurosci **29**: 565-598.

Ihssen, N., W. M. Cox, A. Wiggett, J. S. Fadardi and D. E. Linden (2011). "Differentiating heavy from light drinkers by neural responses to visual alcohol cues and other motivational stimuli." Cereb Cortex **21**(6): 1408-1415.

Innis, R. B., V. J. Cunningham, J. Delforge, M. Fujita, A. Gjedde, R. N. Gunn, J. Holden, S. Houle, S.-C. Huang, M. Ichise, H. Iida, H. Ito, Y. Kimura, R. A. Koeppe, G. M. Knudsen, J. Knuuti, A. A. Lammertsma, M. Laruelle, J. Logan, R. P. Maguire, M. A. Mintun, E. D. Morris, R. Parsey, J. C. Price, M. Slifstein, V. Sossi, T. Suhara, J. R.

Votaw, D. F. Wong and R. E. Carson (2007). "Consensus nomenclature for in vivo imaging of reversibly binding radioligands." Journal of Cerebral Blood Flow & Metabolism **27**(9): 1533-1539.

Ishibashi, K., C. L. Robertson, M. A. Mandelkern, A. T. Morgan and E. D. London (2013). "The simplified reference tissue model with 18F-fallypride positron emission tomography: choice of reference region." Mol Imaging **12**(8).

Jenkinson, M., C. F. Beckmann, T. E. Behrens, M. W. Woolrich and S. M. Smith (2012). "FSL." Neuroimage **62**(2): 782-790.

Kegeles, L. S., M. Slifstein, X. Xu, N. Urban, J. L. Thompson, T. Moadel, J. M. Harkavy-Friedman, R. Gil, M. Laruelle and A. Abi-Dargham (2010). "Striatal and extrastriatal dopamine D2/D3 receptors in schizophrenia evaluated with [18F]fallypride positron emission tomography." Biol Psychiatry **68**(7): 634-641.

Kendler, K. S., C. A. Prescott, M. C. Neale and N. L. Pedersen (1997). "Temperance board registration for alcohol abuse in a national sample of Swedish male twins, born 1902 to 1949." Arch Gen Psychiatry **54**(2): 178-184.

Kessler, R. C., W. T. Chiu, O. Demler, K. R. Merikangas and E. E. Walters (2005). "Prevalence, severity, and comorbidity of 12-month DSM-IV disorders in the National Comorbidity Survey Replication." Arch Gen Psychiatry **62**(6): 617-627.

Kumar, A., K. H. Choi, W. Renthal, N. M. Tsankova, D. E. Theobald, H. T. Truong, S. J. Russo, Q. Laplant, T. S. Sasaki, K. N. Whistler, R. L. Neve, D. W. Self and E. J. Nestler (2005). "Chromatin remodeling is a key mechanism underlying cocaine-induced plasticity in striatum." Neuron **48**(2): 303-314.

Laine, T. P., A. Ahonen, P. Torniainen, J. Heikkila, J. Pyhtinen, P. Rasanen, O. Niemela and M. Hillbom (1999). "Dopamine transporters increase in human brain after alcohol withdrawal." Mol Psychiatry **4**(2): 189-191, 104-185.

Lammertsma, A. A. and S. P. Hume (1996). "Simplified reference tissue model for PET receptor studies." Neuroimage **4**(3 Pt 1): 153-158.

Liu, X. and F. Weiss (2002). "Reversal of ethanol-seeking behavior by D1 and D2 antagonists in an animal model of relapse: differences in antagonist potency in previously ethanol-dependent versus nondependent rats." J Pharmacol Exp Ther **300**(3): 882-889.

Lof, E., P. Olausson, A. deBejczy, R. Stomberg, J. M. McIntosh, J. R. Taylor and B. Soderpalm (2007). "Nicotinic acetylcholine receptors in the ventral tegmental area mediate the dopamine activating and reinforcing properties of ethanol cues." Psychopharmacology (Berl) **195**(3): 333-343.

Logan, J., J. S. Fowler, N. D. Volkow, G. J. Wang, Y. S. Ding and D. L. Alexoff (1996). "Distribution volume ratios without blood sampling from graphical analysis of PET data." J Cereb Blood Flow Metab **16**(5): 834-840.

Maldjian, J. A., P. J. Laurienti and J. H. Burdette (2004). "Precentral gyrus discrepancy in electronic versions of the Talairach atlas." Neuroimage **21**(1): 450-455.

Maldjian, J. A., P. J. Laurienti, R. A. Kraft and J. H. Burdette (2003). "An automated method for neuroanatomic and cytoarchitectonic atlas-based interrogation of fMRI data sets." Neuroimage **19**(3): 1233-1239.

Martinez, D., R. Gil, M. Slifstein, D.-R. Hwang, Y. Huang, A. Perez, L. Kegeles, P. Talbot, S. Evans, J. Krystal, M. Laruelle and A. Abi-Dargham (2005). "Alcohol Dependence Is Associated with Blunted Dopamine Transmission in the Ventral Striatum." Biological Psychiatry **58**(10): 779-786.

Mazziotta, J., A. Toga, A. Evans, P. Fox, J. Lancaster, K. Zilles, R. Woods, T. Paus, G. Simpson, B. Pike, C. Holmes, L. Collins, P. Thompson, D. MacDonald, M. Iacoboni, T. Schormann, K. Amunts, N. Palomero-Gallagher, S. Geyer, L. Parsons, K. Narr, N. Kabani, G. Le Goualher, D. Boomsma, T. Cannon, R. Kawashima and B. Mazoyer (2001). "A probabilistic atlas and reference system for the human brain: International Consortium for Brain Mapping (ICBM)." Philos Trans R Soc Lond B Biol Sci **356**(1412): 1293-1322.

Mazziotta, J., A. Toga, A. Evans, P. Fox, J. Lancaster, K. Zilles, R. Woods, T. Paus, G. Simpson, B. Pike, C. Holmes, L. Collins, P. Thompson, D. MacDonald, M. Iacoboni, T. Schormann, K. Amunts, N. Palomero-Gallagher, S. Geyer, L. Parsons, K. Narr, N. Kabani, G. Le Goualher, J. Feidler, K. Smith, D. Boomsma, H. Hulshoff Pol, T. Cannon, R. Kawashima and B. Mazoyer (2001). "A four-dimensional probabilistic atlas of the human brain." J Am Med Inform Assoc **8**(5): 401-430.

Mazziotta, J. C., A. W. Toga, A. Evans, P. Fox and J. Lancaster (1995). "A probabilistic atlas of the human brain: theory and rationale for its development. The International Consortium for Brain Mapping (ICBM)." Neuroimage **2**(2): 89-101.

McBride, W. J., E. Chernet, W. Dyr, L. Lumeng and T. K. Li (1993). "Densities of dopamine D2 receptors are reduced in CNS regions of alcohol-preferring P rats." Alcohol **10**(5): 387-390.

Mereu, G., F. Fadda and G. L. Gessa (1984). "Ethanol stimulates the firing rate of nigral dopaminergic neurons in unanesthetized rats." Brain Res **292**(1): 63-69.

Mori, S., S. Wakana, P. C. Van Zijl and L. Nagae-Poetscher (2005). MRI atlas of human white matter, Elsevier.

Morris, E. D., C. J. Endres, K. C. Schmidt, B. T. Christian, R. F. Muzic and R. E. Fisher (2004). "Kinetic modeling in positron emission tomography." Emission Tomography: The Fundamentals of PET and SPECT. Academic, San Diego.

Mukherjee, J., B. T. Christian, K. A. Dunigan, B. Shi, T. K. Narayanan, M. Satter and J. Mantil (2002). "Brain imaging of 18F-fallypride in normal volunteers: blood analysis, distribution, test-retest studies, and preliminary assessment of sensitivity to aging effects on dopamine D-2/D-3 receptors." Synapse **46**(3): 170-188.

Mukherjee, J., B. T. Christian, T. K. Narayanan, B. Shi and D. Collins (2005). "Measurement of d-amphetamine-induced effects on the binding of dopamine D-2/D-3 receptor radioligand, 18F-fallypride in extrastriatal brain regions in non-human primates using PET." Brain Res **1032**(1-2): 77-84.

Mukherjee, J., Z. Y. Yang, T. Brown, R. Lew, M. Wernick, X. Ouyang, N. Yasillo, C. T. Chen, R. Mintzer and M. Cooper (1999). "Preliminary assessment of extrastriatal dopamine D-2 receptor binding in the rodent and nonhuman primate brains using the high affinity radioligand, 18F-fallypride." Nucl Med Biol **26**(5): 519-527.

Mukherjee, J., Z. Y. Yang, M. K. Das and T. Brown (1995). "Fluorinated benzamide neuroleptics--III. Development of (S)-N-[(1-allyl-2-pyrrolidinyl)methyl]-5-(3-

[18F]fluoropropyl)-2, 3-dimethoxybenzamide as an improved dopamine D-2 receptor tracer." Nucl Med Biol **22**(3): 283-296.

Nair, N. P., S. Lal, H. I. Iskandar, P. Etienne, P. L. Wood and H. Guyda (1982). "Effect of sulpiride, an atypical neuroleptic, on apomorphine-induced growth hormone secretion." Brain Res Bull **8**(6): 587-591.

Nestler, E. J. and G. K. Aghajanian (1997). "Molecular and cellular basis of addiction." Science **278**(5335): 58-63.

Nevo, I. (1995). "Neurotransmitter and neuromodulatory mechanisms involved in alcohol abuse and alcoholism." Neurochemistry International **26**(4): 305-336.

Noble, E. P., K. Blum, T. Ritchie, A. Montgomery and P. J. Sheridan (1991). "Allelic association of the D2 dopamine receptor gene with receptor-binding characteristics in alcoholism." Arch Gen Psychiatry **48**(7): 648-654.

Nurnberger, J. I., Jr., R. Wiegand, K. Bucholz, S. O'Connor, E. T. Meyer, T. Reich, J. Rice, M. Schuckit, L. King, T. Petti, L. Bierut, A. L. Hinrichs, S. Kuperman, V. Hesselbrock and B. Porjesz (2004). "A family study of alcohol dependence: coaggregation of multiple disorders in relatives of alcohol-dependent probands." Arch Gen Psychiatry **61**(12): 1246-1256.

Oikonen, V. (2018, 14.02.2018). "Reference region input compartmental models." Retrieved 29.10.2018, 2018, from http://www.turkupetcentre.net/petanalysis/model_compartmental_ref.html.

Pabst, A., L. Kraus, E. G. d. Matos and D. Piontek (2013). "Substanzkonsum und substanzbezogene Störungen in Deutschland im Jahr 2012." Sucht **59**(6): 321-331.

Patenaude, B., S. M. Smith, D. N. Kennedy and M. Jenkinson (2011). "A Bayesian model of shape and appearance for subcortical brain segmentation." Neuroimage **56**(3): 907-922.

Pfeffer, A. O. and H. H. Samson (1988). "Haloperidol and apomorphine effects on ethanol reinforcement in free feeding rats." Pharmacol Biochem Behav **29**(2): 343-350.

Politis, M. (2014). "Neuroimaging in Parkinson disease: from research setting to clinical practice." Nat Rev Neurol **10**(12): 708-722.

Repo, E., J. T. Kuikka, K. A. Bergstrom, J. Karhu, J. Hiltunen and J. Tiihonen (1999). "Dopamine transporter and D2-receptor density in late-onset alcoholism." Psychopharmacology (Berl) **147**(3): 314-318.

Riccardi, P., R. Li, M. S. Ansari, D. Zald, S. Park, B. Dawant, S. Anderson, M. Doop, N. Woodward, E. Schoenberg, D. Schmidt, R. Baldwin and R. Kessler (2006). "Amphetamine-induced displacement of [18F] fallypride in striatum and extrastriatal regions in humans." Neuropsychopharmacology **31**(5): 1016-1026.

Robinson, T. (1993). "The neural basis of drug craving: An incentive-sensitization theory of addiction." Brain Research Reviews **18**(3): 247-291.

Robinson, T. E. and K. C. Berridge (2001). "Incentive-sensitization and addiction." Addiction **96**(1): 103-114.

Robinson, T. E. and K. C. Berridge (2003). "Addiction." Annu Rev Psychol **54**: 25-53.

Robinson, T. E. and K. C. Berridge (2008). "Review. The incentive sensitization theory of addiction: some current issues." Philos Trans R Soc Lond B Biol Sci **363**(1507): 3137-3146.

Robinson, T. E. and B. Kolb (2004). "Structural plasticity associated with exposure to drugs of abuse." Neuropharmacology **47 Suppl 1**: 33-46.

Rominger, A., P. Cumming, G. Xiong, G. Koller, G. Boning, M. Wulff, A. Zwergal, S. Forster, A. Reilhac, O. Munk, M. Soyka, B. Wangler, P. Bartenstein, C. la Fougere and O. Pogarell (2012). "[18F]Fallypride PET measurement of striatal and extrastriatal dopamine D 2/3 receptor availability in recently abstinent alcoholics." Addict Biol **17**(2): 490-503.

Rommelspacher, H., C. Raeder, P. Kaulen and G. Brüning (1992). "Adaptive changes of dopamine-D2 receptors in rat brain following ethanol withdrawal: A quantitative autoradiographic investigation." Alcohol **9**(5): 355-362.

Rubio, G., M. Jimenez, R. Rodriguez-Jimenez, I. Martinez, C. Avila, F. Ferre, M. A. Jimenez-Arriero, G. Ponce and T. Palomo (2008). "The role of behavioral impulsivity in the development of alcohol dependence: a 4-year follow-up study." Alcohol Clin Exp Res **32**(9): 1681-1687.

Russell, R. N., W. J. McBride, L. Lumeng, T. K. Li and J. M. Murphy (1996). "Apomorphine and 7-OH DPAT reduce ethanol intake of P and HAD rats." Alcohol **13**(5): 515-519.

Salimov, R. M., N. B. Salimova, L. N. Shvets and A. I. Maisky (2000). "Haloperidol administered subchronically reduces the alcohol-deprivation effect in mice." Alcohol **20**(1): 61-68.

Sari, Y., R. L. Bell and F. C. Zhou (2006). "Effects of chronic alcohol and repeated deprivations on dopamine D1 and D2 receptor levels in the extended amygdala of inbred alcohol-preferring rats." Alcohol Clin Exp Res **30**(1): 46-56.

Schmidt, L. G., M. Dettling, K. J. Graef, A. Heinz, S. Kuhn, J. Podschus and H. Rommelspacher (1996). "Reduced dopaminergic function in alcoholics is related to severe dependence." Biological Psychiatry **39**(3): 193-198.

Schuckit, M. A. and T. L. Smith (2000). "The relationships of a family history of alcohol dependence, a low level of response to alcohol and six domains of life functioning to the development of alcohol use disorders." J Stud Alcohol **61**(6): 827-835.

Schuckit, M. A. and T. L. Smith (2006). "An evaluation of the level of response to alcohol, externalizing symptoms, and depressive symptoms as predictors of alcoholism." J Stud Alcohol **67**(2): 215-227.

Schultz, B. B. (1985). "Levene's Test for Relative Variation." Systematic Zoology **34**(4): 449-456.

Siessmeier, T., Y. Zhou, H. G. Buchholz, C. Landvogt, I. Vernaleken, M. Piel, R. Schirrmacher, F. Rosch, M. Schreckenberger, D. F. Wong, P. Cumming, G. Grunder and P. Bartenstein (2005). "Parametric mapping of binding in human brain of D2 receptor ligands of different affinities." J Nucl Med **46**(6): 964-972.

Slifstein, M., D.-R. Hwang, Y. Huang, N. Guo, Y. Sudo, R. Narendran, P. Talbot and M. Laruelle (2004). "In vivo affinity of [18F]fallypride for striatal and extrastriatal dopamine D2 receptors in nonhuman primates." Psychopharmacology **175**(3): 274-286.

Slifstein, M., L. S. Kegeles, X. Xu, J. L. Thompson, N. Urban, J. Castrillon, E. Hackett, S. A. Bae, M. Laruelle and A. Abi-Dargham (2010). "Striatal and extrastriatal dopamine release measured with PET and [18 F] fallypride." Synapse **64**(5): 350-362.

Slifstein, M., R. Narendran, D. R. Hwang, Y. Sudo, P. S. Talbot, Y. Huang and M. Laruelle (2004). "Effect of amphetamine on [(18)F]fallypride in vivo binding to D(2) receptors in striatal and extrastriatal regions of the primate brain: Single bolus and bolus plus constant infusion studies." Synapse **54**(1): 46-63.

Smith, S. M., M. Jenkinson, M. W. Woolrich, C. F. Beckmann, T. E. Behrens, H. Johansen-Berg, P. R. Bannister, M. De Luca, I. Drobnjak, D. E. Flitney, R. K. Niazy, J. Saunders, J. Vickers, Y. Zhang, N. De Stefano, J. M. Brady and P. M. Matthews (2004). "Advances in functional and structural MR image analysis and implementation as FSL." Neuroimage **23 Suppl 1**: S208-219.

Spreckelmeyer, K. N., M. Paulzen, M. Raptis, T. Baltus, S. Schaffrath, J. Van Waesberghe, M. M. Zalewski, F. Rosch, I. Vernaleken, W. M. Schafer and G. Grunder (2011). "Opiate-induced dopamine release is modulated by severity of alcohol dependence: an [(18)F]fallypride positron emission tomography study." Biol Psychiatry **70**(8): 770-776.

Stefanini, E., M. Frau, M. G. Garau, B. Garau, F. Fadda and G. L. Gessa (1992). "Alcohol-preferring rats have fewer dopamine D2 receptors in the limbic system." Alcohol Alcohol **27**(2): 127-130.

Surti, S., A. Kuhn, M. E. Werner, A. E. Perkins, J. Kolthammer and J. S. Karp (2007). "Performance of Philips Gemini TF PET/CT scanner with special consideration for its time-of-flight imaging capabilities." J Nucl Med **48**(3): 471-480.

Talairach, J. and P. Tournoux (1988). Co-planar stereotaxic atlas of the human brain. 3-Dimensional proportional system: an approach to cerebral imaging.

Thanos, P. K., J. M. Katana, C. R. Ashby, Jr., M. Michaelides, E. L. Gardner, C. A. Heidbreder and N. D. Volkow (2005). "The selective dopamine D3 receptor antagonist SB-277011-A attenuates ethanol consumption in ethanol preferring (P) and non-preferring (NP) rats." Pharmacol Biochem Behav **81**(1): 190-197.

Thanos, P. K., N. D. Volkow, P. Freimuth, H. Umegaki, H. Ikari, G. Roth, D. K. Ingram and R. Hitzemann (2001). "Overexpression of dopamine D2 receptors reduces alcohol self-administration." J Neurochem **78**(5): 1094-1103.

Thielen, R. J., E. A. Engleman, Z. A. Rodd, J. M. Murphy, L. Lumeng, T. K. Li and W. J. McBride (2004). "Ethanol drinking and deprivation alter dopaminergic and serotonergic function in the nucleus accumbens of alcohol-preferring rats." J Pharmacol Exp Ther **309**(1): 216-225.

Tiihonen, J., J. Kuikka, K. Bergstrom, P. Hakola, J. Karhu, O. P. Ryynanen and J. Fohr (1995). "Altered striatal dopamine re-uptake site densities in habitually violent and non-violent alcoholics." Nat Med **1**(7): 654-657.

Tiihonen, J., H. Vilkman, P. Rasanen, O. P. Ryynanen, H. Hakko, J. Bergman, T. Hamalainen, A. Laakso, M. Haaparanta-Solin, O. Solin, M. Kuoppamaki, E. Syvalahti and J. Hietala (1998). "Striatal presynaptic dopamine function in type 1 alcoholics measured with positron emission tomography." Mol Psychiatry **3**(2): 156-161.

Tupala, E., H. Hall, K. Bergstrom, T. Mantere, P. Rasanen, T. Sarkioja and J. Tiihonen (2003). "Dopamine D2 receptors and transporters in type 1 and 2 alcoholics measured with human whole hemisphere autoradiography." Hum Brain Mapp **20**(2): 91-102.

Tupala, E., H. Hall, K. Bergström, T. Särkioja, P. Räsänen, T. Mantere, J. Callaway, J. Hiltunen and J. Tiihonen (2001). "Dopamine D2/D3-receptor and transporter densities in nucleus accumbens and amygdala of type 1 and 2 alcoholics." Molecular Psychiatry **6**(3): 261-267.

Tzourio-Mazoyer, N., B. Landeau, D. Papathanassiou, F. Crivello, O. Etard, N. Delcroix, B. Mazoyer and M. Joliot (2002). "Automated anatomical labeling of activations in SPM using a macroscopic anatomical parcellation of the MNI MRI single-subject brain." Neuroimage **15**(1): 273-289.

Urban, N. B. L., L. S. Kegeles, M. Slifstein, X. Xu, D. Martinez, E. Sakr, F. Castillo, T. Moadel, S. S. O'Malley, J. H. Krystal and A. Abi-Dargham (2010). "Sex Differences in Striatal Dopamine Release in Young Adults After Oral Alcohol Challenge: A Positron Emission Tomography Imaging Study With [11C]Raclopride." Biological Psychiatry **68**(8): 689-696.

Vandehey, N. T., J. M. Moirano, A. K. Converse, J. E. Holden, J. Mukherjee, D. Murali, R. J. Nickles, R. J. Davidson, M. L. Schneider and B. T. Christian (2010). "High-affinity dopamine D2/D3 PET radioligands 18F-fallypride and 11C-FLB457: a comparison of kinetics in extrastriatal regions using a multiple-injection protocol." J Cereb Blood Flow Metab **30**(5): 994-1007.

Vengeliene, V., A. Bilbao, A. Molander and R. Spanagel (2008). "Neuropharmacology of alcohol addiction." Br J Pharmacol **154**(2): 299-315.

Vengeliene, V., F. Leonardi-Essmann, S. Perreau-Lenz, P. Gebicke-Haerter, K. Drescher, G. Gross and R. Spanagel (2006). "The dopamine D3 receptor plays an essential role in alcohol-seeking and relapse." FASEB J **20**(13): 2223-2233.

Vernaleken, I., L. Peters, M. Raptis, R. Lin, H. G. Buchholz, Y. Zhou, O. Winz, F. Rosch, P. Bartenstein, D. F. Wong, W. M. Schafer and G. Grunder (2011). "The applicability of SRTM in [(18)F]fallypride PET investigations: impact of scan durations." J Cereb Blood Flow Metab **31**(9): 1958-1966.

Vetreno, R. P. and F. T. Crews (2014). "Current hypotheses on the mechanisms of alcoholism." Handb Clin Neurol **125**: 477-497.

Volkow, N. D., G.-J. Wang, H. Begleiter, B. Porjesz, J. S. Fowler, F. Telang, C. Wong, Y. Ma, J. Logan, R. Goldstein, D. Alexoff and P. K. Thanos (2006). "High Levels of Dopamine D2 Receptors in Unaffected Members of Alcoholic Families." Arch Gen Psychiatry **63**(9): 999.

Volkow, N. D., G.-J. Wang, J. S. Fowler, J. Logan, R. Hitzemann, Y.-S. Ding, N. Pappas, C. Shea and K. Piscani (1996). "Decreases in Dopamine Receptors but not in Dopamine Transporters in Alcoholics." Alcoholism: Clinical and Experimental Research **20**(9): 1594-1598.

Volkow, N. D., G. J. Wang, L. Maynard, J. S. Fowler, B. Jayne, F. Telang, J. Logan, Y. S. Ding, S. J. Gatley, R. Hitzemann, C. Wong and N. Pappas (2002). "Effects of alcohol detoxification on dopamine D2 receptors in alcoholics: a preliminary study." Psychiatry Res **116**(3): 163-172.

Volkow, N. D., G. J. Wang, F. Telang, J. S. Fowler, J. Logan, M. Jayne, Y. Ma, K. Pradhan and C. Wong (2007). "Profound decreases in dopamine release in striatum in detoxified alcoholics: possible orbitofrontal involvement." J Neurosci **27**(46): 12700-12706.

Vollstadt-Klein, S., S. Wichert, J. Rabinstein, M. Buhler, O. Klein, G. Ende, D. Hermann and K. Mann (2010). "Initial, habitual and compulsive alcohol use is characterized by a shift of cue processing from ventral to dorsal striatum." Addiction **105**(10): 1741-1749.

von der Goltz, C. and F. Kiefer (2009). "Learning and memory in the aetiopathogenesis of addiction: future implications for therapy?" Eur Arch Psychiatry Clin Neurosci **259 Suppl 2**: S183-187.

Wakana, S., A. Caprihan, M. M. Panzenboeck, J. H. Fallon, M. Perry, R. L. Gollub, K. Hua, J. Zhang, H. Jiang and P. Dubey (2007). "Reproducibility of quantitative tractography methods applied to cerebral white matter." Neuroimage **36**(3): 630-644.

Warner, L. A., H. R. White and V. Johnson (2007). "Alcohol initiation experiences and family history of alcoholism as predictors of problem-drinking trajectories." J Stud Alcohol Drugs **68**(1): 56-65.

Wiesbeck, G. A., C. Mauerer, J. Thome, F. Jakob and J. Boening (1995). "Alcohol Dependence, Family History, and D2 Dopamine-Receptor Function as Neuroendocrinologically Assessed with Apomorphine." Drug and Alcohol Dependence **40**(1): 49-53.

Wise, R. A. (1988). "The neurobiology of craving: implications for the understanding and treatment of addiction." J Abnorm Psychol **97**(2): 118-132.

Woolrich, M. W., S. Jbabdi, B. Patenaude, M. Chappell, S. Makni, T. Behrens, C. Beckmann, M. Jenkinson and S. M. Smith (2009). "Bayesian analysis of neuroimaging data in FSL." Neuroimage **45**(1 Suppl): S173-186.

World Health Organization. (2014). "Global status report on alcohol and health-2014."

Wrase, J., F. Schlagenhauf, T. Kienast, T. Wüstenberg, F. Bermpohl, T. Kahnt, A. Beck, A. Ströhle, G. Juckel, B. Knutson and A. Heinz (2007). "Dysfunction of reward processing correlates with alcohol craving in detoxified alcoholics." NeuroImage **35**(2): 787-794.

Yoder, K. K., E. D. Morris, C. C. Constantinescu, T. E. Cheng, M. D. Normandin, S. J. O'Connor and D. A. Kareken (2009). "When what you see isn't what you get: alcohol cues, alcohol administration, prediction error, and human striatal dopamine." Alcohol Clin Exp Res **33**(1): 139-149.

Zimmermann, U. S., D. Blomeyer, M. Laucht and K. F. Mann (2007). "How gene-stress-behavior interactions can promote adolescent alcohol use: the roles of predrinking allostatic load and childhood behavior disorders." Pharmacol Biochem Behav **86**(2): 246-262.

Zimmermann, U. S., I. Mick, M. Laucht, V. Vitvitskiy, M. H. Plawecki, K. F. Mann and S. O'Connor (2009). "Offspring of parents with an alcohol use disorder prefer higher levels of brain alcohol exposure in experiments involving computer-assisted self-infusion of ethanol (CASE)." Psychopharmacology (Berl) **202**(4): 689-697.

Eidesstattliche Versicherung

„Ich, David Paul Weber, versichere an Eides statt durch meine eigenhändige Unterschrift, dass ich die vorgelegte Dissertation mit dem Thema: Optimizing the Automated Analysis of Dopamine D2 Receptor Imaging for Research into Alcohol Use Disorders / Optimierung der automatischen Analyse von Dopamin D2 Rezeptor Bildgebung für die Untersuchung von Alkoholgebrauchsstörungen selbstständig und ohne nicht offengelegte Hilfe Dritter verfasst und keine anderen als die angegebenen Quellen und Hilfsmittel genutzt habe.

Alle Stellen, die wörtlich oder dem Sinne nach auf Publikationen oder Vorträgen anderer Autoren/innen beruhen, sind als solche in korrekter Zitierung kenntlich gemacht. Die Abschnitte zu Methodik (insbesondere praktische Arbeiten, Laborbestimmungen, statistische Aufarbeitung) und Resultaten (insbesondere Abbildungen, Graphiken und Tabellen) werden von mir verantwortet.

Ich versichere ferner, dass ich die in Zusammenarbeit mit anderen Personen generierten Daten, Datenauswertungen und Schlussfolgerungen korrekt gekennzeichnet und meinen eigenen Beitrag sowie die Beiträge anderer Personen korrekt kenntlich gemacht habe (siehe Anteilserklärung). Texte oder Textteile, die gemeinsam mit anderen erstellt oder verwendet wurden, habe ich korrekt kenntlich gemacht.

Meine Anteile an etwaigen Publikationen zu dieser Dissertation entsprechen denen, die in der untenstehenden gemeinsamen Erklärung mit dem/der Erstbetreuer/in, angegeben sind. Für sämtliche im Rahmen der Dissertation entstandenen Publikationen wurden die Richtlinien des ICMJE (International Committee of Medical Journal Editors; www.icmje.og) zur Autorenschaft eingehalten. Ich erkläre ferner, dass ich mich zur Einhaltung der Satzung der Charité – Universitätsmedizin Berlin zur Sicherung Guter Wissenschaftlicher Praxis verpflichte.

Weiterhin versichere ich, dass ich diese Dissertation weder in gleicher noch in ähnlicher Form bereits an einer anderen Fakultät eingereicht habe.

Die Bedeutung dieser eidesstattlichen Versicherung und die strafrechtlichen Folgen einer unwahren eidesstattlichen Versicherung (§§156, 161 des Strafgesetzbuches) sind mir bekannt und bewusst."

Datum   Unterschrift

Anteilserklärung an etwaigen erfolgten Publikationen

David Paul Weber hatte folgenden Anteil an den folgenden Publikationen:

Publikation 1 (Posterpräsentation mit zitierbarem Abstract): D. P. Weber, T. Gleich, T. Kodalle, G. Spitta, C. Lange, O. Butler, W. Brenner, A. Heinz, J. Gallinat, R. Buchert; Assessment of dopamine D2/3 receptor status in alcohol use disorders using F-18-fallypride PET and reference tissue approaches: methodological considerations; Dreiländertagung 2017 der Deutschen Gesellschaft für Nuklearmedizin

Beitrag im Einzelnen (bitte detailliert ausführen):

Entwicklung der Forschungsfrage zu den Methodenvergleichen gemeinsam mit Dr. Buchert. Programmierung der Skripte zur automatischen Bildauswertung gemeinsam mit Dr. Buchert. Eigenständige statistische Datenauswertung. Eigeständige Erstellung des Posterentwurfs, inklusive Erstellung der Abbildungen. Mitarbeit bei der Überarbeitung des Posters.

_____

Unterschrift, Datum und Stempel des/der erstbetreuenden Hochschullehrers/in

_____

Unterschrift des Doktoranden/der Doktorandin

Lebenslauf

Mein Lebenslauf wird aus datenschutzrechtlichen Gründen in der elektronischen Version meiner Arbeit nicht veröffentlicht.

Mein Lebenslauf wird aus datenschutzrechtlichen Gründen in der elektronischen Version meiner Arbeit nicht veröffentlicht.

Publikationen

Posterpräsentation mit zitierbarem Abstract: D. P. Weber, T. Gleich, T. Kodalle, G. Spitta, C. Lange, O. Butler, W. Brenner, A. Heinz, J. Gallinat, R. Buchert; Assessment of dopamine D2/3 receptor status in alcohol use disorders using F-18-fallypride PET and reference tissue approaches: methodological considerations; Dreiländertagung 2017 der Deutschen Gesellschaft für Nuklearmedizin

Danksagung

Meinem Erstbetreuer Professor Dr. med. Winfried Brenner danke ich für die Möglichkeit an der Klinik für Nuklearmedizin zu promovieren, für die Empfehlung der Forschungsgruppe und für die Überlassung des Themas.

Meinem Zweitbetreuer Dr. rer. nat. Ralph Buchert danke ich von Herzen für die hervorragende mehrjährige Betreuung. Vielen lieben Dank für die bereichernde Zusammenarbeit, die interessanten Diskussionen, sowie all die Zeit und Energie, die in dieses Projekt und in die Förderung meiner Arbeit geflossen sind.

Ich möchte mich auch ausdrücklich bei allen Mitwirkenden der LeAD-Studie für ihre konstruktive Arbeit bedanken, insbesondere dem gesamten Team des Unterprojekts 5.

Ein besonderer Dank gilt auch allen Patientinnen, Patienten, Probandinnen und Probanden für die Bereitschaft an dieser Studie mitzuwirken. Ohne ihre Mithilfe wäre keine derartige Studie möglich gewesen.

Zu guter Letzt möchte ich meinen Eltern, meiner Schwester, meinen Freunden und vor allem auch meiner Freundin Anita danken für alle Geduld, Unterstützung und Motivation.